Final Report - Ending on April 30, 1983

NASA-Ames Agreement No. NAG 2-225

"NEW POLYMERS FOR COMPOSITES"

A Summary of Research on Polystyrylpyridines

Principal Investigator:

Eli M. Pearce
Director, Polymer Research Institute

Polytechnic Institute of New York
333 Jay Street
Brooklyn, New York 11201

TABLE OF CONTENTS

LIST OF FIGURES

PATR I. STYRYLPYRIDINE AND ITS DERIVATIVES

LIST OF TABLE

PART I. STYRYLPYRIDINE AND ITS DERIVATIVES

PART II. SYNTHESIS, CHARACTERIZATION, AND THERMAL STABILITY OF STYRYLPYRIDINE BASED POLYMERS

PART I. STYRYLPYRIDINE AND ITS DERIVATIVES

PART I: STYRYLPYRIDINE AND ITS DERIVATIVES

I. INTRODUCTION

It is well known that substituents in the benzene ring may influence aromatic reactions. Many reactions have been investigated, especially those affecting a side chain. Substituents change the distribution of electron density and therefore influence the reactivity of a molecule by affecting bond strengths and repulsion forces. The influence of substituents in the pyridine reaction is analogous to the behavior of the substituents on benzene. There is some literature concerning the condensation of aromatics aldehydes with 2- or 4- position of methyl pyridine in the presence of acetic anhydride[1-5]. Bennett and Pratt[6] first used acetic anhydride as a condensing agent in the preparation of 2', 4'-dinitro-2-stilbazole. Acetic anhydride, acting as a Lewis acid catalyst, is now found to be generally applicable, and gives purer products and higher yield than other Lewis acids, such as $ZnCl_2$ or HCl[7,8].

A. P. Phillips[9] studied the reactions of dinitro derivatives of xylenes with aromatic aldehydes in aniline and zinc chloride. From his results, a resonable mechanism was proposed which added several intermediate steps to the Mills' mechanism[10]. Phillips suggested the following mechanism:

EQUATION 1

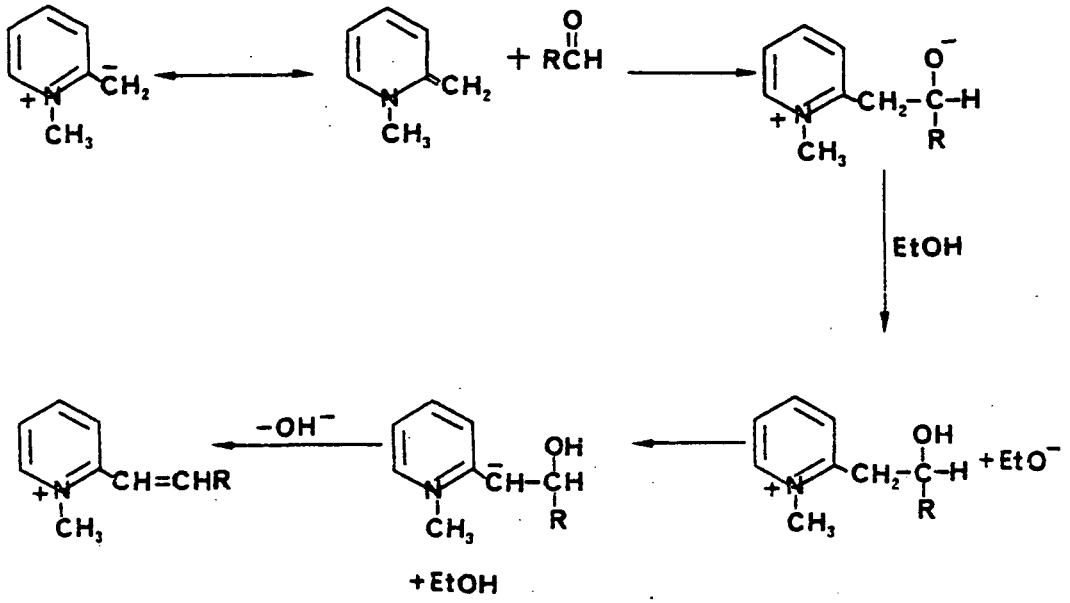

It is evident that simple aromatic hydrocarbons such as benzene, and its nitrogen analog, pyridine, show many gross similarities. For example, they have approximately the same resonance energy[11] , absorb at approximately the same wavelength (maximum at 255 mμ), and undergo anionoid and cationoid reactions[12]. The ultra-violet absorption spectra of aqueous solutions of pyridine and its homologs have been reviewed by Anderson[13]. In general, the main absorption peaks of the ionized and unionized form of a given base lie at approximately the same wavelength, but the extinction coefficient of the unionized base is only about half of that of the ionized base. Furthermore,

H. C. Brown[14] showed that the pK_a's of 3-,2-,and 4-methyl pyridine are in the order $3 < 2 < 4$. The methyl group in 3-picoline was found to have a non-acidic hydrogen and was unreactive toward aldehydes and, thus, no condensation was observed[15].

The absorption spectra of different derivatives of styrylpyridine have almost identical maximum wavelength (maximum at 290 $\pm$ 10 mμ)[5] and the shape of the spectra were approximately identical. E. R. Blout[5] attributed this to charge delocalization and the length of the conjugated absorbing system:

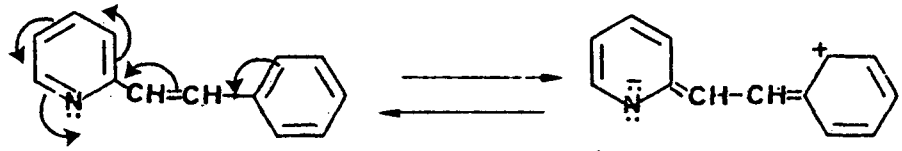

The reactivity of methyl derivatives of pyridine depends on its position in the pyridine ring. Thus, reactivity is a very important factor in the stability of the products (styrylpyridine). Previous studies[16] concentrated on the condensation reaction of methyl triazine with benzaldehyde.

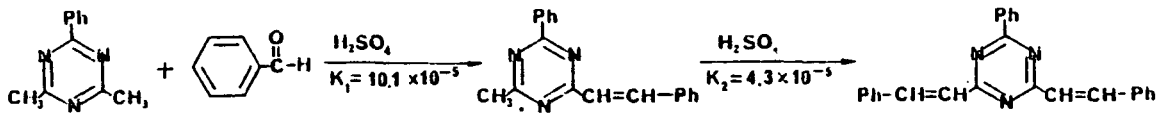

in the presence of sulfuric acid as a catalyst. The reaction rates were in the following order: methyl >styrl >pyridine. This effect could be caused by

the increase of delocalization of the electronic charge in the phenyl group. No information about the reactivity and activation energy for different methyl group positions on pyridine has been reported.

In this study, various methyl pyridines were reacted with benzaldehyde in acetic anhydride at a constant temperature and varying reaction times.

II. EXPERIMENTAL

II-A Formation of Various Styrylpyridine (SP)

(I) 2-styrylpyridine (2-SP)

(II) 4-styrylpyridine (4-SP)

(III) 2,4-di-(p-styryl)pyridine (2,4-DSP)

(IV) 2,6-di-(p-styryl)pyridine (2,6-DSP)

(V) 2,4,6-tri-(p-styryl)pyridine (2,4,6-TSP)

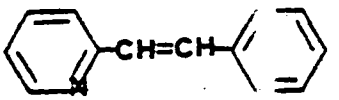

(I)

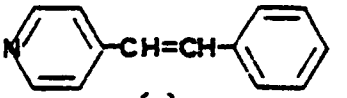

(II)

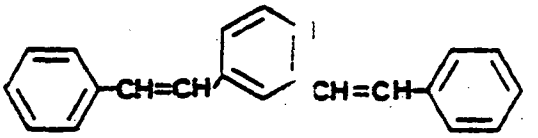

(III)

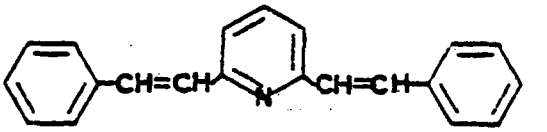

(IV)

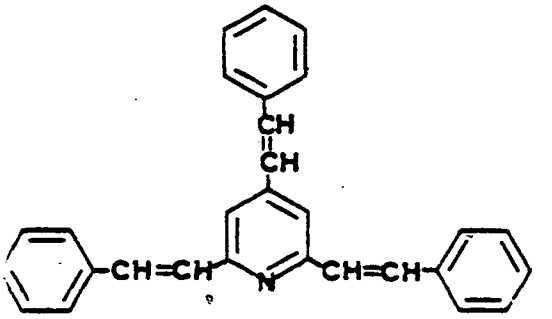

(V)

Methyl pyridine condensation products were prepared in the usual manner[5,7] by refluxing for approximately 9-15 hours the appropriate methyl pyridine and benzaldehyde in acetic acid and acid anhydride. The molar ratio of methyl pyridine to benzaldehyde varied from 1:1.2 to 1:3.6 depending on the particular styrylpyridine. After steam distillation a brown solid residue remained in the reaction vessel. The residue was recrystallized from n-hexane. Table 1 shows the chemical and physical constants. UV, IR, and proton and carbon-13 NMR spectra are shown in Fig. 1,2,3, and 4, respectively. The assignments for each of the characteristic peaks in the IR spectra are listed in Table 2.

II-B Formation of Derivatives of Styrylpyridine

(VI) 2-(p-hydroxystyryl)pyridine[17] (2-(p-OH)SP)

(VII) 4-(p-hydroxystyryl)pyridine[18] (4-(p-OH)SP)

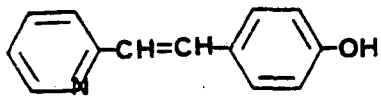

(VI)

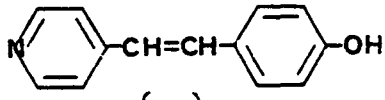

(VII)

A solution of 9.8 ml (0.1 mole) picoline, 14.6 gram (0.12 mole) of p-hydroxybenzaldehyde, and 18.8 ml (0.2 mole) of acetic anhydride was refluxed for 12 hours. The unreacted picoline and acetic anhydride were distilled off in vacuo. The rest of the solution was added to 75 ml of 3N HCl and refluxed for 1 hour. The color of the solution

Table 1. The chemical and physical constant for 2-SP, 4-SP, 2,4-DSP, 2,6-DSP, 2,4,6-TSP, 2-(p-OH)SP, 4-(p-OH)SP, 2,4-D(p-OH)SP, 2,6-D(p-OH)SP, and 2,4,6-T(p-OH)SP.

component	m.p. °C (lit.)	m.p. °C (observed, DSC) onset	melted (max.)	λmax (MeOH)	Log ε	at 800 °C
2-SP	90-91[a]	87.3	90.7	310[i]	4.41	0.8%
4-SP	127[b]	128.4	131.1	307[i]	4.51	1.0%
2,4-DSP	174[c]	170.5	173.7	307; 296[i]	4.54; 4.55	6.5%
2,6-DSP	167.5[d]	163.5	166.7	330; 290[i]	4.40; 4.57	4.0%
2,4,6-TSP	187-188[e]	180.1	185.2	300[i]	4.77	14.0%
2-(p-OH)SP	219-220[f]	214.6	217.1	308	4.11	3.0%
4-(p-OH)SP	271[g]	276.1	280.3	330	4.53	5.9%
2,4-D(p-OH)SP		253.5	257.4	340	4.71	55.0%
2,6-D(p-OH)SP	254 (decomp.)[h]	252.7	257.5	339; 324	4.54; 4.55	59.5%
2,4,6-T(p-OH)SP		258.2	262.2	317; 310	4.42; 4.43	

2-SP: 2-(p-styryl)pyridine.
4-SP: 4-(p-styryl)pyridine.
2,4-DSP: 2,4-di(p-styryl)pyridine.
2,6-DSP: 2,6-di(p-styryl)pyridine.
2,4,6,-TSP: 2,4,6-tri(p-styryl)pyridine.
2-(p-OH)SP: 2-(p-hydroxystyryl)pyridine
4-(p-OH)SP: 4-(p-hydroxystyryl)pyridine.
2,4-D(p-OH)SP: 2,4-di(p-hydroxystyryl)pyridine.
2,6-D(p-OH)SP: 2,6-di(p-hydroxystyryl)pyridine.
2,4,6-T(p-OH)SP: 2,4,6-tri(p-hydroxystyryl)pyridine

a : H. Bauath, Ber., 20, 2719(1887).
b : C. Friedlander, Ber., 38, 159(1905).
c : F. Schuster, Ber., 25, 2398(1905).
d : G. R. Clemo and W. M. Gourlay, J. Chem. Soc., 478(1938).
e : Koenigs and Bentheim, Ber., 38, 3908(1905).
f : M. X. Hubacher and S. Doernberg, J. Pharmaceutical Sciences, 53, 1067(1964).
g : W. A. Lees and A. Burawoy, Tetrahedron, 19, 419(1963).
h : E. D. Bergmann and S. Pinchas, J. Org. Chem., 15, 1184(1950).
i : E. R. Blout and V.W. Eager, J. Am. Chem. Soc., 67, 1315 (1945).

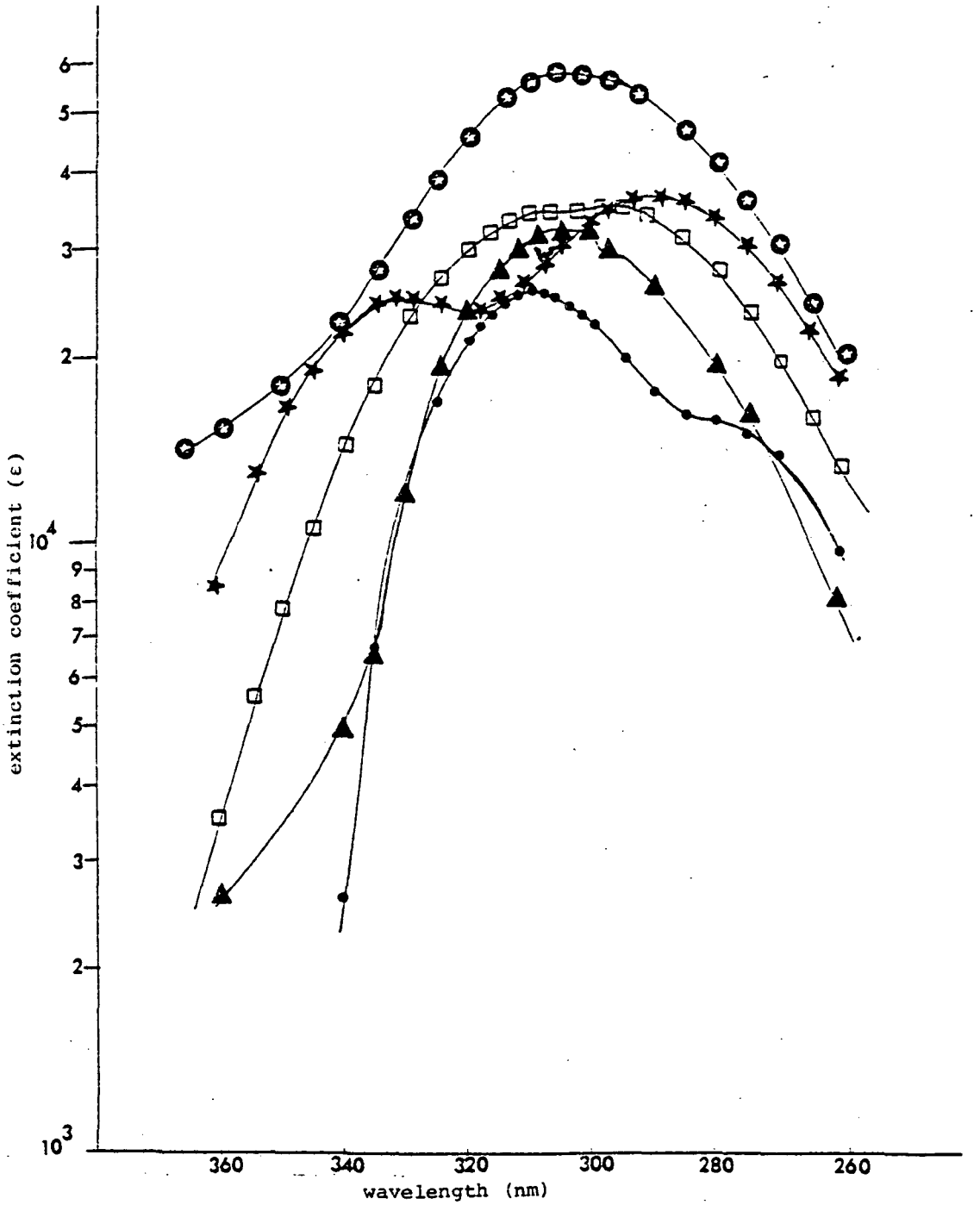

Figure 1. Ultraviolet spectra in methanol of
• 2SP, ▲ 4SP, □ 2,4DSP, ✱ 2,6DSP,
✪ 2,4,6TSP.

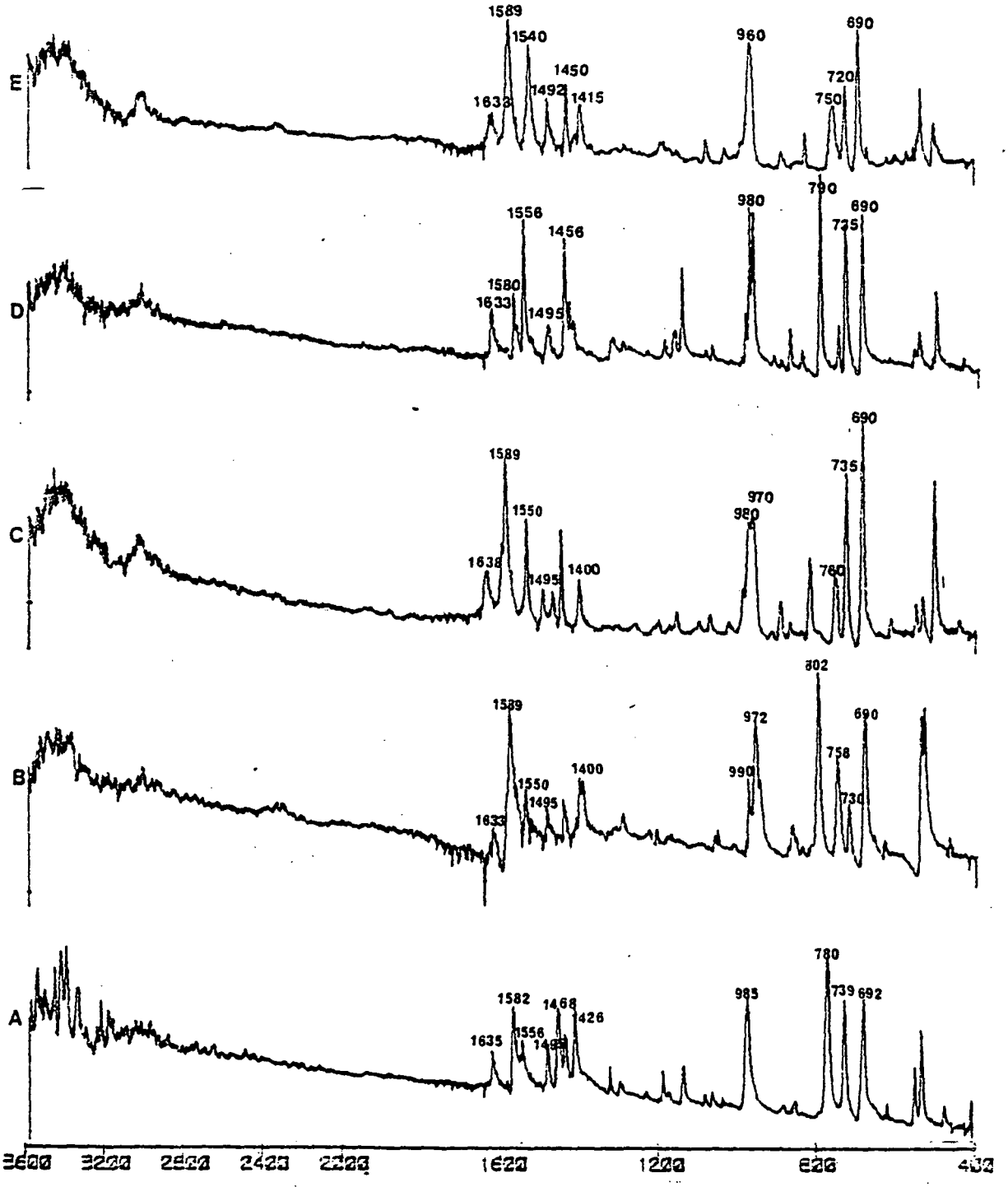

Figure 2. The IR spectrum of various styrylpyridines: (A) 2-SP, (B) 4-SP, (C) 2,4-DSP, (D) 2,6-DSP, and 2,4,6-TSP. (KBr pellet).

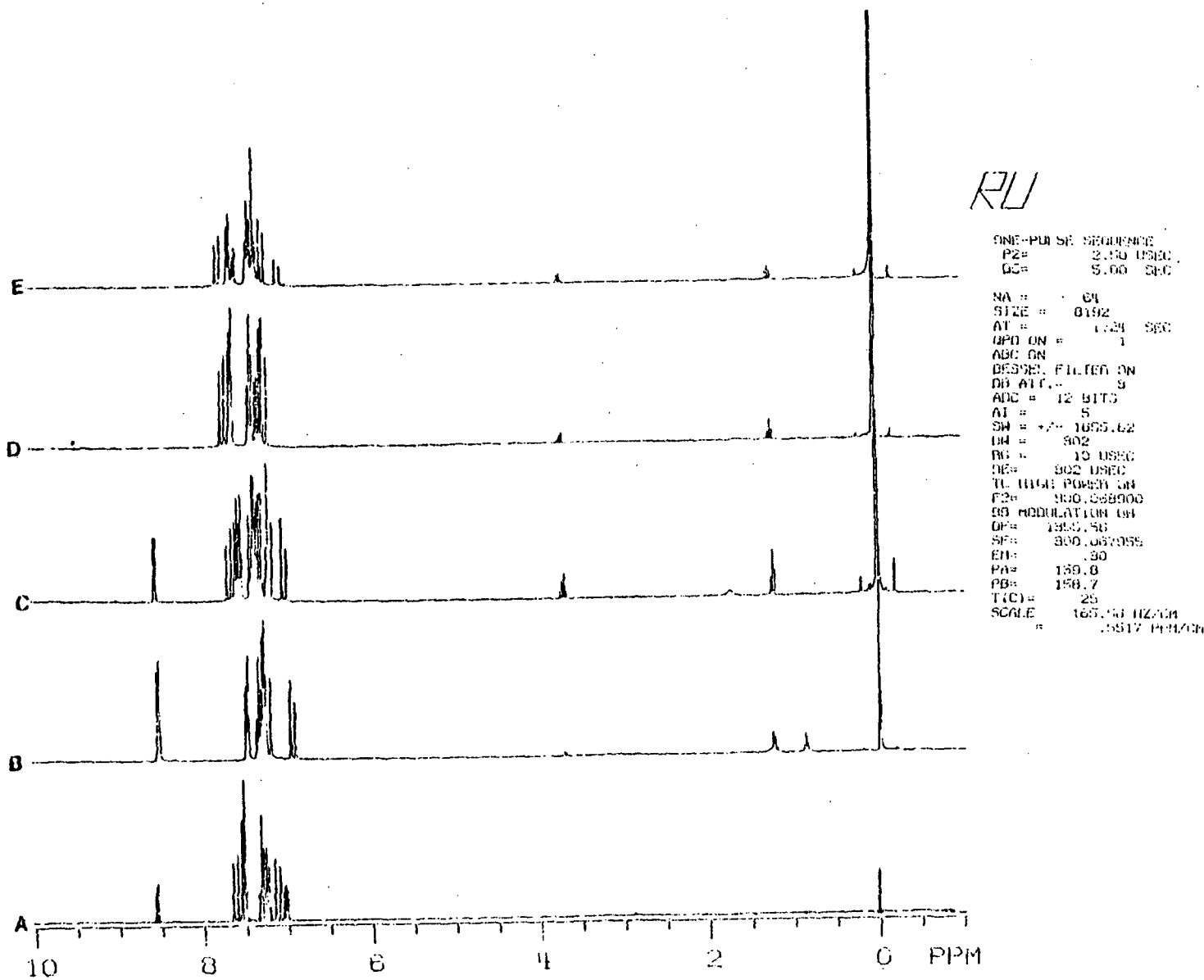

Fig. 3. H^1 NMR Spectra of (A) 2-SP, (B) 4-SP, (C) 2,4-DSP, (D) 2,6-DSP, and (E) 2,4,6-TSP in d-chloroform.

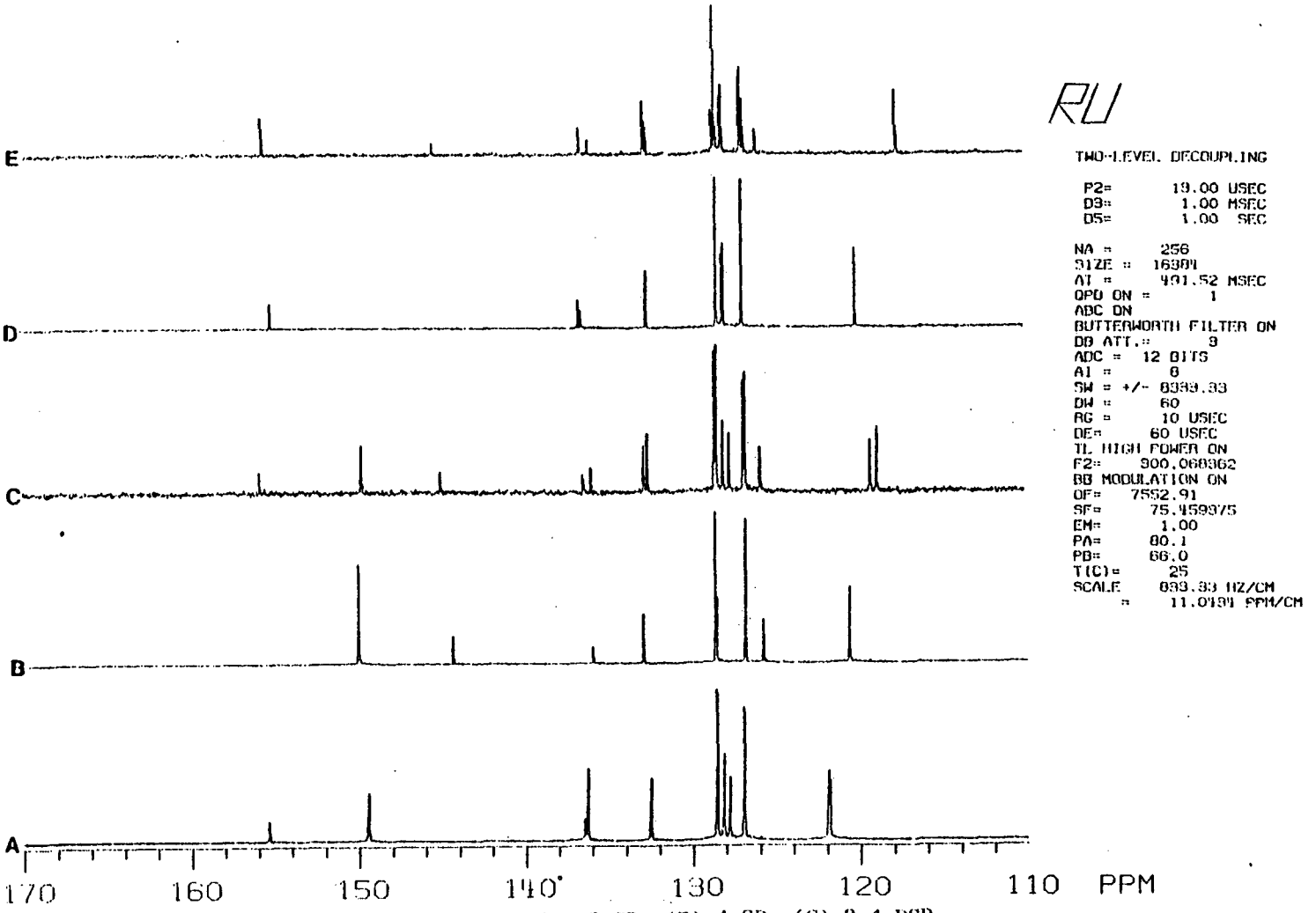

Fig. 4. C-13 NMR Spectra of (A) 2-SP, (B) 4-SP, (C) 2,4-DSP, (D) 2,6-DSP, and (E) 2,4,6-TSP in d-chloroform.

Table 2. The assignment of the IR spectrum for 2-SP, 4-Sp, 2,4-DSP, 2,6-DSP, and 2,4,6-TSP. KBr pellet.

vibration mode	wavelength (cm^{-1})				
	2-SP	4-SP	2,4-DSP	2,6-DSP	2,4,6-TSP
C=C stretching vibration of benzene	1635, 1510 1495	1638, 1550 1495, 1450	1638, 1537 1595, 1450	1633, 1556 1495, 1456	1633, 1492 1450
C=C stretching vibration of pyridine	1582, 1465, 1426	1589, 1420	1590, 1400	1580	1589, 1540 1415
C-H out-of-plane bending vibration of the hydrogen atom remaining on the ethylene	985	990, 972	970, 980	980	960
C-H out-of-plane bending vibration of the hydrogen atom remaining on the benzene (5 adjacent hydrogen)	780, 692	758, 690	760, 687	795, 690	750, 690
C-H out-of-plane bending vibration of the hydrogen atom remaining on the pyridine	739	730	735	735	720
C-H out-of-plane bending vibration of the hydrogen atom remaining on the benzene (2 adjacent hydrogen)		802			

turned dark brown (dark red for 4-picoline). A precipitate formed after neutralization with NaOH(pH=7) (Na_2CO_3 for 4-picoline). The greenish gray precipitate (pale yellow for 4-picoline) melted at 209-214 °C (269-272 °C for 4-picoline). Recrystallization from 95% ethanol (1 gram in 18 ml of ethanol) was followed by sublimation at 1 mm Hg and 200 °C[20]. The chemical and physical constants are listed in Table 1. UV, IR, and proton and carbon-13 NMR spectra are shown in Figs. 5, 6, 7, and 8, respectively. The assignment for each of the characterization peaks in the IR spectra are listed in Table 3.

(VIII) 2,4-di-(p-hydroxystyryl)pyridine (2,4-D(p-OH)SP)

(IX) 2,6-di-(p-hydroxystyryl)pyridine (2,6-D(p-OH)SP)

Formation of di-(p-acetoxystyryl)pyridine

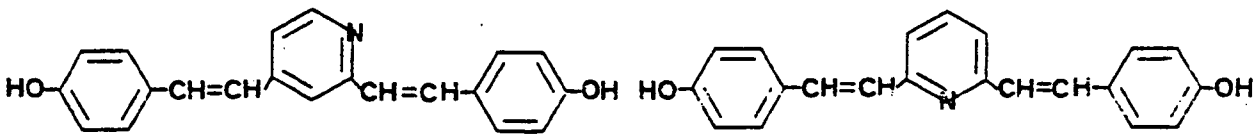

(VIII) (IX)

A mixture of lutidine (o.1 mole), p-hydroxybenzaldehyde (30.5 gram; 0.25 mole), and acetic anhydride (37.0 ml; 0.4 mole) was refluxed for 21 hours using an oil bath maintained at 155-160 °C in a nitrogen atmosphere to protect it from air. After 21 hours, the solution was poured into 600 ml of water and stirred for about 1 hour to remove the excess actic anhydride. A solid product was obtained by filtering, washing twice with water and recrystallizing from ethanol.

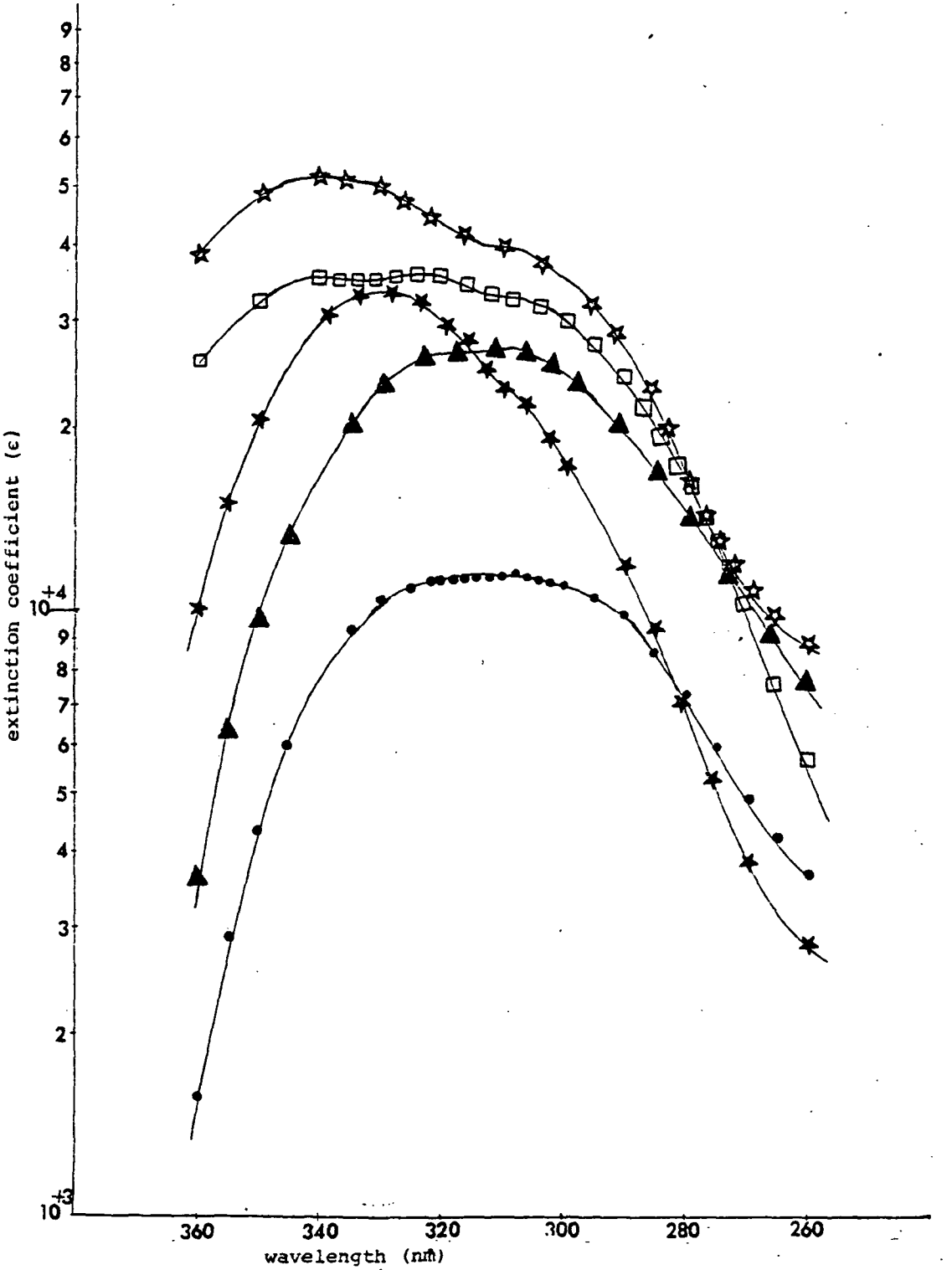

Figure 5. Ultraviolet spectra in methanol of ● 2-(p-OH)SP, ★ 4-(p-OH)SP, ☆ 2,4-D(p-OH)SP, □ 2,6-D(p-OH)SP, and ▲ 2,4,6-T(p-OH)SP.

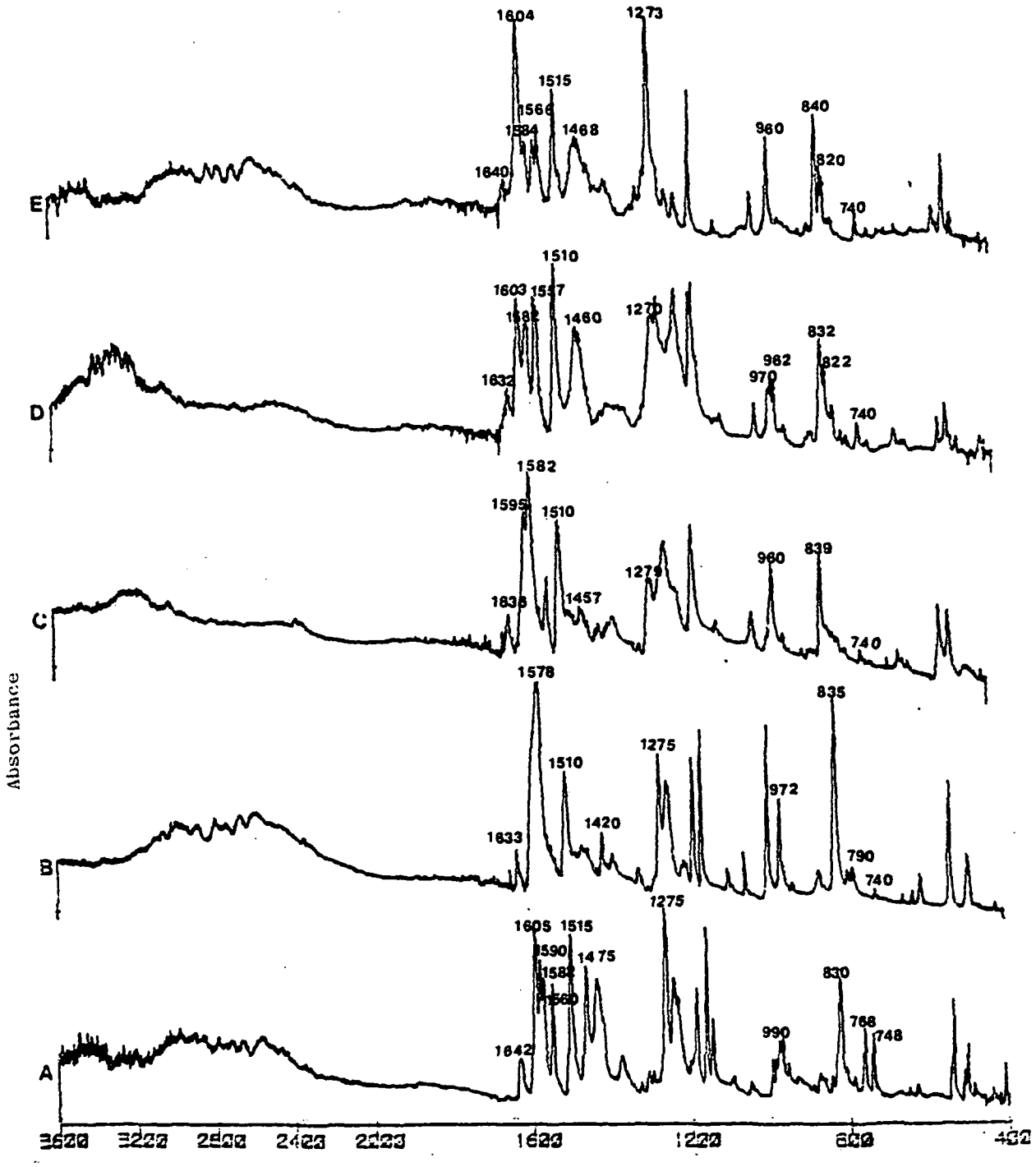

Figure 6. The IR spectrum of various components: (A) 2-(p-OH)SP, (B) 4-(p-OH)SP, (C) 2,4-D(p-OH)SP, (D) 2,6-D(p-OH)SP, and (E) 2,4,6-T(p-OH)SP. (KBr pellet)

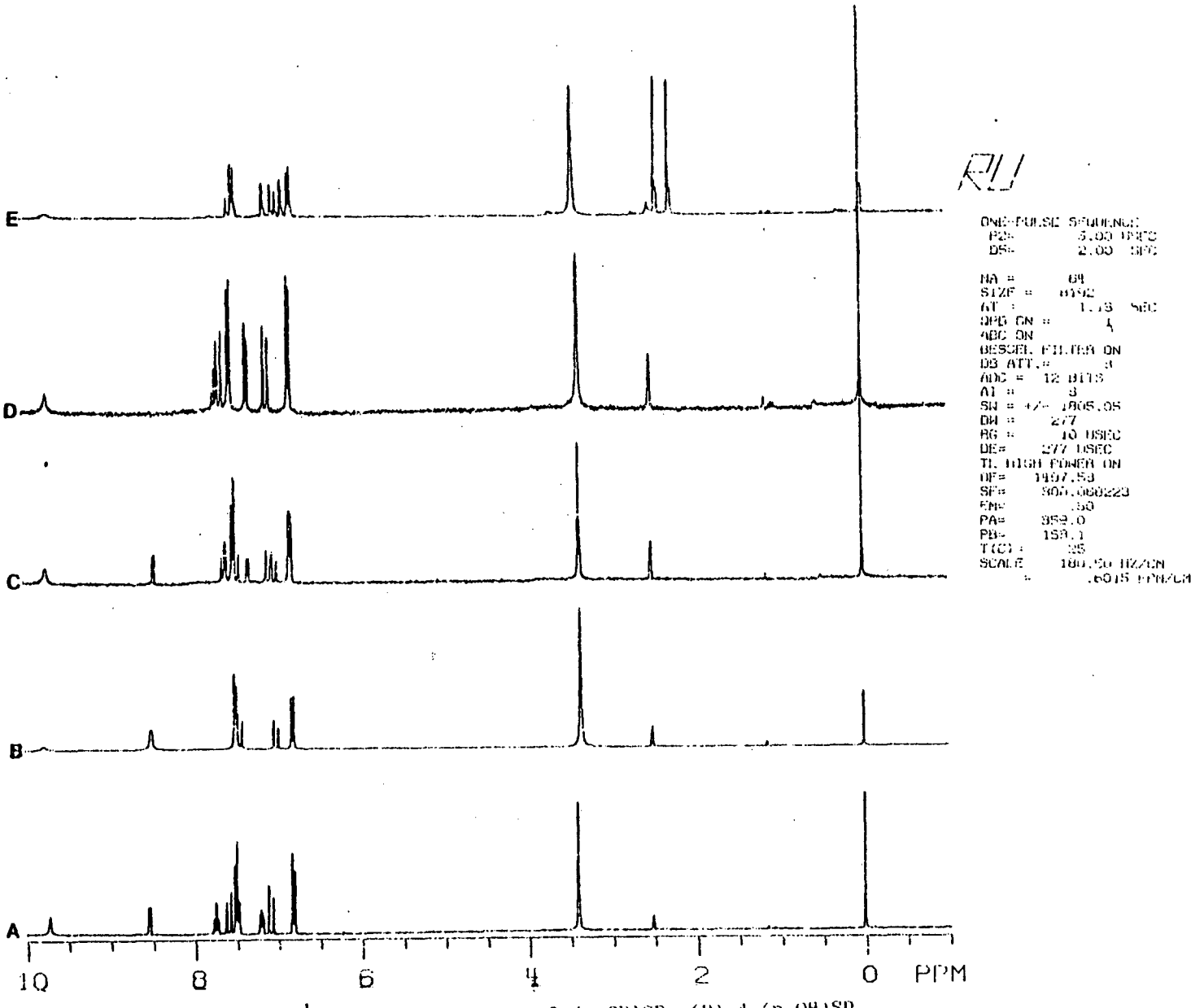

Fig. 7. H^1 NMR Spectra of (A) 2-(p-OH)SP, (B) 4-(p-OH)SP, (C) 2,4-D(p-OH)SP, (D) 2,6-D(p-OH)SP, and (E) 2,4,6-T(p-OH)SP in d-DMSO.

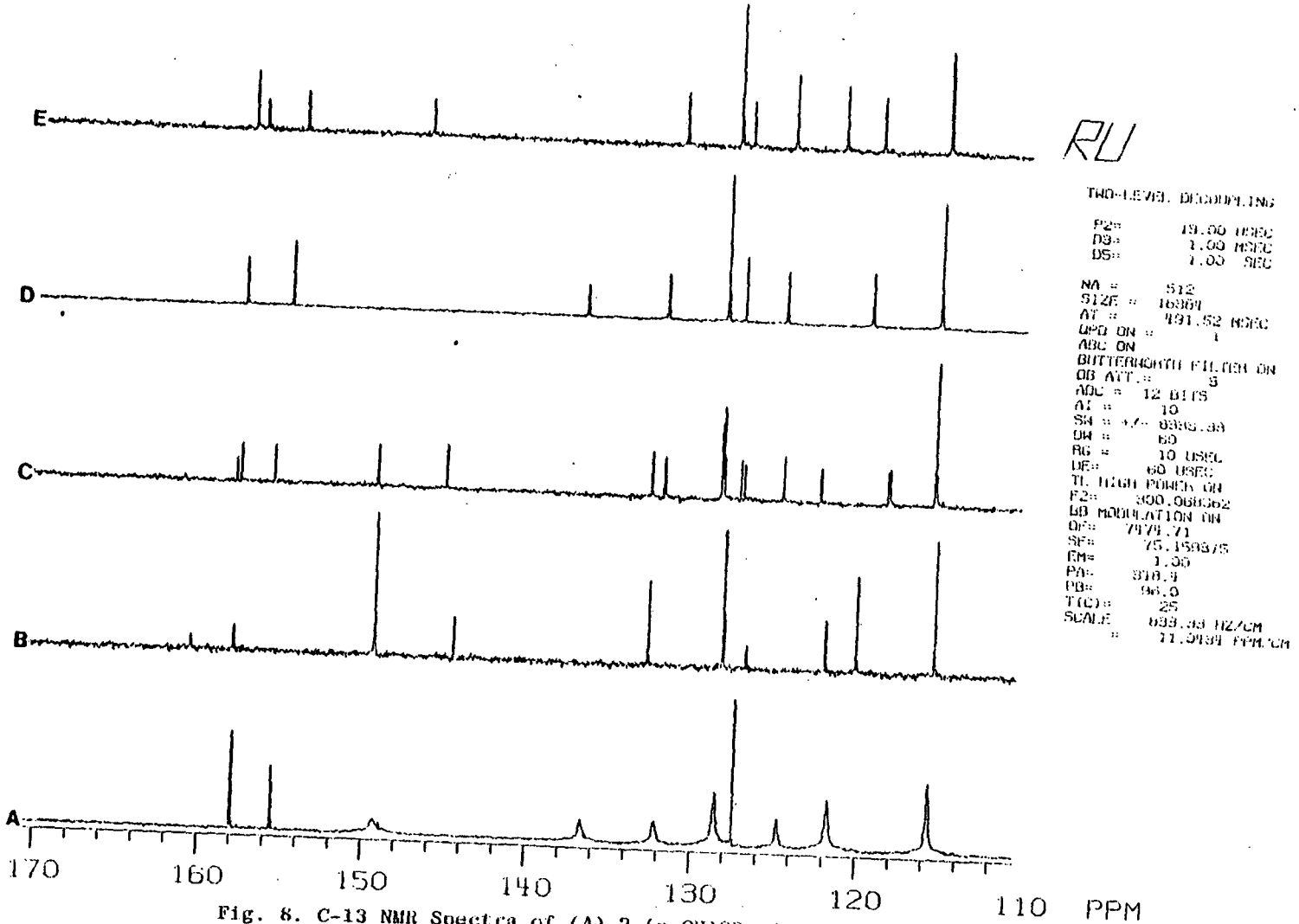

Fig. 8. C-13 NMR Spectra of (A) 2-(p-OH)SP, (B) 4-(p-OH)SP, (C) 2,4-D(p-OH)SP, (D) 2,6-D(p-OH)SP, and (E) 2,4,6-T(p-OH)SP in DMSO.

Table 3. The assignment of the IR spectrum for 2-(p-OH)SP, 4-(p-OH)SP, 2,4-D(p-OH)SP, 2,6-D(p-OH)SP, and 2,4,6-T(p-OH)SP. KBr pellet.

vibration mode	wavelength (cm^{-1})				
	2-(p-OH)SP	4-(p-OH)SP	2,4-D(p-OH)SP	2,6-D(p-OH)SP	2,4,6-T(p-OH)SP
C=C stretching vibration of benzene	1642, 1605 1515	1633, 1578 1510	1635, 1595 1578, 1510	1632, 1603 1557, 1510	1640, 1604 1557, 1515
C=C stretching vibration of pyriding	1590, 1582 1560, 1475	1420	1582, 1457	1582, 1562 1460	1584, 1566 1468
 -O	1275	1275	1279	1270	1273
C-H out-of-plane bending vibration of the hydrogen atom remaining on the ethylene	990, 980	972	960	970, 962 955	960
C-H out-of-plane bending vibration of the hydrogen atom remaining on the benzene	830, 768	835, 790,	839	832, 822	840, 820
C-H out-of-plane bending vibration of the hydrogen atom remaining on the pyridine	748	738	740	740	740

Formation of di-(p-hydroxystyryl)pyridine

A mixture of di(p-acetoxystyryl)pyridine (6.0 gram) was refluxed with o.75N alcoholic potassium hydroxide (60 ml) for 1.5 hours. The hydrochloride hydrate was obtained by adding hydrochloride acid and then recrystallized from water. Ten grams of di-(p-hydroxystyryl)pyridine hydrochloride hydrate were dissolved in 50 ml of 10% NaOH, resulting in a dark red solution; the solution was acidified with 50% acetic acid; the precipitate obtained was recrystallized from 95% ethanol. The chemical and physical constants are listed in Table 1. UV, IR, and proton and C-13 NMR spectra are shown in Figs. 5, 6, 7, and 8, respectively. The assignments for each of the characteristic peaks in the IR spectra are listed in Table 3.

(X) 2,4,6-tri-(p-hydroxystyryl)pyridine

(2,4,6-T-(p-OH)SP)

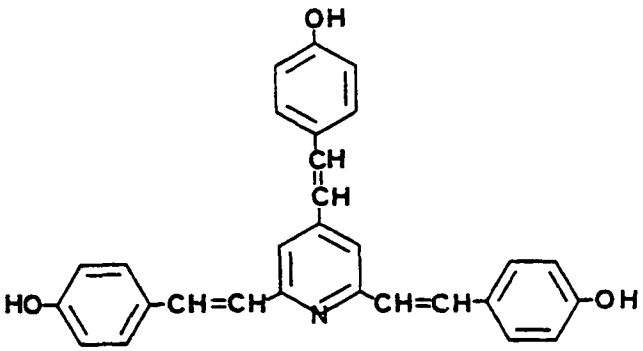

(X)

A mixture of collidine (0.2 mole), p-hydroxybenzaldehyde (0.9 mole), and $ZnCl_2$ (0.006 mole) was refluxed for 15 hours (175-180 ^{o}C) in a nitrogen atmosphere. After 15 hours, 200 ml of ethanol was added followed by dilution

with 20 ml of 0.2N HCl. The p-hydroxybenzaldehyde was removed by steam distillation. Thirty ml of 0.2N NaOH was added to make the solution basic. This was followed by steam distillation again to remove excess collidine. The viscous residue was extracted with ether and then evaporated. The solid product was dissolved in 20 ml of 0.1N NaOH solution, reprecipitated after acidification with 50% acetic acid, and recrystallied from 95% ethanol. The chemical and physical constants are listed in Table 1. UV, IR, and proton and C-13 NMR spectra are shown in Figs. 5, 6, 7, and 8, respectively. The assignments for each of the characteristic peaks in the IR are shown in Table 3.

II-C. Ultra-Violet Spectroscopic Studies

(a) Styrylpyridine and their derivatives

Ultra-violet absorption spectra of 1.0×10^{-5} to 1.0×10^{-6} M styrylpyridines and their derivatives in purified methanol[20] were obtained from a Beackman Acta III Spectrophotometer. The wavelengths of this photometer were calibrated with the absorption band from 360 mμ to 260 mμ of methanol.

(b) Kinetic study on the formation of 2-styrylpyridine and 4-styrylpyridine

A 500 ml three-neck-flask was fitted with a thermometer and a condenser with a drying tube. All the

equipment was dried and flushed with nitrogen for 10 minutes. Picoline (9.90 ml, 0.1 mole), benzaldehyde (203.3 ml, 2 mole), acetic acid (28.7 ml, 0.5 mole), and acetic anhydride (47.2 ml, 0.5 mole) was placed in the flask. The mixtures were heated at constant temperature by using an oil bath with a heat controller. The solution changed to light yellow in a few minutes and subsequently to dark brown. At various intervals, 5 ml of solution from the reaction vessel were pipetted into a 50 ml volumetric flask and diluted with methanol to 50 ml (solution A). Subsequently, 0.1 ml of solution A was pipetted into a 100 ml volumetric flask and diluted with methanol to 100 ml (solution B). The final concentration of solution for the various styrylpyridines was about 1.0×10^{-5} to 1.0×10^{-6} M. The UV spectrum of solution B was then taken and the absorbance of the spectral maximum of each styrylpyridine was measured (303 $m\mu$ for 4-styrylpyridine and 310 $m\mu$ for 2-styrylpyridine). This absorbance at different times (A_t) is proportional to the concentration of styrylpyridine at time t, since the system exhibits no absorbance at these wavelengths at t=0. In view of the large excess of the benzaldehyde reagent, the reaction may be assumed to be a first order reaction and, thus, the reaction rate can be obtained from a plot of

$$\ln \frac{A_\infty - A_t}{A_\infty - A_o}$$ again time (hours), were A is the maximum

absorbance of styrylpyridine at infinite time and can be calculated from the initial concentration of picoline. The results on reaction rate studies are shown in Figures 9 and 10, and Table 4.

(c) Yield study on the formation of 2,4-distyrylpyridine and 2,6-distyrylpyridine

The procedures were the same as those in II-C(b) except that almost equivalent weights of the starting materials were used. For example, lutidine (0.086 eq.), benzaldehyde (0.1030 eq., a slight excess), acetic acid (0.086 eq.), and acetic anhydride (0.086 eq.) were placed in the flask. The mixtures were heated at 130°C by using an oil bath with a heat controller. At various time intervals, the reaction solution was precipitated by adding water, and the product recrystallized from n-hexane The results of the distyrylpyridine yield formation are shown in Figure 11.

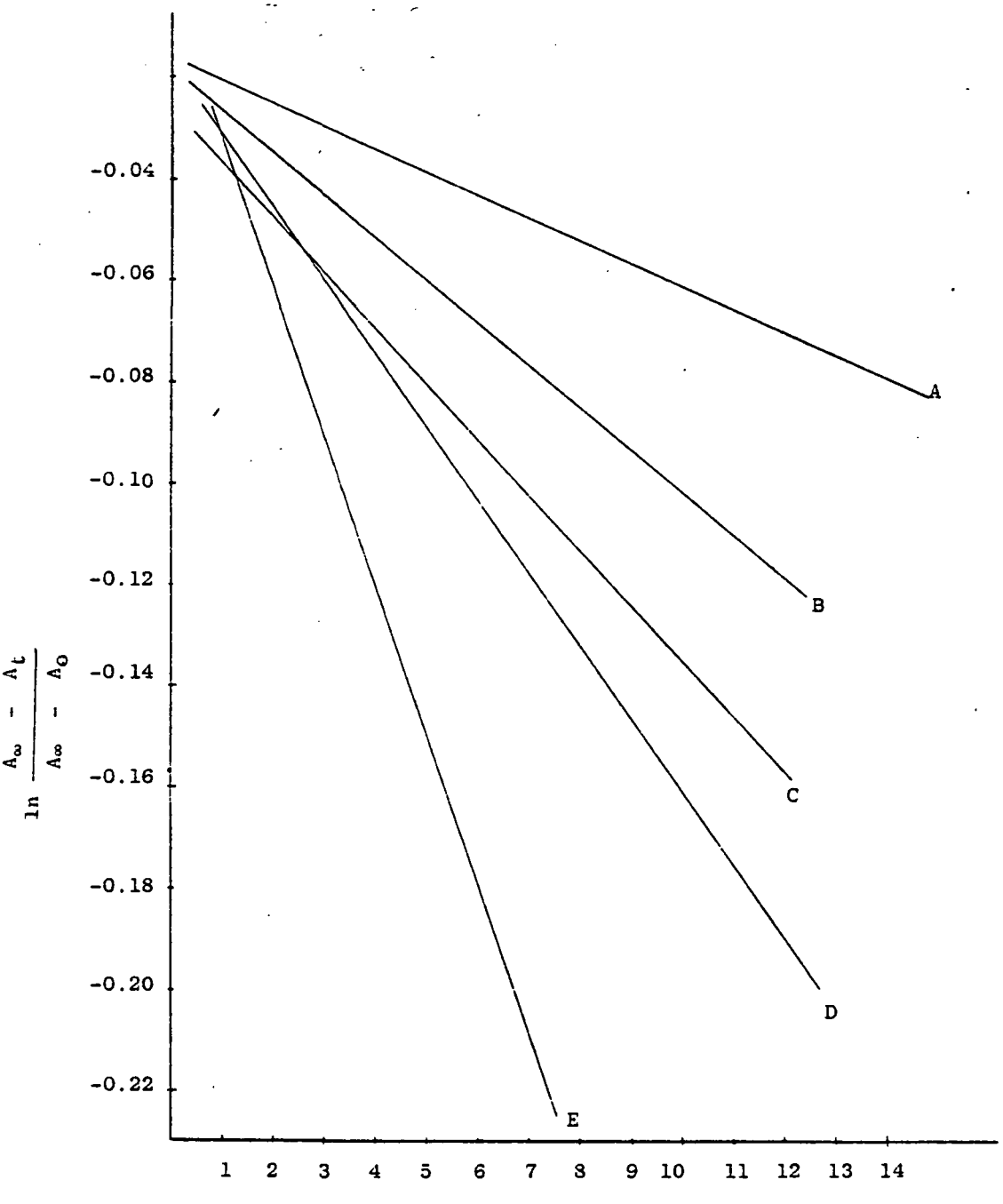

Fig. 9. Determination of the rate constant for the reaction of 2-picoline with excess benzaldehyde in acetic acid and acetic anhydride at various temperatures (A) 100°C, (B) 110°C, (C) 120°C, (D) 130°C, and (E) 145°C.

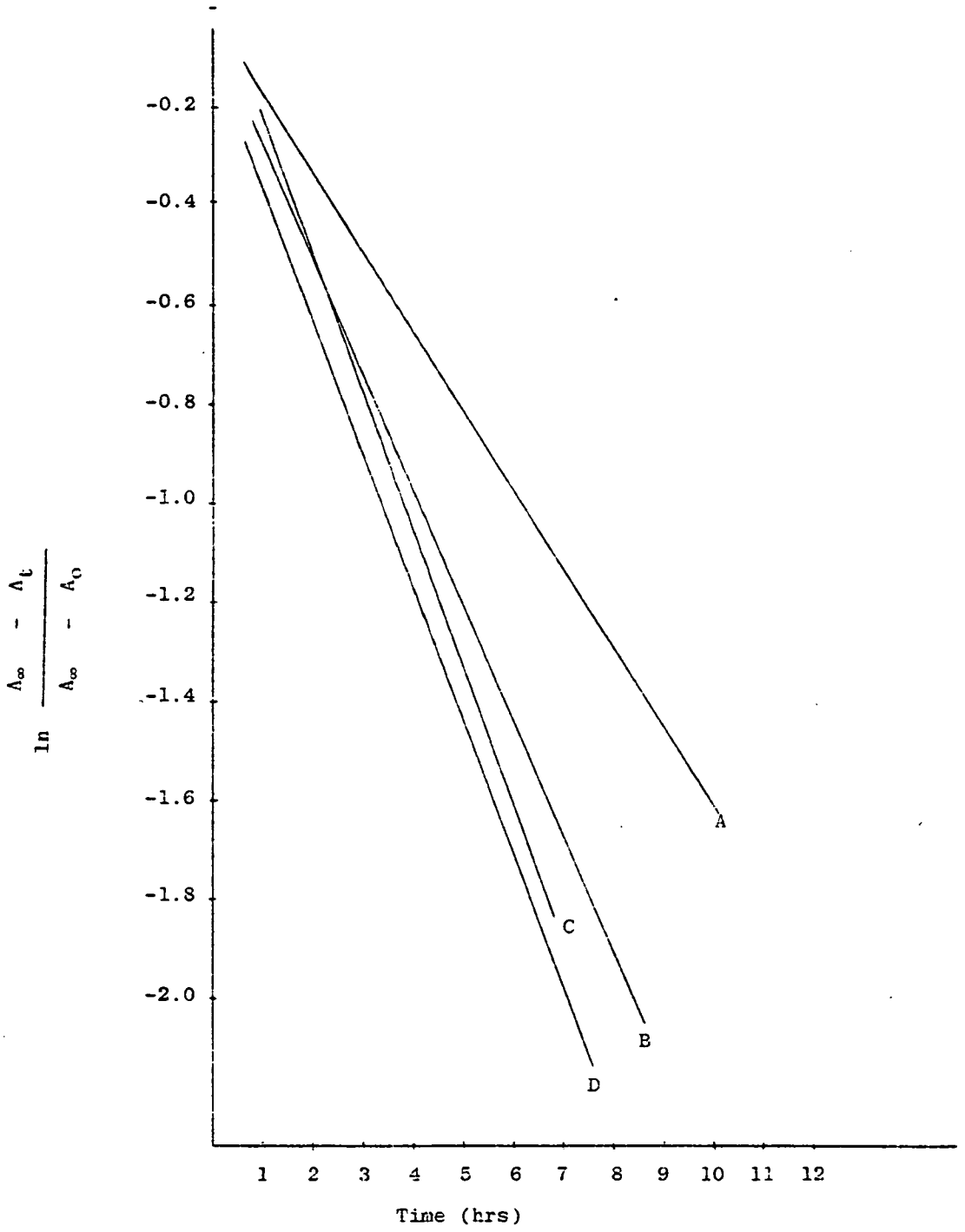

Fig. 10. Determination of the rate constant for the reaction of 4-picoline with excess benzaldehyde in acetic acid and acetic anhydride at various temperatures (A) 100°C, (B) 110°C, (C) 120°C and (D) 130°C.

Table 4. The rate constant for 2-picoline and 4-picoline at different temperatures.

	rate constant (sec^{-1})	
Temperature	2-picoline	4-picoline
145°C	8.47×10^{-6}	9.56×10^{-5}
130°C	5.64×10^{-6}	7.38×10^{-5}
120°C	4.30×10^{-6}	6.22×10^{-5}
110°C	3.11×10^{-6}	6.57×10^{-5}
100°C	1.25×10^{-6}	4.44×10^{-5}

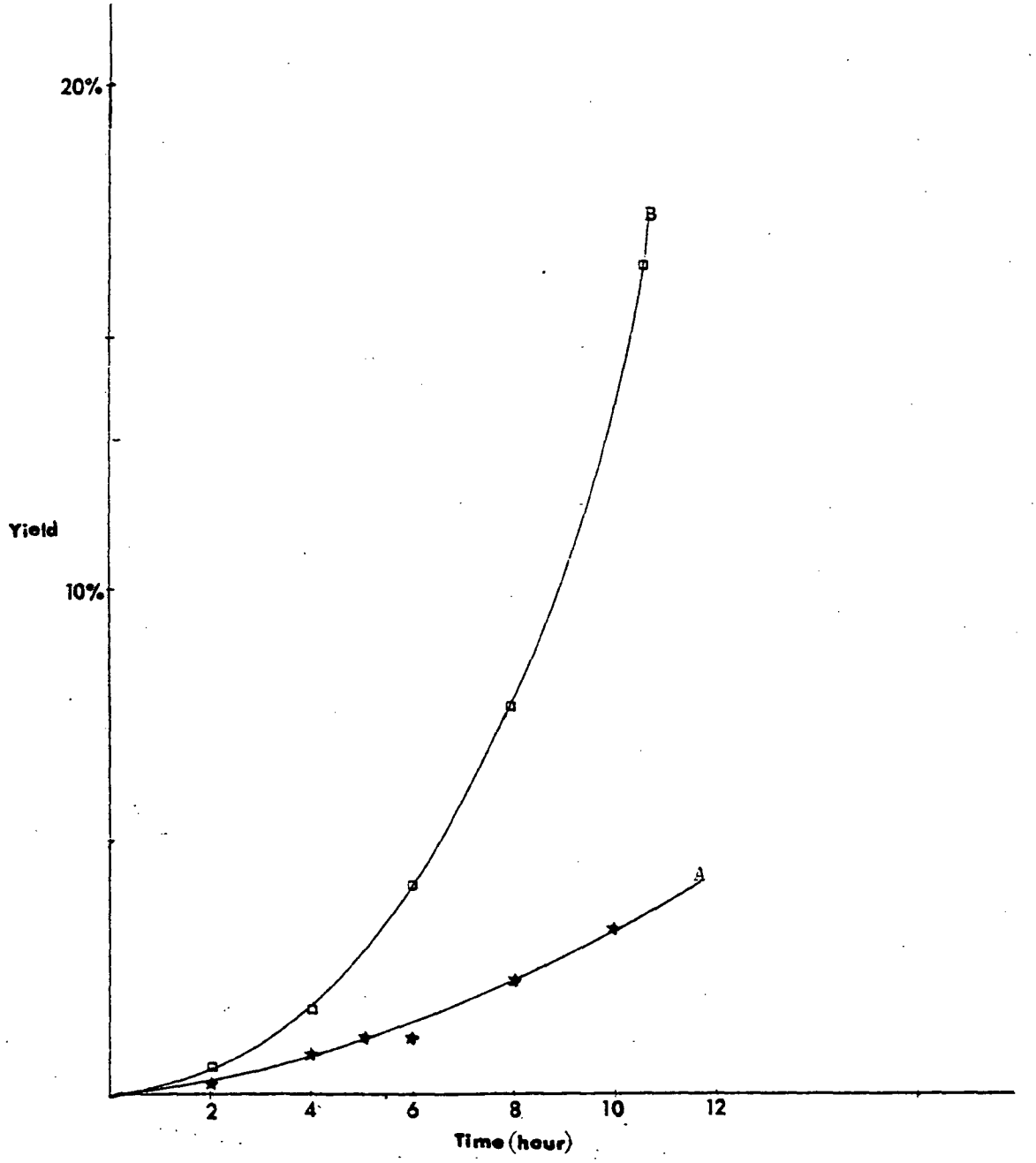

Figure 11. Yield percentage of (A) 2,4DSP, and (B) 2,6DSP (isolated from condensation reaction).

Continued from Fig. 11.

Yield percentage of 2,4-DSP and 2,6-DSP.
(The products were isolated from condensation reaction).

component %yield time	2,4-DSP	2,6-DSP
2 hr	0.12	0.17
4 hr	0.78	1.66
6 hr	1.02	4.12
8 hr	2.27	7.66
10 hr	3.25	16.46

III. RESULTSNAND DISCUSSION

A. Ultra-Violet Spectroscopy

Pure compouds of the methyl pyridine series are particularly diffcult to prepare, partly for the following reasons: (1) there are no conventient synthestic methods[21], (2) they have similar boiling points and (3) they are difficult to free from water. Purvis[22], at an earlier date, had commented upon the large number of near coincidences in the wavelengths of bands in pyridine and picoline. Kohlrausch[23] showed that a 3-picoline sample contained 2,6-lutidine even after extensive treatment. Therefore, for this study the purity of the samples was established by freezing point[24], followed by vacuum distillation. Figs. 12, 13, and 14 show the UV spectra of pyridine, 2-picoline and 2,6-lutidine in H_2O, 0.2N H_2SO_4, 0.1N NaOH and a mixture of acetic acid and acetic anhydride in methanol. There was no particular shift in the position of the maximum wavelength in the different solvents for each component as Herington had reported[21]. However there was a small shift in the position of the main peak at 290 mμ to longer wavelengths due to the different methyl positions on the pyridine ring, in the order, pyridine> 2-picoline> 2,6-lutidine. Brown and Barbaras[25] have discussed the relationship between structure and basicity in the methyl pyridine series pointing out that inductive effects and resonance

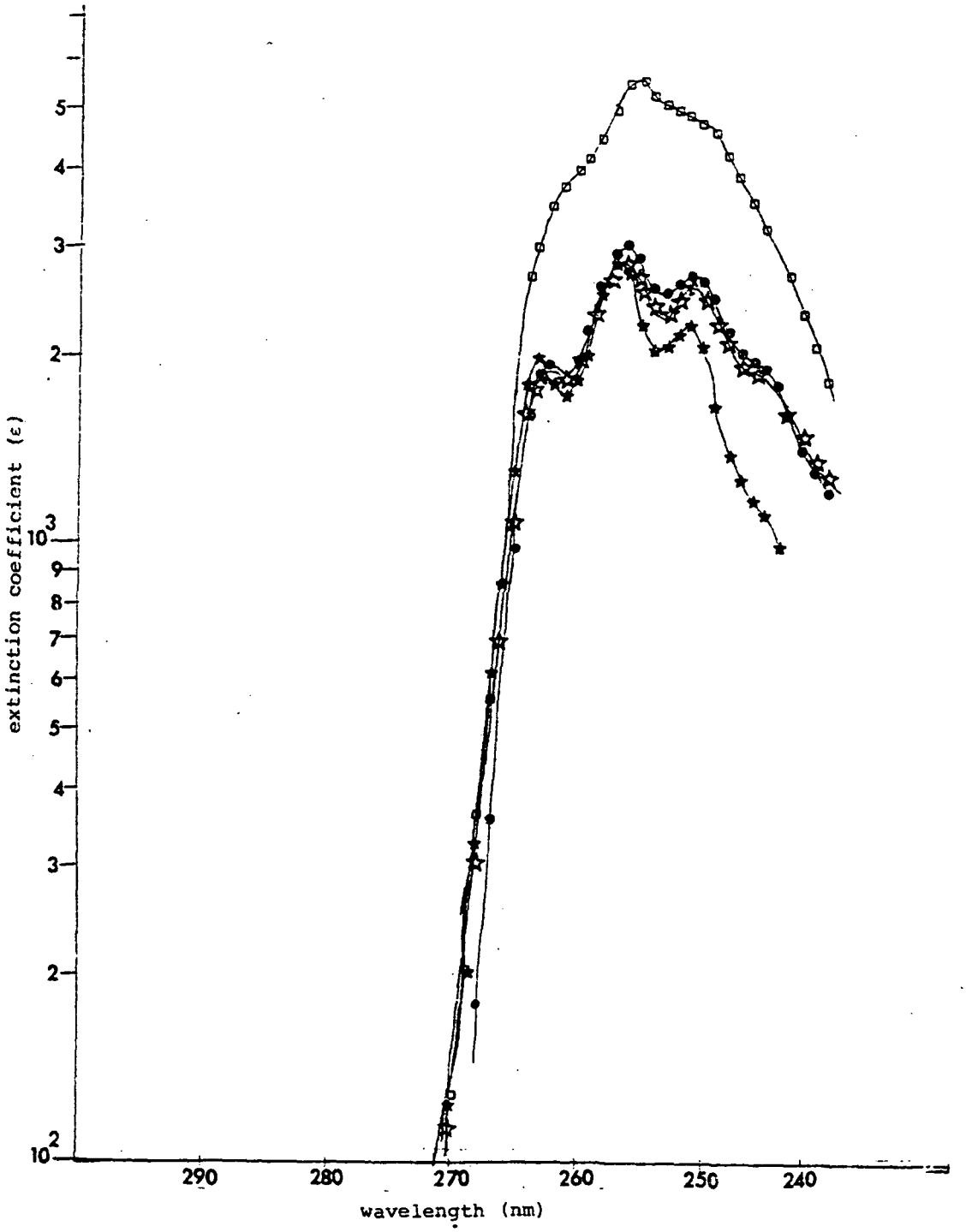

Figure 12. Ultraviolet spectra of pyridine in different solutions: ● H_2O, ▫ 0.1N H_2SO_4, ✯ 0.1N NaOH, and ★ acetic acid and acetic anhydride in methanol.

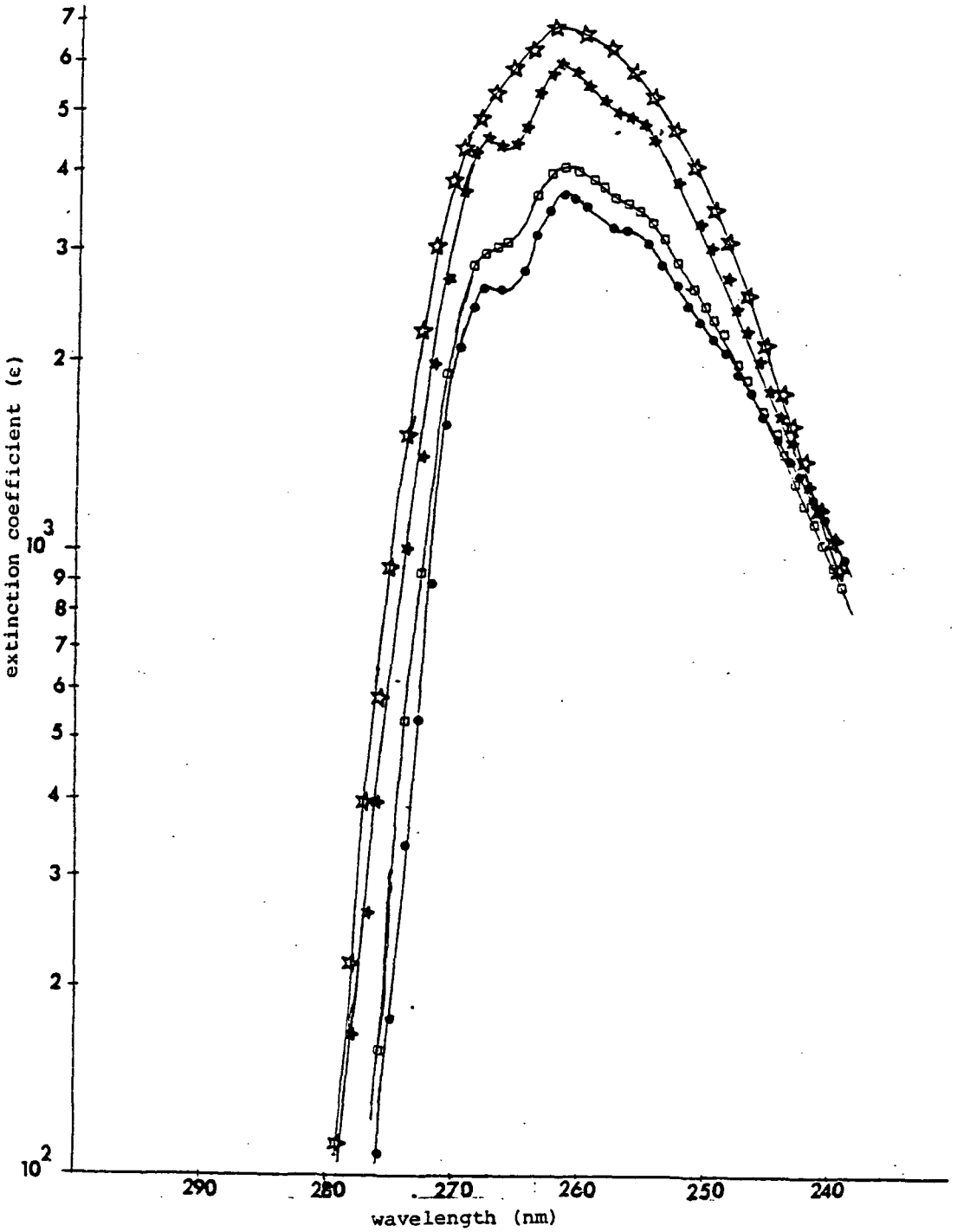

Figure 13. Ultraviolet spectra of 2-picoline in different solutions: ▫ H_2O ☆ 0.1N H_2SO_4, ● 0.1N NaOH, and ★ a mixture of acetic acid and acetic anhydride in methanol.

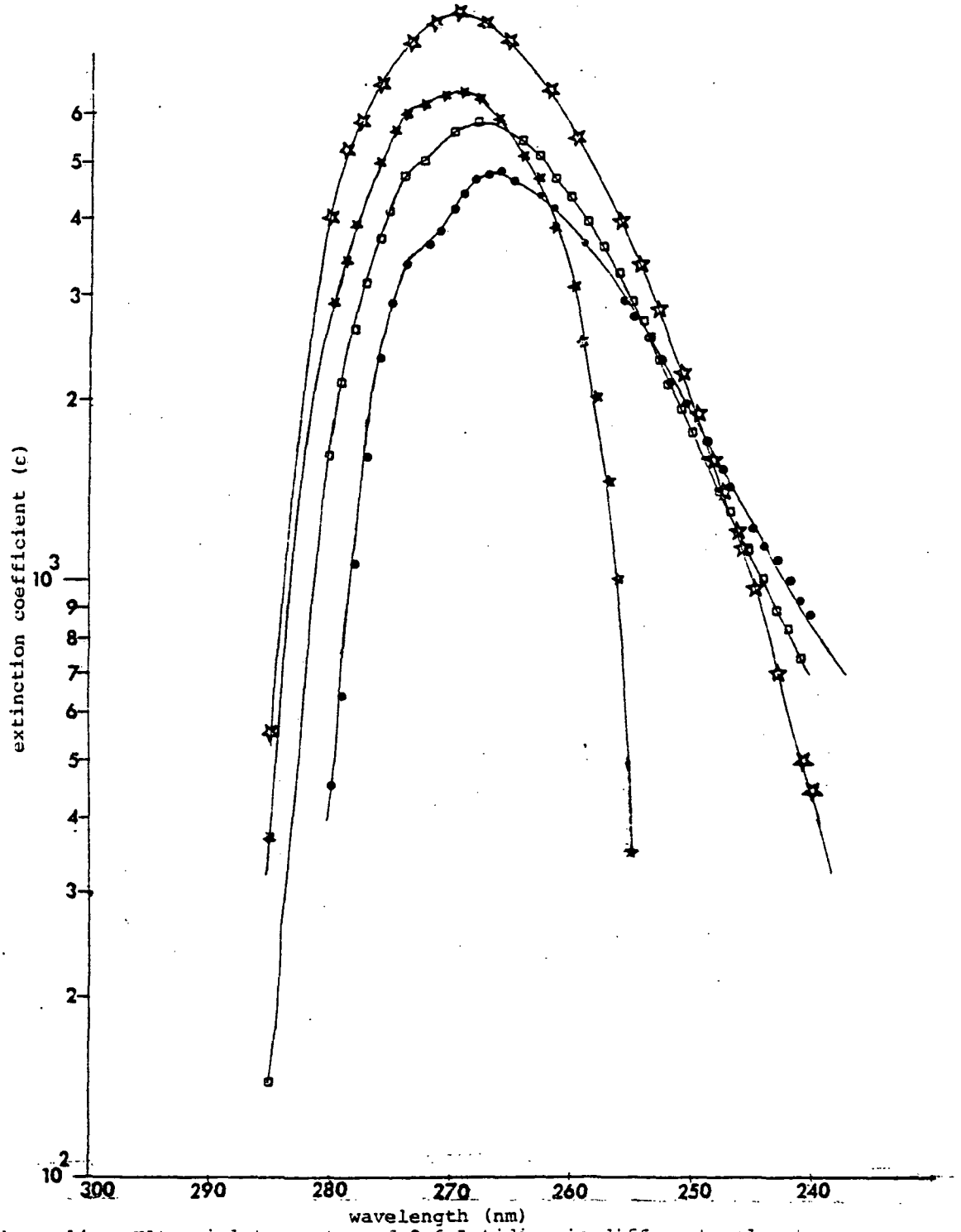

Figure 14. Ultraviolet spectra of 2,6 Lutidine in different solvents: ▫ H_2O, ✯ 0.1N H_2SO_4, • 0.1N NaOH, and ★ acetic acid and acetic anhydride in methanol.

effects will change the relative base strengths of the methyl pyridines. Therefore, inductive and resonance effects increasing electron density on the nitrogen atom, and causing $\pi \longrightarrow \pi^*$ (or $n \longrightarrow \pi^*$) transitions, result in this shift to longer wavelength.

It is well known that increasing the number of benzene rings (chromophoric groups) in a molecule shifts the position of maximum wavelength if the additional chromophoric groups are conjugated with the initial absorbing system[26]. In the case of our pyridine derivatives, one absorption maximum of 2,4-di-(p-styryl)pyridine (2,4-DSP), 2,6-di(p-styryl)pyridine (2,6-DSP), and 2,4,6-tri-(p-styryl)pyridine (2,4,6-TSP) was at the same wavelength as the 2-styrylpyridine (2-SP) and 4-styrylpyridine (4-SP) as shown in Fig. 1. In 2,4-DSP and 2,6-DSP, a second absorption peak was observed: a principal band occured at 290 m_μ for both compounds and a subsidiary band which occurred at 310 m_μ and 355 m_μ , respectively, associated with forms in which there is increased or decreased electron density on the nitrogen atom and a positive ornegative charge delocalized over the remaining portion of the molecule. This is illustrated below:

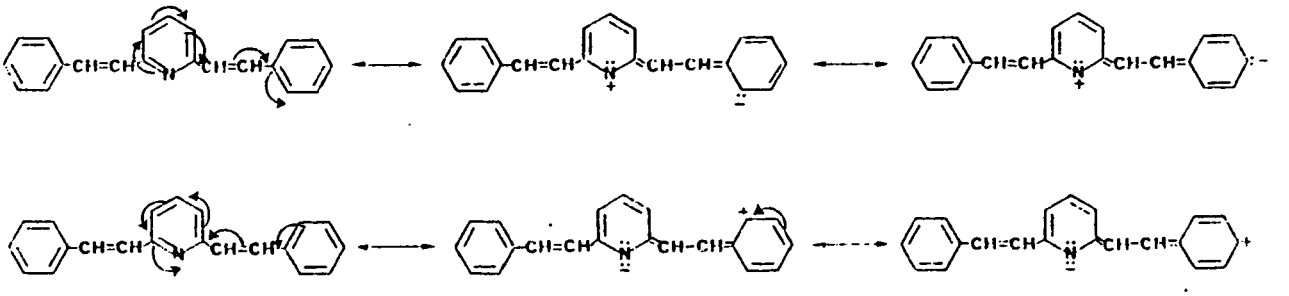

The role of subsitituents and their effect on charge distribution can be seen from the position of the maxima absorption for 2-(p-hydroxystyryl)pyridine (2-(p-OH)SP), 4-(p-hydroxystyryl)pyridine (4-(p-OH)SP), 2,4-di-(p-hydroxystyryl)pyridine (2,4-D(p-OH)SP, 2,6-di-(p-hydroxystyryl)pyridine (2,6-D(p-OH)SP), and 2,4,6-tri-(p-hydroxystyryl)pyridine (2,4,6-T(p-OH)SP). These compounds show maximum absorption at 325 ± 10 mμ (Fig. 5). The shift of the maximum wavelength toward longer wavelength compared with the unsubstituted styrylpyridine may be attributed to both an increase in the number of resonance structures of the absorbing system and the increased charge separation due to electron donating properties of the hydroxyl group and electron accepting properties of the nitrogen atom. This is illustrated below:

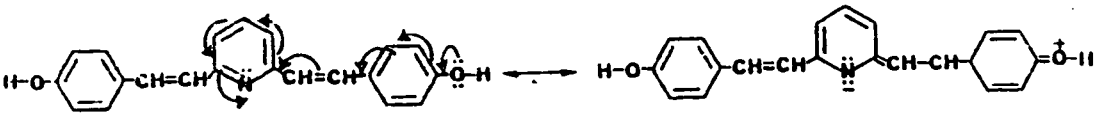

B. Kinetic Study

Although the mechanism of the condensation of picoline methiodides with aromatic aldehyde (eq. 1) has been reported by A. P. Phillips[9], Knoevengel[27] claimed that active hydrogen in 2-picoline can be removed by a base, followed by condensation with aldehydes usually not containing an α-hydrogen. In the presence of acetic acid and acetic anhydride solution, the acitve hydrogen in 2-picoline cannot be removed by an acid catalyst. Therefore, summarizing these two proposals, a resonable reaction sequence is shown below:

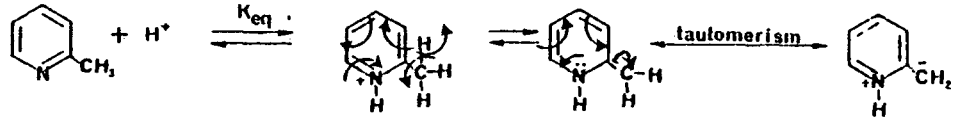

eq. 2

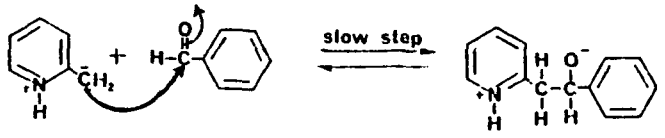

eq. 3

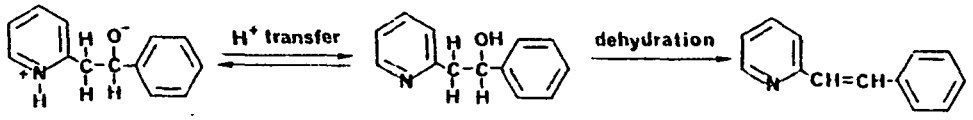

eq. 4

In acidic medium dehydration of the intermediate was faster than its formation, so the rate determining step is the formation of the intermediate shown in eq. 3[28].

The rate for equation 3 can be expressed by

rate = k (benzaldehyde)(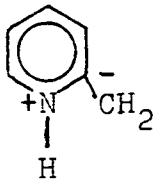), and the

eequilibrium constant for equation 2,

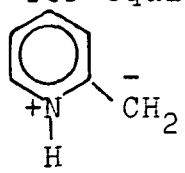

$$K_{eq} = \frac{\text{(picoline) (H}^+\text{)}}{}$$, and thus

$$\text{rate} = k\, K_{eq}\, \text{(picoline) (H}^+\text{) (benzaldehyde)} \quad \text{---- eq. 5}$$

Since the acid catalyst is not consumed and benzaldehyde was used in twenty-fold excess during the entire reaction, the concentrations of benzaldehyde and acetic acid can be considered constant, and the rate coefficient can be rewritten to give

$$k' = k\, K_{eq}\, \text{(H+) (benzaldehyde)}$$

Thus, the rate law was simplifed to

$$\text{rate} = \frac{d(\text{picoline})}{dt} = -k' \text{ (picoline)} \quad \text{------ eq. 6}$$

Since this is a pseudo-first-order rate law, eq. 6 could be intergrated directly. Noting the concentration of $(\text{picoline})_o$ at t=0 and at a subsequent time, $(\text{picoline})_t$, then

$$-\{\ln (\text{picoline})_t - \ln (\text{picoline})_o\} = k' t.$$

The concentration of picoline at time t can be measured from the difference between the ultraviolet absorbance of

2-styrylpyridine at time t and infinite time t_∞ . Therefore, the apparent activation energy refers to k' rather than to k, and k' contains K_{eq} and k.

The equilibrium constant (K_{eq}) is a function of temperature. In order to obtain the activation energy for 2-styrylpyridine and 4-styrylpyridine, equation 6 was simplified bt assuming that the equilibrium constant is independent of temperature because of the relatively small differences in reaction temperatures used in our study ($100^{o}$to 145^{o}). The activation energy E_a from

$$k' = A \exp(-E_a/RT) \text{ ----------eq. 7}$$

was determined by a plot of log k' vs 1/T (Fig. 15). From Table 5, it can be seen that the rate of the 4-picoline reaction with benzaldehyde was faster than the corresponding 2-picoline under the same conditions. The increase of the rate of 4-picoline as compared to 2-picoline is also characterized by a decrease in the activation energy (Table 5) due to increased inductive effects. This may arise not only from ionic charges but also from the action of dipoles within the reacting molecules[29]. Electron shifts associated with inductive effects of 2-picoline and 4-picoline may be represented as:

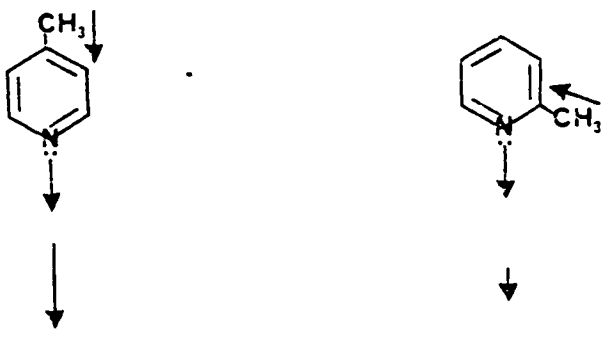

total
inductive
effect

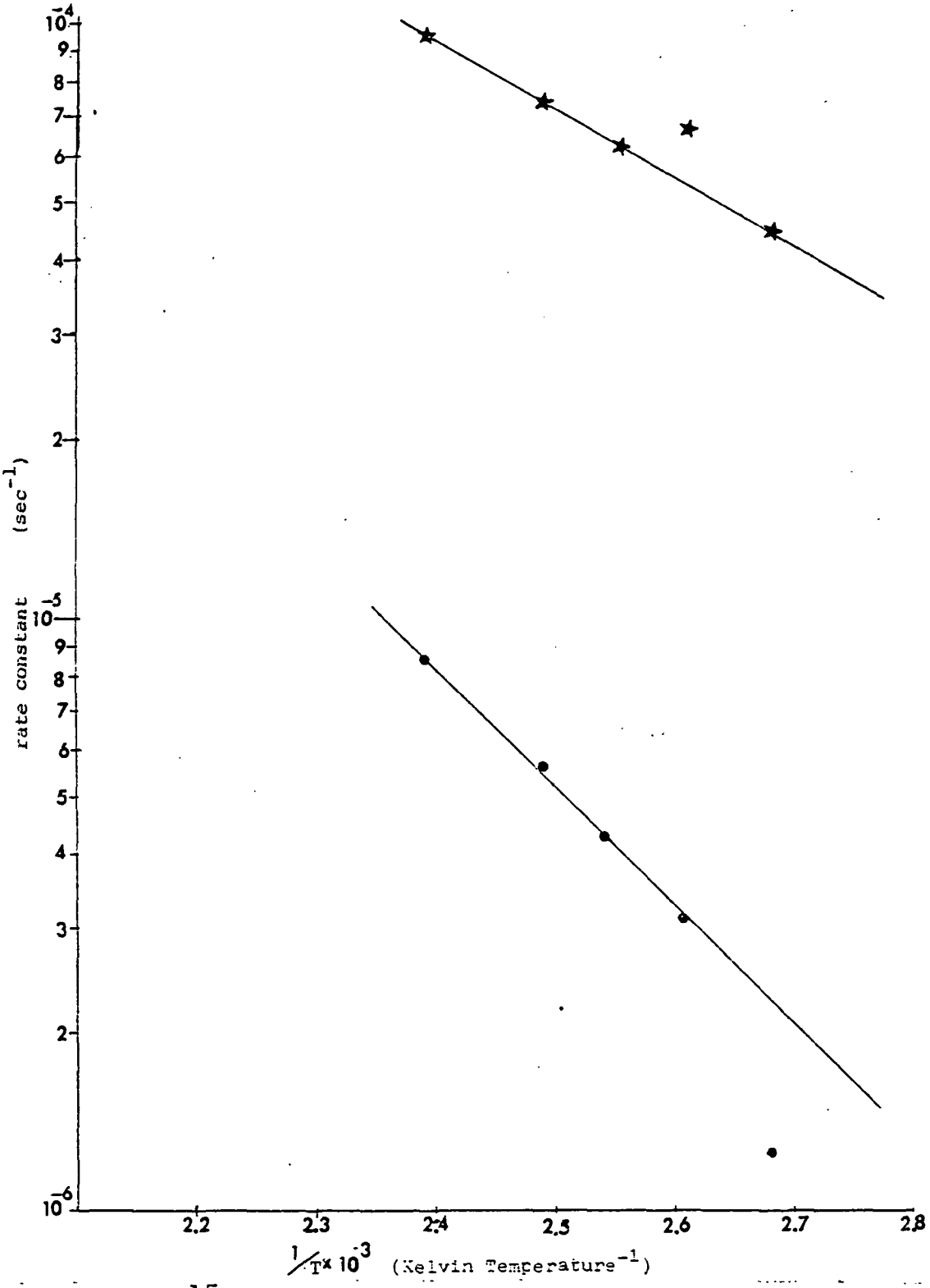

Figure 15. Ln of the rate constant for the condensation reaction of (A) 2-picoline, (5) 4-picoline with the excess benzaldehyde in acetic annydride as a function of 1/T.

Table 5. The acivation energy for the condensation reaction of the different picolines with excess benzaldehyde in acetic anhydride.

	2-picoline	4-picoline
activation energy	34.14KJ/mole	20.38 KJ/mole

Therefore, the total positive inductive effects of the 4-picoline molecule is greater than of the 2-picoline. Hence, the 4-picoline will facilitate the removal of the H^+ ion from the methyl group or hinder its return to the methyl group. This allows the intermediate to form quite readily.

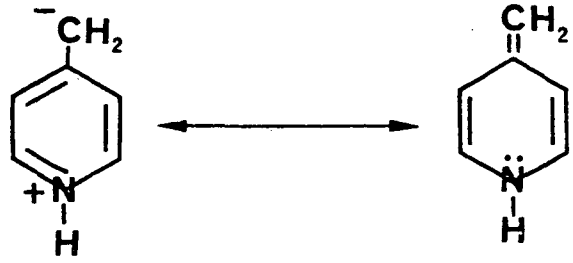

The yield of distyrylpyridine under the same reaction conditions was 2,6-DSP> 2,4-DSP (see Fig. 11). The upward curvature of the plots is expected since monostyrylpyridine has to be found before the distyryl derivative. Applying the inductive effect explanation to predict the yields of 2,4-DSP and 2,6-DSP, the order should be 2,4-DSP > 2,6-DSP because the 4-picoline on the pyridine ring was more reactive than the 2-position. However, the results were opposite to this. A possible explanation may be that the negative inductive effect of styryl (-C=C- 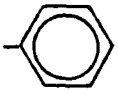) in the 4-position. Further reaction of the intermediates may also provide an explanation of the experimantal results.

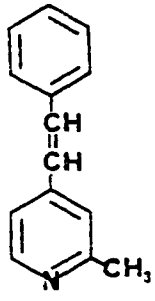

2-methyl-4-styrylpyridine

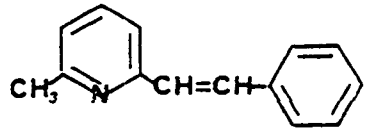

2-methyl-6-styrylpyridine

There was only one possible way to form the intermediate of 2,4-lutidine, while the intermediate of 2,6-lutidine may be formed in two ways. The styryl group could act as an electron withdrawing group (negative inductive effect), making it difficult to remove the H^+ ion from the methyl group for the next condensation. On this basis, the order of di-styrylpyridine yield would be 2,6-DSP> 2,4-DSP.

C. The Thermal Analysis Study of Various Styrylpyridine

The chemical bonds in the backbone of the molecule have certain bond energies which can be calculated from their corresponding dissociation energies, because the thermal stability of the molecule is related to the dissociation energies of the various bonds. Several factors may contribute to bond energies:

1. Secondary or Van der Waals bonding forces, which determine the cohesion or the forces of attraction between the chain molecules.

2. The resonance stabilization of certain cyclic structures such as benzene, pyridine, naphthalene, etc.

3. The type of reaction which occurs after bond cleavage. If the activation energy of the next reaction step is high, recombination may occur.

Therefore, bond strength (bond energy) can serve as a guide for the synthesis of polymers of high thermal stability.

The thermogravimetric analyses of various styrylpyridine compounds under nitrogen are shown in Figs. 14 and 15. The weight loss and decomposition temperature increased as the number of conjugated double bonds and phenyl groups increased. This can be explained by resonance stabilization which also was confirmed by van Krevelen's suggestion[30] that phenyl groups and double bonds contribute to char-formation tendency(CFT). Also, for the styrylpyridine system, Diels-Alder reactions may occur during thermal degradation, resulting in the formation of highly-crosslinked char. The 2,6-DSP has a greater tendency to form a highly crosslinked char than 2-SP because 2,6-DSP behaves as if it were "polymerized" through the Diels-Alder reaction between the double bond and another molecule containing the pyridine group. Hydroxystyrylpyridine showed increased Diels-Alder reaction when compared to unsubstituted styrylpyridines. This indicated that the hydroxy group promotoed the Diels-Alder reaction ("polymerized") of these derivative styrylpyridine.

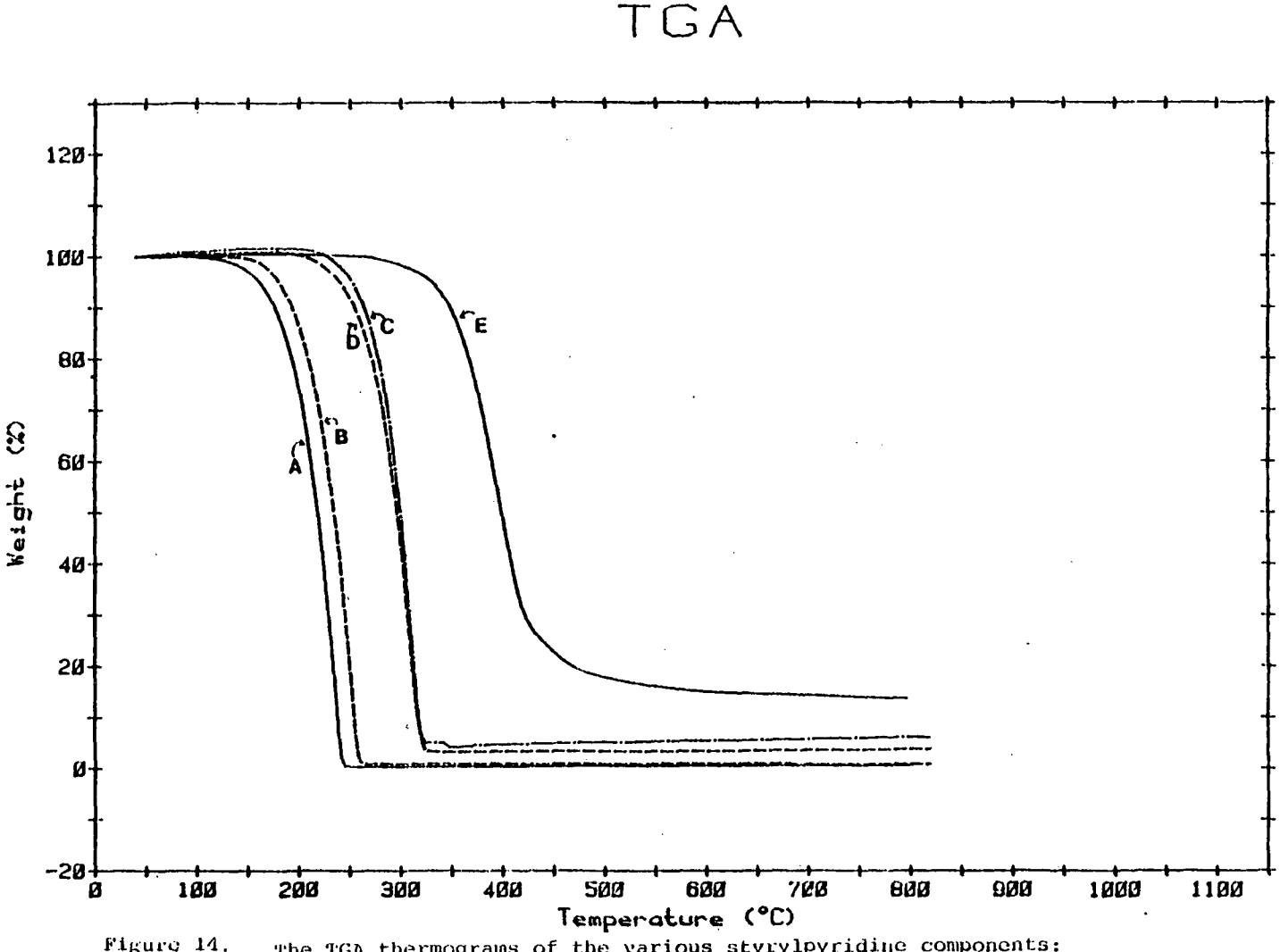

Figure 14. The TGA thermograms of the various styrylpyridine components: (A) 2SP, (B) 4SP, (C) 2,4DSP, (D) 2,6DSP, and (E) 2,4,6TSP at ATM: N_2 (flow rate 0.5 LPM) and heating rate: 20°C/min.

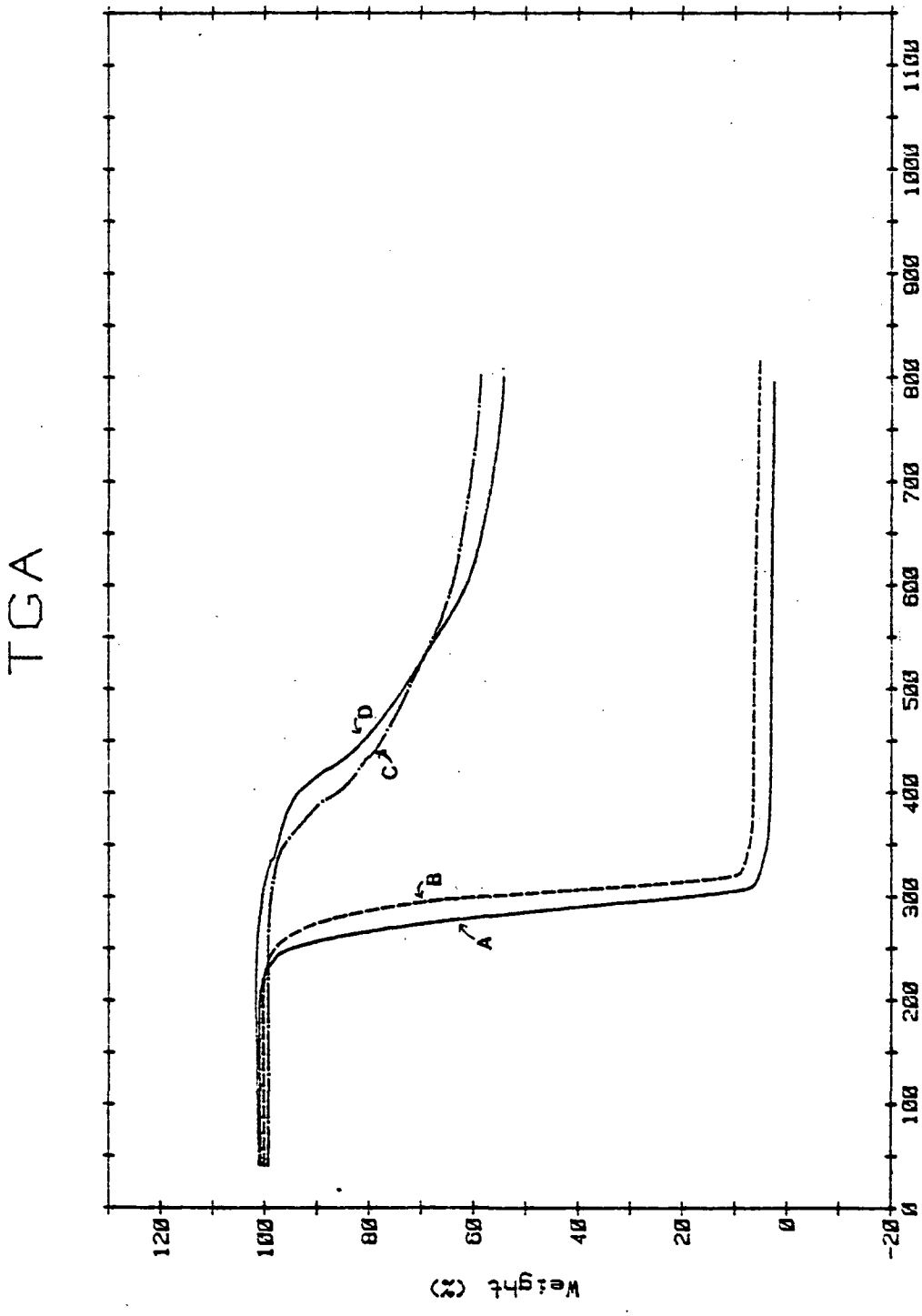

Figure 15. The TGA thermograms of the various hydroxystyrylpyridine components: (A) 2-(p-OH)SP, (B) 4-(p-OH)SP, (C) 2,4-D(p-OH)SP, and (D) 2,6-D(p-OH)SP, ATM : N_2 (flow rate 0.5 LPM) and heating rate : 20 °C/min.

IV. CONCLUSION

The mechanism of the reaction of methyl pyridine with benzaldehyde involves the transition state:

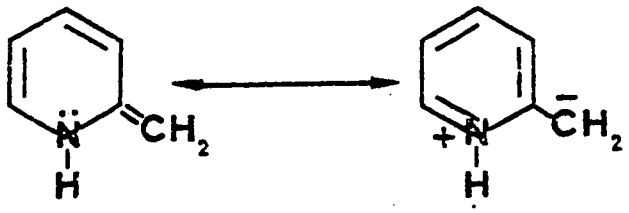

Acetic anhydride was one of the most effective Lewis aid catalysts for this reaction, since it allowed formation of increased product with high purity. The order of reactivity of methyl pyridine measured by the yield of styrylpyridine under the same conditions was 4-picoline> 2-picoline. The 2,6-DSP was produced faster than the 2,4-DSP from the corresponding lutidines. Positive inductive effects in picoline caused accelerated removeal of the H^+ ion from the methyl group. Negative inductive effects in lutidine (since the intermediate is methyl pyridine, and the styryl group is acting as an electron withdrawing group) cause decreased removal of the H^+ ion from the secondary methyl group.

The activation energy of the condensation reaction between different methyl pyridine compounds and excess benzaldehyde, as measured by ultra-violet spectrophotometry, is found to be 34.14 KJ/mole for 2-picoline and 20.38 KJ/mole for 4-picoline. The yield of styrylpyridine increased

with increasing reaction time and temperature.

The maximum wavelength was not greatly shifted by substituting another styryl group on the pyridine ring, but the hydroxy derivatives of styrylpyridine showed a large shift in the position of the maximum wavelength as compared to styrylpyridine. This was explained by an increase in the number of resonance structures in the absorbing system and the easier charge delocalization due to the electron donating properties of the hydroxy group.

V. BIBLIOGRAPHY

1. M. C. Chiang and W. H. Hartung, J. Org. Chem., 10, 21 (1945).

2. E. D. Bergmann and S. Pinchas, J. Org. Chem., 15, 1184 (1950).

3. L. Horwitz, J. Am. Chem. Soc., 77, 1687 (1955).

4. L. Horwitz, J. Org. Chem., 21, 1039 (1056).

5. E. R. Blout and V. W. Eager, J. Am. Chem. Soc., 67, 1315 (1945).

6. G. M. Bennett and W. L. C. Pratt, J. Chem. Soc., 1465 (1929).

7. B. D. Shaw and E. A. Wagstaff, J. Chem. Soc., 77 (1933).

8. E. A. Wagstaff, J. Chem. Soc., 276 (1934).

9. A. P. Phillips, J. Org. Chem., 13, 622 (1948).

10. W. H. Mills and R. Raper, J. Chem. Soc., 2466 (1925).

11. R. T. Morrison and R. N. Boyd, "Organic Chemistry", 4th Edition, Allyn and Bacon, Inc., Boston, 1983, 36 kcal/mole for benzene, pp 579; 23 kcal/mole for pyridine, pp 1276.

12. H. Bowen, Chem. Soc. Lond., Ann. Rep., 40, 25 (1943).

13. R. J. L. Anderson, J. D. Cox and E. F. G. Herington, Transaction Faraday Soc., 50, 918 (1950).

14. H. C. Brown and X. R. Mihn, J. Am. Soc., 77, 1723 (1955).

15. N. V. Sidgewick, "The Organic Chemistry of Nitrogen", New Edition revised and rewritten by Taylor and Baker, Oxford Clarendon Press, London, 1937, pp. 534.

16. Van Hans-Gregor Elias and Erich Greth, Die Makromol. Chem., 123, 203 (1969).

17. M. X. Hubacher and S. Doernberg, J. Pharm. Sci., 53 (9), 1067 (1964).

18. W. A. Lees and A. Burawoy, Tetrahedron, 19, 419 (1963).

19. D. Papa and E. Schwenk, J. Chem Soc., 73, 253 (1951).

20. A. J. Gordon and R. A. Ford, "The Chemists' Companion: A Handbook of Practical Data Techniques and References". Wiley, New York, 1972, pp. 434.

21. E. F. G Herington, Disc. Faraday Soc., 9, 26 (1950).

22. J. E. Purvis, J. Chem. Soc., 97, 692 (1910).

23. E. Herz, L. Kahovec and K. W. F Kohlrausch, Z. Physik. Chem., B, 53, 124 (1943).

24. E. F. G. Herington and R. Handley, J. Chem. Soc., 199 (1950).

25. H. C. Brown and G. K. Barbaras, J. Am. Chem. Soc., 69, 1137 (1947).

26. J. R. Dyer, "Application of Absorption Spectroscopy of Organic Compounds", Prentice-Hall, Inc., N. J., 1965, ppll.

27. E. Knoevenagel, Chem. Zentr., II, 179, 1702 (1905).

28. W.P. Jencks, "Catalysis in Chemistry and Enzymology", McGraw-Hill, New York, 1967, Chapter 10, pp. 501.

29. E S. Gould, "Mechanism and Structure in Organic Cemistry" Holt-Rinehart and Winston, Inc., New York, 169, Chapter 7, pp. 203.

30. D. W. van Krevelen and P. J. Hoftyzer, "Properties of Polymers", Elsevier, New York, 1976, Chapter 21, pp. 459-465.

PART II. SYNTHESIS, CHARACTERIZATION AND THERMAL STABILITY OF STYRYLPYRIDINE BASED POLYMERS

PART II: Synthesis, Characterization and Thermal Stability of Styrylpyridine Based Polymers

I. INTRODUCTION

The rapidly growing use of polymers in a variety of applications has created a great deal of concern for their performance with regard to their properties and characteristics such as flammability, high impact, polymer-polymer compatibility, photostability, etc.

Initial goals in flammability research have focused on the use of additives in polymers. More recently, the research has concentrated on the structure-flammability relationships and their application in the synthesis of high-temperature resistant polymers which inherently possess improved flammability behavior.

One objective of this research was to utilize the polystyrylpyridine (PSP) structure in designing new and better flame resistant polymers. The PSP unit has certain structural features which meet the general criteria for good flammability behavior in high temperature systems. The structural characteristics of polymers possessing high temperature stable properties are: (1) strong chemical bonds in the polymer backbone, (2) no rearrangement capabilities, (3). maximum resonance stabilization and, (4) lack of ring strain[1]. Epoxy resins, polyesters,

polycarbonates, and polymeric triazines containing PSP units were systematically prepared to study their flammability and thermal degradation behavior.

The developments in the area of organic photochemistry have given assistance to the interpretation of photodegradation processes and to the search for novel methods of UV stabilization. In this study, the photodegradations of styrylpyridine based arylates have also been investigated and interpretations were based on spectroscopic observations.

A. Flammability of Polymers

A brief description of the process leading to polymer combustion[2] can be shown by the following scheme:

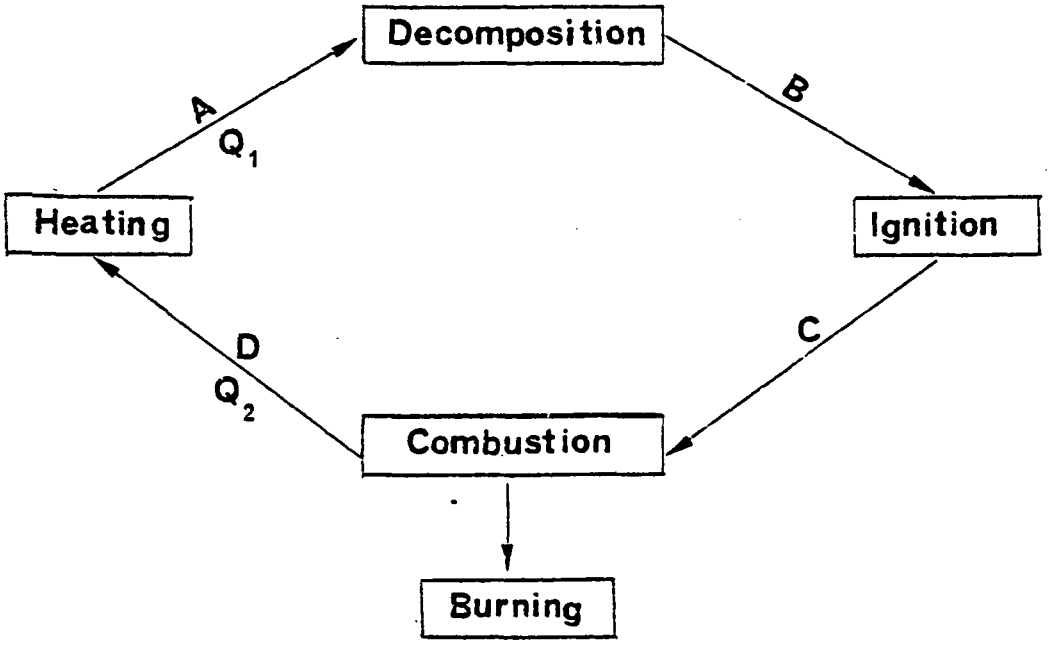

If Q_1 is the heat transferred to the polymer, and if it is larger than the bond strength within the polymer backbone, then the polymer will begin to decompose. As the polymer decomposes at least two categories of products may be formed: (1) low molecular weight products which contain the combustible gases, and (2) highly crosslinked C-C bonded char. If the concentration of combustible gases and oxygen is high enough, the combustible products will ignite and the polymer will burn. The burning process generates additional heat, Q_2, which is transferred to the polymer itself. If Q_2 is larger than Q_1, the polymer undergoes further decomposition, ignition, and combustion. This cycle continues until the polymer is completely consumed.

Flame retardation can be achieved by interrupting the burning process at one of the stages shown in the above scheme. At stage A decomposition of a polymer is usually initiated by breaking the backbone to form active free radicals. This process can be interrupted by the formation of a strong chemical bond in the backbone which results from a high maximization resonance energy of ring or double bond character. Materials used in the stages B and C to prevent ignition and combustion usually are the chemicals which generate non-combustible gases, such as H_2O, HX, CO_2, and NH_3 upon decomposition. These non-combustible gases may act as gas phase diluents for the

combustible decomposition products obtained from the polymer. In addition, the structures remaining in the condensed phase can form highly crosslinked C-C char during the decomposition. The minimized diffusion of oxygen and volatile, combustible small molecules back into the polymer matrix and the reduction of heat transferred from the flame to the polymers have decreased the flame retardant properties of polymer[3]. Flame inhibitors, such as CO_2 , H_2O , HX , X_2 , atc., in stage C can decrease the amount of heat (Q_2) transferred to the polymer in stage D.

There are many ways to measured the flammability of materials. A test that has been widely used in the laboratory since its initial development in 1966 in the Oxygen Index Test (OI)[4] . The char yield test, is also quite reliable for systems in which char formation is the preimary mechanism[5] .

In general, the polymeric material increases its thermal and heat resistance with increasing aromatic ring content in the repeating units. A high char yield was shown to be related to a decrease in flammability and can be correlated to an increased oxygen index[5] . An increase in char formation usually decreases the production of combustible carbon-containing gases. These systems also show a decrease in exothermicity, and thermal

conductivity at the surface of the burning material[6]. The char formation and oxygen index have been shown to depend on the structure of the polymer backbone as well as on a variety of substituent effects[5,7].

B. Styrylpyridine Based Polymers: Epoxy Resins

B-1. Epoxy Resin Preparation and Determination of Their Structure

Epoxy resins can be synthesized by various methods[8]. Two important methods are: (1) a mixture of diol and epichlorohydrin is heated to about 60°C and solid sodium hydroxide is added slowly. The properties of the epoxy resin (made by the "taffy process"), such as the equivalent weight, softening temperature and specific gravity[9], depend on the initial feed ratio of the epichlorohydrin to diol. (2) A mixture of diol and epichlorohydrin is heated to 60°C, in the presence of a basic catalyst which allows formation of higher molecular weight epoxy resin. This is the "fusion process". A major difference between the two processes is the degree of polymerization (n). In the "taffy process" n is a series of numbers (n=0,2,3, . . .), in the fusion process n is an even number (n= 0,2,4,6, . . .).

Lee[10] first synthesized a nitro-substituted epoxy resin by epoxidizing a bisphenol prepared from a distyryl-benzene derivative. Epoxy resins containing nitro group

substituents can be used to formulate pyrotechnic binders. Also, some nitro epoxies are known to char heavily when burned[11,12]. Possible high temperature chemical reactions between the double bonds in the backbone to account for this were not mentioned.

The infrared spectrum of epoxy resin was obtained by FT-IR. The characteristic bands at 1250 cm^{-1} and 950-810 cm^{-1} [13] are due to symmetric and assymetric stretching of the epoxy ring (C-C). Unfortunately, the band near 1250 cm^{-1} overlaps with the phenoxide group (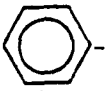 -O) asymmetric stretching band. The band near 910 cm^{-1} may be characterized as an epoxy ring stretching vibration.

In order to understand the structure of epoxy resin prepared from 2,6-di-(p-hydroxystyryl)pyridine with epichlorohydrin in NaOH solution, liquid chromatography was used to purify the epoxy resin. For identifying the actual structure of the epoxy resin, FT-IR and C-13 NMR spectroscopy were applied.

B-2. Determination of Epoxy Equivalent Weight (EEW)

Epoxy resins were analyzed for epoxy or oxirane content which is reported as epoxy equivalent weight (EEW), i.e., the weight of resin in grams containing one gram equivalent of an epoxy group.

If the epoxy chains were assumed to be completely linear with no side chain and possessing terminal epoxy groups, then the EEW would be one half the average molecular weight of a diepoxy resin and one-third of the average molecular weight of a triepoxy resin[14].

Analytically, epoxy resin groups are determined by the reaction with hydrogen bromide in glacial acetic acid and by back titration with standard base[15,16]. Other functional groups present may cause interference problems and result in a poor end point. Pyridium chloride-pyridine is a recommended reagent for the analysis of bisphenol diglycidyl ether resin[17,18].

Other methods of characterization include infrared, near infrared spectroscopy[14], proton[19] and carbon-13 nuclear magnetic resonance[20]. Each method has individual advantages that depend on the characteristics of the resin such as the extent of undesirable side reactions and the presence of impurities and additives in the commercial resins which may interfere with the desired reactions.

M.G. Rogers[21] has found that an estimation of the number of branches in the molecule can be obtained from proton NMR. It is assumed that branches occur only through hydroxy groups so that for every branch point in the non-linear molecule there is one hydroxy-carbinol methine

pair less than in the linear molecule of equal molecular weight. Trichloro acetyl isocyanate[22] has been used to react with the hydroxy group and thus to produce a downfield shift of the associated methylene and methine proton NMR. Therefore, if N is the number of branch points, then the number of carbinol methines in a branched molecule is equal to n-N, where n is the number of repeat units and the number of benzylic methyl protons in the molecule is (6n + 6). Thus:

$$N = n-6A(n + 1)$$

where A is the area ratio of the carbinol methine protons to the benzylic methyl protons. The disadvantage of this method is that n must be known.

A proton NMR method to determine the epoxide equivalent weight (EEW) has been developed for commercial epoxy resins[19]. The precision and accuracy of determining EEW by proton NMR is the same as by the conventional ASTM method. The proton NMR is advantageous over ASTM because it can be carried out in a shorter time period, is free of interferring chemical reactions, and requires a small amount of the sample. However, the overlap of proton NMR signals due to the internal solvent and the epoxy resin may present some difficulty in the choice of a suitable internal standard.

In order to obtain the EEW of styrylpyridine based epoxy resin, carbon-13 FT-NMR is applied and the interpretation of calculations is based on the proposed equation.

B-3. Curing Agent-Trimethoxyboroxine (TMB)

TMB has been applied as a curing agent for epoxy resins and is useful in encapsulating of electronic compounds[23,24], aircraft panels[25,26] and epoxy resin forms[27,28]. Brunner and Waghorn[24] first used TMB to cure DGEBA (bisphenol A and epichlorohydrin) and obtained a hard coating which was useful for encapsulating electronic components. Later, Lee and Neville[29] investigated this epoxy resins and concluded that TMB is an anhydride and can be used as a primary curing agent or a co-curing agent for epoxy resins. Recently, Lopata and Riccitiello[30] have studied the DGEBA-boroxine system by differential thermal analysis (DTA) and observed the characteristic exothermic peak (uncured and cured with TMB) between 300-400°C, with the major exotherm at 430°C. Furthermore, the kinetics of the TMB-induced thermal polymerization of epoxy resins[31] have been studied in order to understand the polymer structure of epoxy resins (crosslinked) with TMB. The result is based on the model compound phenylglycidyl ether (PGE), since the epoxy resin produces a three-dimensional gel network structure early in the cure cycle. The proposed mechanism involves five steps (Figure 1),

Figure 1. The mechanism for the trimethoxyboroxine-induced thermal polymerization of phenyl glycidyl ether.

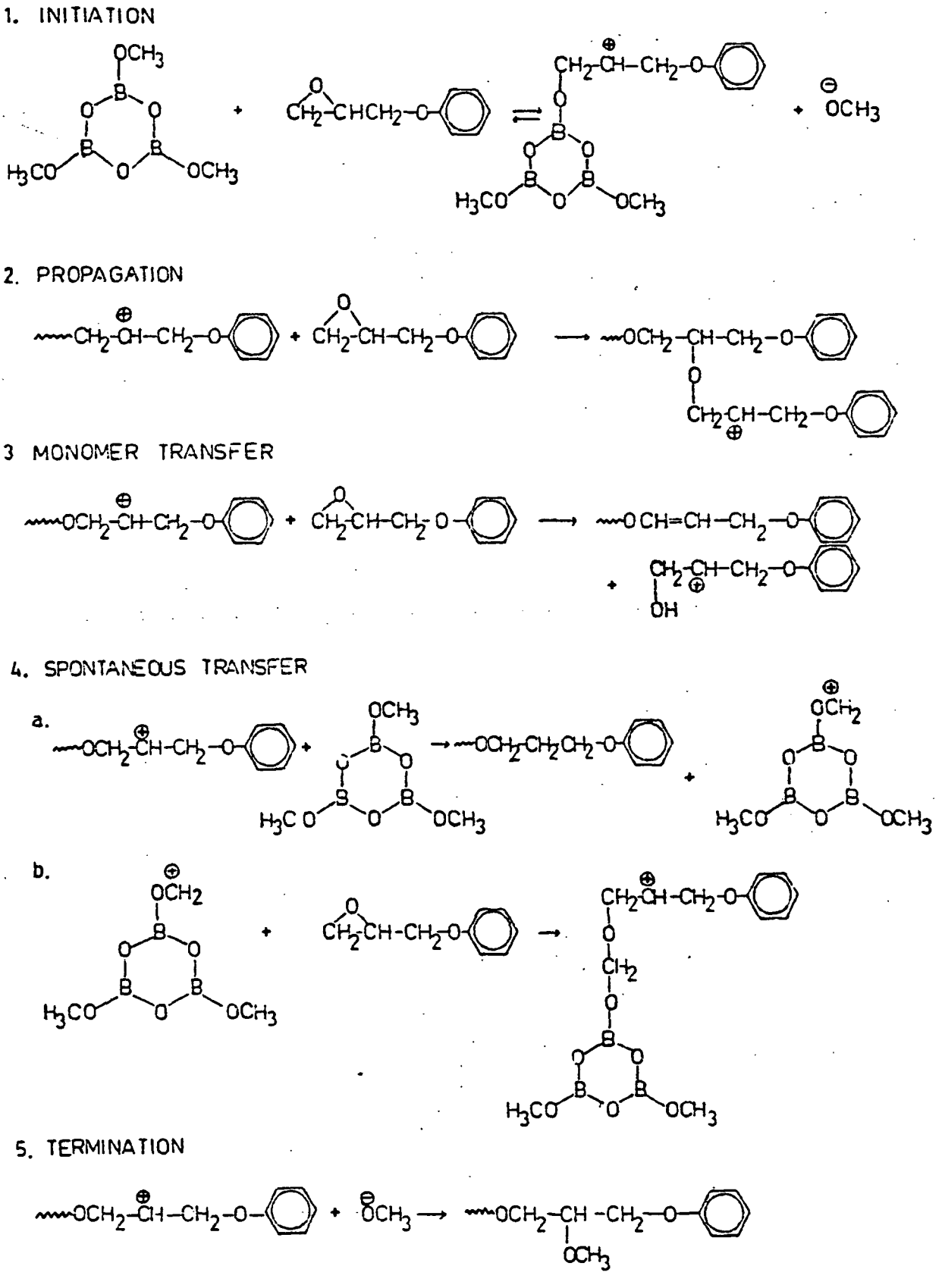

E. S. Lopata and S. R. Riccitiello, J. Appl. Polymer Sci., 21, 91 (1977).

each step was supported by IR and proton and Boron NMR. Lin and Pearce[32] have studied highly crosslinked diglycidyl ether of epoxy resins with good thermal stability by curing these with TMB. They have found that the reactivity of three different resins toward TMB as measured by differential scanning calorimetry (DSC) was DGEBA (diglycidyl ether of bisphenol A) > DGEBF (diglycidyl ether of phenolphthalein) > DGEPP (diglycidyl ether of 9,9-bis-(4-hydroxyphenyl) fluorene). For the same curing conditions the order of crosslinking density was DGEBA > DGEPP > DGEBF. Furthermore[33], the proposed mechanisms of thermal degradation of compounds cured with TMB was supported by studies using FT-IR under various conditions.

Cured glycidyl ethers of various styrylpyridines with TMB have been studied by thermal analysis to understand the effect of the double bond in the backbone in thermal properties.

B-4. Thermal Stability and Degradation Mechanism

The thermal stability of a material is identified by a specific temperature, without reference to the test method, surrounding atmosphere, and time involved[34,35,36]. The softening temperature has been used as a measure of the thermal stability of a material, with a higher temperature usually, but not always, being indicative of increased thermal stability. This process is reversible

and a function of temperature only. Another mechanism is to irreversibly decompose the structure with heat. This process is both temperature and time dependent. Therefore, the thermal stability of a material can be expressed either by temperature or by a temperature-time unit limit in which the material can be used[34].

Thermal stability is related to the dissociation energies and thus to the decomposition temperatures of a polymeric material. In the past decades, intensive research has been undertaken to improve the thermal stability of existing polymers by introducing structural modifications to increase the dissociation energy or by synthesizing an entirely new class of inorganic and organic-inorganic polymers[36]. These polymers may be characterized by higher decomposition temperatures and greater char formation, which may be related to the polymer oxygen index.

W. W.Wright's[1] conclusions regarding the relationship between structure and thermal stability are as follows:

(1) p-linked rings give the highest thermal stability.

(2) Substitution of any group for hydrogen on the ring normally reduces stability.

(3) Stability is reduced by the presence of flexible linking groups. Of those investigated the least deleterious are -CO-, -COO-, -CONH-, -S-, -SO-, and -O-.

(4) The best heterocyclic polymers have stabilities equivalent to that of poly-p-phenylene.

Therefore, polymers of higher thermal stability (i.e. heat resistant and thermal resistant) can be obtained by increasing the bond strength between atoms in the main chain[36], adding some degree of aromatization and cyclization during the thermal reaction, curing with an effective agent to increase surface conductivity during the burning[32], or forming a cardo polymer[37]

In order to obtain polymers of high thermal stability, the styrylpyridine based epoxy resin was prepared, and then cured with TMB. The degree of thermal stability was based upon the TGA and OI results.

Degradation is an irreversible chemical process. An understanding of the degradation mechanism may show the importance of the particular chemical structure for the stabilization of the polymer.

There is much literature concerning oxidative thermal degradation of epoxy resins[38,39]. The most important proposed degradation mechanisms are shown in Figs. 2-4. These were supported by the analyses of the final products using the mass spectrometer, thermal analyzer (TGA, DTA) and infrared spectrometer. Thermal analysis including DTA and TGA, yields some information on thermal stability,

Figure 2. Degradation scheme of epoxide proposed by Neiman.

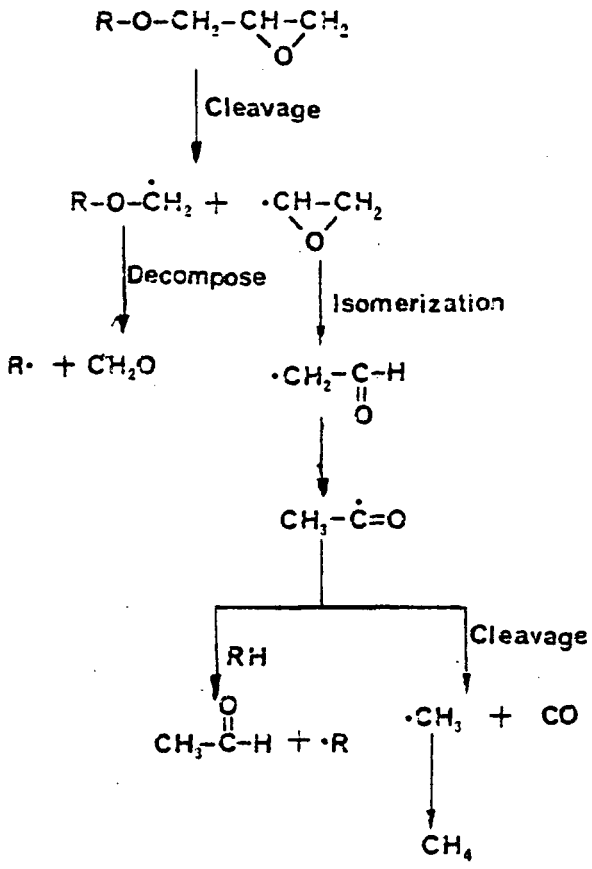

M. B. Neiman, B. M. Kovarskaya, L. I. Golubenkova, A. S. Strizkova, I. I. Levantoskaya, and M. S. Akutin, J. Polym. Sci., 56, 383 (1962).

Figure 3. Degradation scheme of epoxide proposed by Anderson.

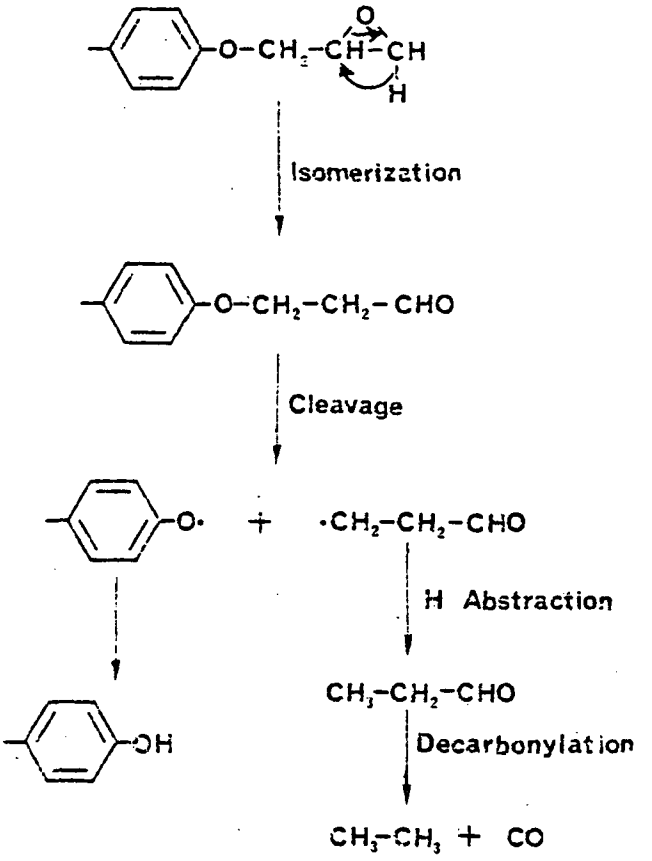

H. C. Anderson, J. Appl. Polym. Sci., 6, 484 (1962).

Figure 4. Degradation scheme of epoxide proposed by Lee.

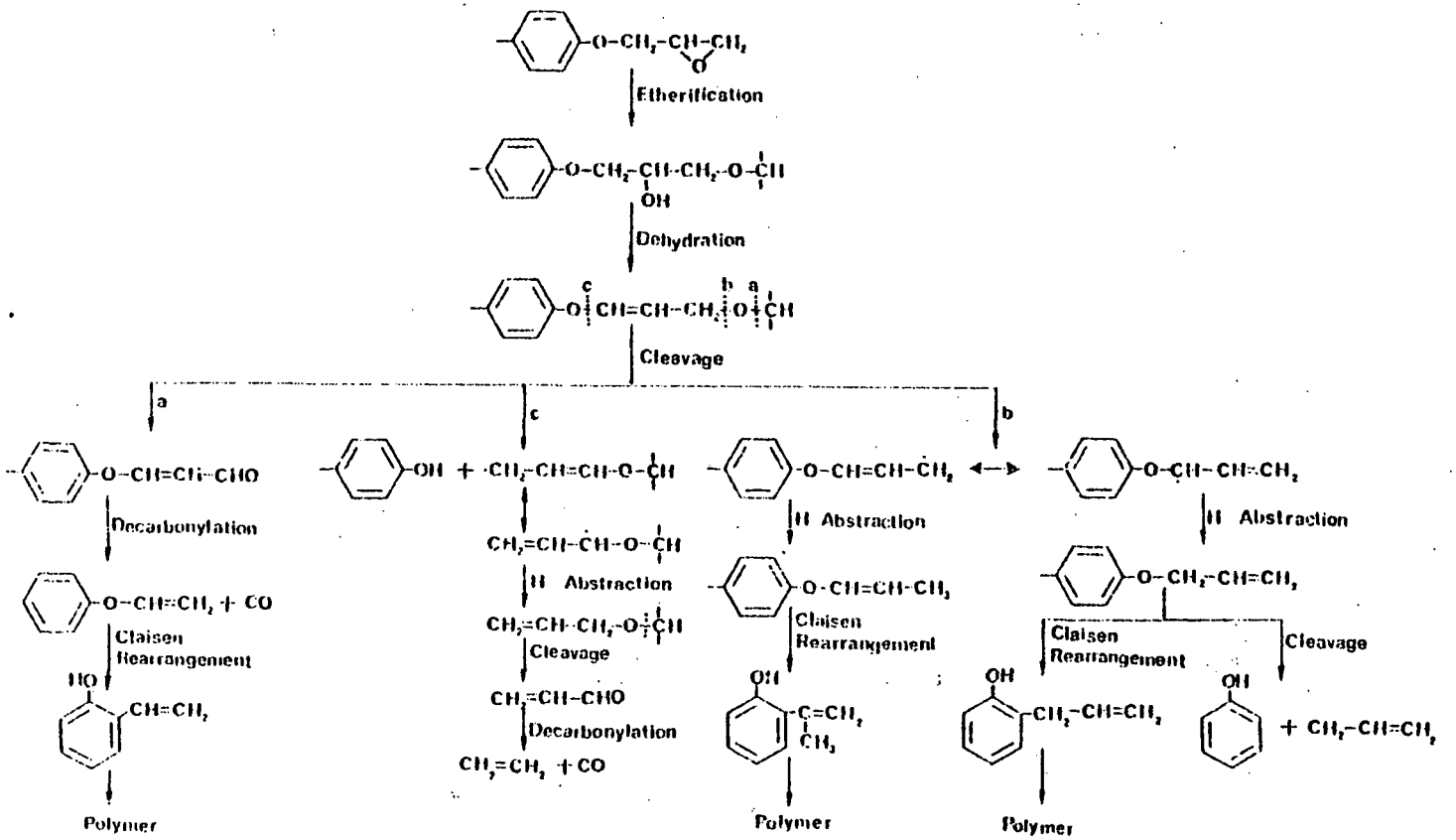

L. H. Lee, J. Polym. Sci., A, 3, 859 (1965).

but, does not provide enough information for interpreting the degradation mechanism route. The final product analysis may lead to an erroneous degradation mechanism because other interim reactions may have occurred. Conventional dispersive IR spectrometry may overcome some of the difficulties of product analysis and may be able to show chemical changes during the degradation process. However, due to its low sensitivity, the characteristic bands may overlap with the strong absorption band of the major component, and hence it is difficult to detect the relatively small changes of the bands in the position.

FT-IR has been used to study the oxidation and thermal degradation of polybutadiene[39,40,41], and the oxidative thermal and photo degradation of various epoxy resins (DGEBA)[26]. The information on degradation mechanism may be obtained by examining the difference between the spectra of the pure polymer and the oxidized or photo-degraded polymer.

In this study, FT-IR is used to understand the mechanisms for the thermal degradation of 2,6-DGESP by interpreting the characteristic peak changes occurring during the thermal degradation.

C. Styrylpyridine Based Polymers: Polyarylates

C-1. Flammability Study

In polymer chemistry, it is important to establish the relation between structure and property of a polymer. Only when this is known can we prepare polymers having properties specified in advance.

It is known that an increase in char yield is usually associated with improved flammability behavior[5]. This can be understood if one considers that the volatile flammable producrs can only diffuse with difficulty through a char layer, and that thermal conductivity of a char layer is relatively poor[6]. The structure of the polymer can contribute to the amount of char formed based on the character of the functional groups present and the nature of the backbone[5,7].

Ritchie[42] found that for a series of unsaturated polyesters and their copolymers, the temperatures at which carbon dioxide is eliminated lie in the range 280-345°C depending on the structure of the polyester. Aliphatic polyesters and their copolymers have less thermal stability than the polyarylates. Z. Jedlinski[43] has studied the influence of chemical structure on fourteen aromatic copolymers, containing naphthalene rings in the backbone, and found that the thermal stability increases as the number of condensed naphthalene rings increased and the

symmetry of the copolymer chain increased. van Krevelen[44] and Parker[25] have correlated char yield with the aromaticity of polymers. Lin and Pearce[45] have confirmed the general relationships between char yield and oxygen indices for phenolphthalein related polyesters and polycarbonates.

In this study, styrylpyridine based polyesters, polycarbonates and their related model compounds were synthesized and characterized by TGA and OI to determine the effect of structure on thermal stability.

C-2. Photo-Stability and Fries Rearrangement

Polymers containing certain chromophores can absorb light to undergo photochemical reactions involving the formation of free radicals, photoionization, cyclization, intramolecular rearrangement, and fragmentation. These can cause discoloration, extraction, distortion, shrinkage, surface cracking, and electrical failures of the polymeric material. These effects will affect the color, toughness, tensile strength, and the mechanical and electrical properties of polymers. In order to prevent these failures, many polymers have been protected against photodegradation by the addition of stabilizers. These stabilizers fall into three general types[46]: light screens, ultraviolet absorbers, and quenching compounds. Studies on stabilization mechanisms show that these substances must be compatible with the polymer and stable to ultraviolet

irradiation, and elevated temperature[47-50]. Finding stabilizers with such properties is often a difficult problem. Thus, the synthesis of polymers capable of self-stabilization due to some structural feature or to stabilizing groups inherent in the molecule has received considerable attention in recent years[51,52].

The energy of photons from sunlight may be sufficient to break many of the single bonds[53] encountered in polymeric systems. Chemical reactions thus can be one mode of dissipation of absorbed electronic energy. However, in addition to photochemical processes, there are a number of radiative and non-radiative photophysical processes that do not lead to a net chemical reaction yet are alternate modes for dissipation of absorbed energy[46,54] (Fig 5).

In a major photostabilization process, all the excitation energy must be dissipated by only photophysical processes. Let us consider the mechanism of the photostabilizer in photophysical processes in more detail.

For UV absorbers, the mechanism is to convert electronic energy into vibrational energy by a radiationless route without a change in spin multiplicity ($S_1 \rightarrow S_o$, $S_2 \rightarrow S_1$). It has been found that o-hydroxybenzophenones (III) are common UV absorbers[48].

Figure 5. Photophysical processes of molecules.

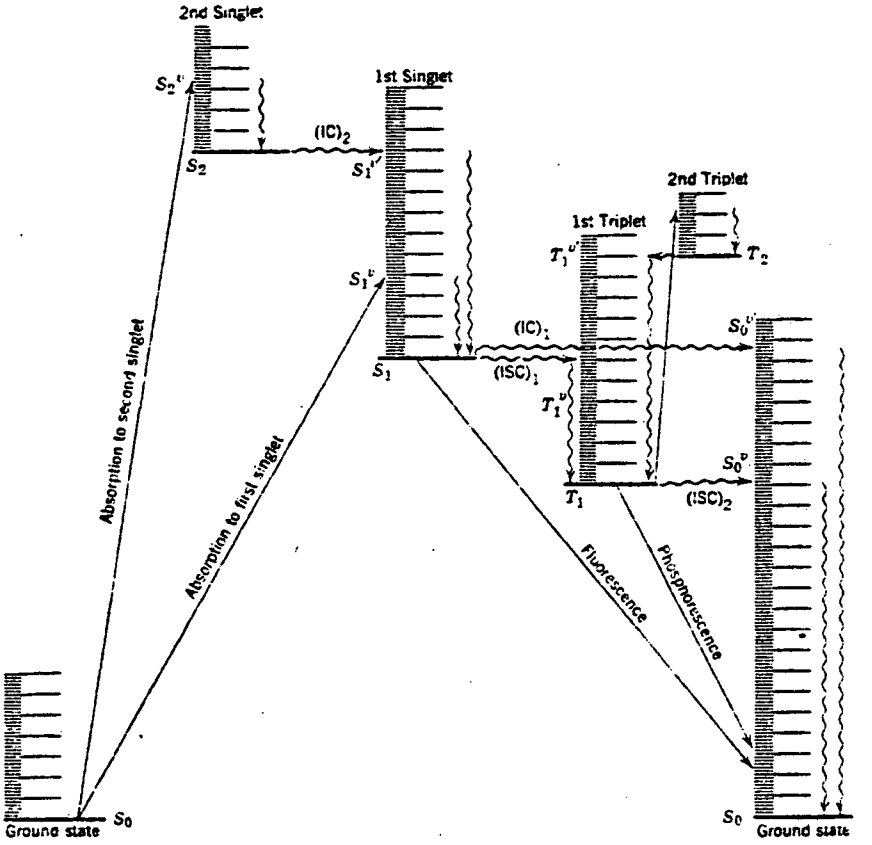

Excited states and photophysical transitions between these states in a "typical" organic molecule. Radiative transitions between states are given by solid lines, radiationless processes by wavy lines; IC = internal conversion, ISC = intersystem crossing. Vertical wavy lines are vibrational relaxation processes. Vibrational and rotational levels are shown approximately equally spaced for convenience in presentation. Actually they blend into a continuum at large quantum numbers. Higher electronic states exist but are omitted for convenience. Photodissociation and possible relationless transitions from upper vibrational levels of the excited states have been omitted for simplicity of presentation.

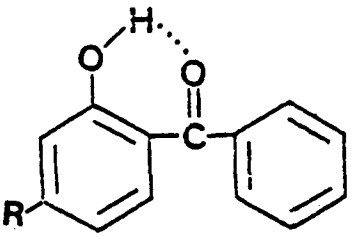

(A)
o-hydroxybenzophenones

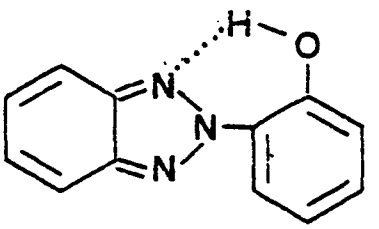

(B)
o-hydroxyphenyl-
benzotriazoles

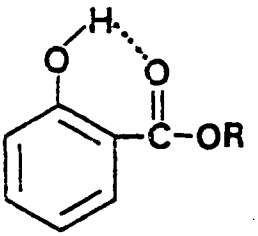

(C)

silicylates

All these compounds have a common structural feature, the intramolecular hydrogen bond, which can efficiently deactivate the electronically excited states of the ultraviolet absorber. The mechanism of this phenomenon can be interpreted as an intramolecular charge-trasnfer transition[55,56].

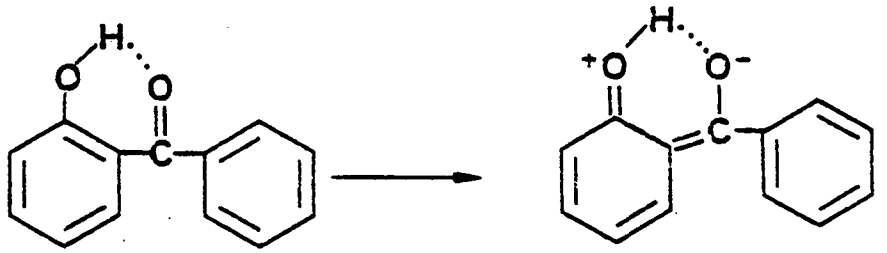

The photo-self-protective (Photo-Fries) mechanism involves the dissipation of energy by a molecular rearrangement following the absorption of ultraviolet light[57]. The mechanism is shown below:

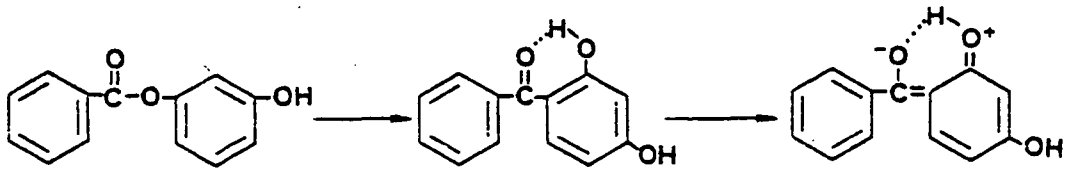

(I)
resorcinol monobenzoate

I is almost as effective as o-hydroxybenzophenone in dissipating damageable UV light because monobenzoate is converted by sunlight into o-hydroxybenzophenone by a Photo-Fries rearrangement.

It has been known that the polymers containing the same choromophores as the low molecular molecules just discussed above have similar photo-chemical reactions[58]. Many Fries-arrangements of the polyaryesters[51,59,60] and polycarbonates[52] to o-hydroxybenzophenone have been studied in recent years. The reaction scheme is the following:

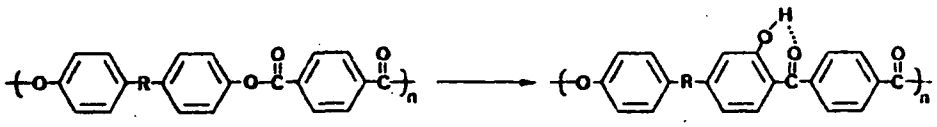

A Friedel-Crafts type inter-chain electrophilic aromatic substitution also can occur[46].

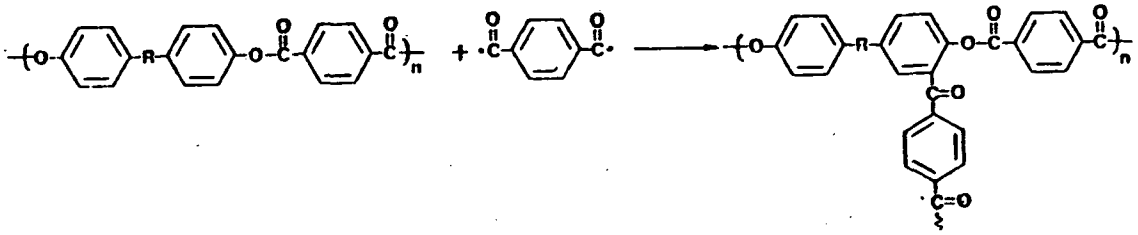

This effect can decrease the formation of o-hydroxybenzophenone.

During the course of this project, the chemical changes which occur during UV irradiation of the styrylpyridine based model compound of the ester and carbonate were investigated. The results obtained from the model compounds provide information about the mechanism of rearrangement in polymers, and for less sterically hindered systems information concerning dimerization and isomerization may also be obtained.

D. Styrylpyridine Based Polymer: Triazine (PST)

Research on the polycyclotrimerization of monomers containing multiple carbon-nitrogen bonds has been widely developed only during the past decade due to technological demands for high heat-resistant and thermally stable polymers. The construction of the space shuttle resulted in some of the most notable applications of these polymeric materials to technology.

Numerous subsequent studies established[61-64] that the cyclotrimerization reaction is more readily undergone by nitriles with electronegative substituents in the α-position relative to the nitrile group. Electronegative substituents lower electron density at the carbon atom of the nitrile group and hence electrophilic reactivity of such nitriles[64]. Compounds containing the C≡N group tend to form stable cyclic trimers because trimerization involves decreased bond enthalpy. In addition the cyclic trimer is stabilized because the favorable valence angles (about 120°)[65,66] create a Pπ — Pπ aromatic system with high resonance energy[67,68].

The mechanism of the synthesis of s-triazines from nitriles has been proposed[61,62]. A possible mechanism is[70]:

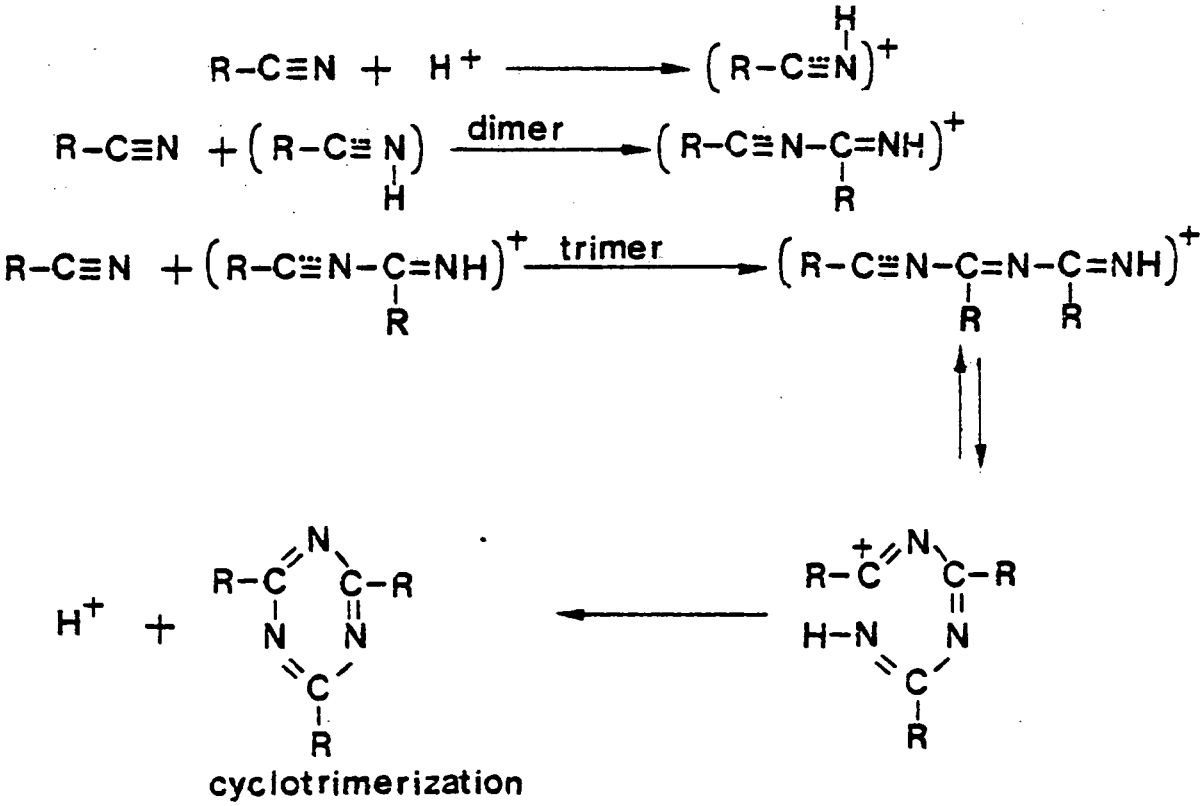

It should be noted that the cyclotrimerization of nitriles may be accompanied by several secondary processes, particularly, linear polymerization of cyano groups with formation of an azomethine structure[70].

Anderson[71] first reported that aromatic dinitriles form aromatic polymers containing the s-triazine ring in the backbone. Thermostable polymers with triazine rings formed from aromatic dinitriles under the influence of chlorosulfonic acid ($ClSO_3H$) were obtained. The structure of polytriazines was characterized by the disappearance of the C≡N absorption band in the infrared (2264 cm^{-1}) and the appearance of a new band at 1550 cm^{-1} [67,72] for the C≡N band in the s-triazine ring. Unfortunately, the information obtained from the infrared spectra of the polytriazines was uninterpretable because the absorption of both the aromatic monomers and triazine link fall in approximately the same region. Therefore, Anderson proceeded to hydrolyze the triazine in the presence of concentrated hydrochloric acid and the product, a dicarboxylic acid, was used to confirm the structure.
B. B. Wildi[73] polymerized 2,4,6-tricyano-s-triazines. This resulted in the formation of both the polyazomethine (linear polymer) and polytriazine structure. Information concerning the thermostability of these polymers was not given. It was anticipated that polymers encapped with

nitrile groups or having nitriles pendant from the main chain could be crosslinked by catalytic trimerization to give the thermally stable triazine ring. J. Verborgt[74] adapted this idea for the syntheiss of crosslinked aromatic polyethers and polysulfones and found that the char yield and viscosity increased dramatically.

In this study, FT-IR was used to examine the structural changes occurring as the nitrile functional groups trimerize to form the polytriazine. In addition, the thermal stability of various polytriazine isomers were examined by comparisons at different reaction times.

II. EXPERIMENTAL

A. Preparation of Diglycidyl Ether of Styrylpyridine (DGESP)

A-1. Synthesis of Diglycidyl Ether of Styrylpyridine[75]

A mixture of 5.0g (0.01587 mole) of 2,6-di(p-hydroxystyryl)pyridine and 12.4 ml (0.1587 mole) of epichlorohydrin was heated to 90~100°C. During a period of 1 hour, 1.3 gm of NaOH in 50 ml of water was added to the reaction mixture with vigorous stirring. After adding NaOH, a "taffy" yellow gum rose to the top of the reaction mixture. The mixture was filtered. The coagulated yellow solid was washed with hot water twice to decompose unreacted epichlorohydrin. The resin was heated to 160°C under reduced pressure (~1mmHg) to remove water and unreacted epichlorohydrin. The reaction schemes for conversion of hydroxy-terminated styrylpyridine to glycidyl ether are shown in Figure 6.

A-2. Characterization of DGESP - Liquid Chromatography

Silica gel with the mesh number 200 to 400 mesh ASTM and particle size 0.040-0.063mm (E M reagents), and chloroform (Fisher certified ACS grade) were used as absorbent and elution solvent. The column employed had an inner diameter of 2.5 cm and a height of 50.0cm. Ten to fifteen grams of DGESP was dissolved in 100ml of

Figure 6. The synthesis scheme for the diglycidyl ether of styrylpyridine.

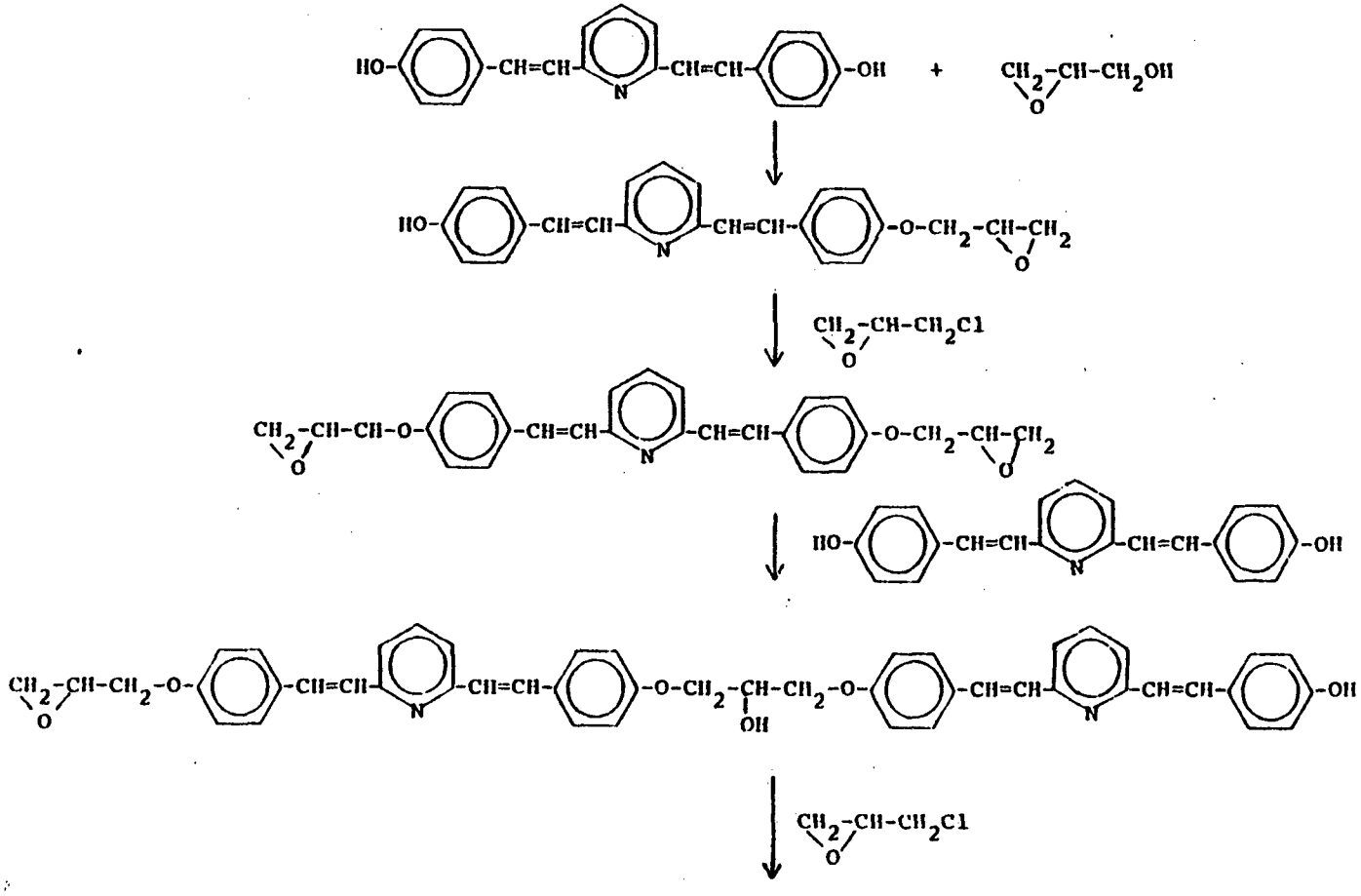

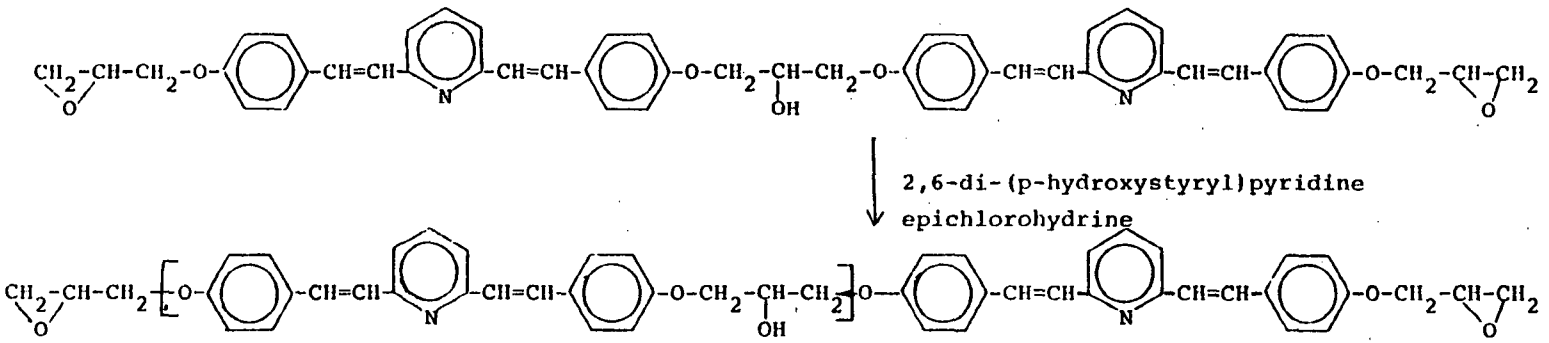
2,6-di-(p-hydroxystyryl)pyridine
epichlorohydrine

chloroform. Three different colors - red, yellow, and pink, were observed in the column after elution. The red colored material eluted first and followed by the yellow material. The pink colored material stayed on the top of the column. A higher acetone content elution was then added in order to remove the slowly moving pink material. The elution rate was 5ml per minute and the solution was collected in 50ml portions. The first portion (red color) contained a high content of epoxy ring. The solvent was removed with the rotoevaporator. The characterization data is shown in Table 1.

Epoxy Equivalent Weight Determination

Determination of the epoxy content of DGESP by the ASTM method (15.76) failed to provide reproducible results due to the reaction of hydrogen bromide with pyridine and the ambiguous end-point upon titration.

The carbon-13 FT-NMR measurements in $CDCl_3$ of the DGESP epoxy resins in 10mm o.d. sample tube were carried out by NT FT-NMR 300 Spectrometer system. A 90^{o} (10μsec) pulse was used with gaged decoupling to depress the NOE (number Overhauser effect)[77]. The number of scans was 512. The calculation of degree of polymerization is shown on page 106.

Table 1. The characterization data for glycidyl ethers of styrylpyridine

epoxy resin	epoxy eq.wt.[a]	degree of polymerization	softening T_m[b] point	exotherm peak[c]	OI[d]	Y_{800}[e]
2,4-DGESP	-	-	290-300	302.8-310.5 345.4-392.6 220-260.1	25.2%	46.5%
2,6-DGESP	213.5	0.04	175.3	289.5-305 334-355	24.7%	46.2%
2,4,6-TGESP	-	-	-	131.3-201.0 329-337.2	23.8%	36.0%

a: measured by C-13 NMR
b: measured by TMA
c: measured by DSC
d: OI (oxygen index)
e: Y_{800} char yield at 800°C, measured by TGA

A-3. Thermal Crosslinking Mechanism Study of DGESP by FT-IR

The DGESP resins were dissolved in the chloroform and then coated on an aluminum plate following by drying in a vacuum oven for 24 hours (30°C). The aluminum plate was mounted on the microheater in the reflectance attachment of the sample compartment of the FT-IR spectrometer* (Fig. 7). Spectra were taken under nitrogen with controlled temperature. The difference spectrum was obtained by subtracting the two spectra of interest.

*Digilab FTS-20B Fourier Transform Spectrometer.

A-4. Curing the Epoxy Resin (DGESP) with TMB and Thermal Cured Epoxy Resin (without TMB)

TMB (Aldrich; 99%, bp 130°C, n_D^{20}1.3996) was used as the curing agent. In order to obtain consistent results, 9.5gm of TMB was mixed with 1 equivalent of epoxy resin[25,30]. The mixture of the DGESP-TMB system was red in color. The curing was carried out in a nitrogen filled, sealed glass tube at 135°C for 3 hours, 180°C for 3 hours and another 3 hours at 220°C.

The above procedure was applied with equal amounts of epoxy resin (DGESP) using different equivalent weights of TMB.

An equal amount of epoxy resin (DGESP) (0.5gm) without TMB was sealed in a glass tube under nitrogen followed

Figure 7. Schematic diagram of reflectance attachment.

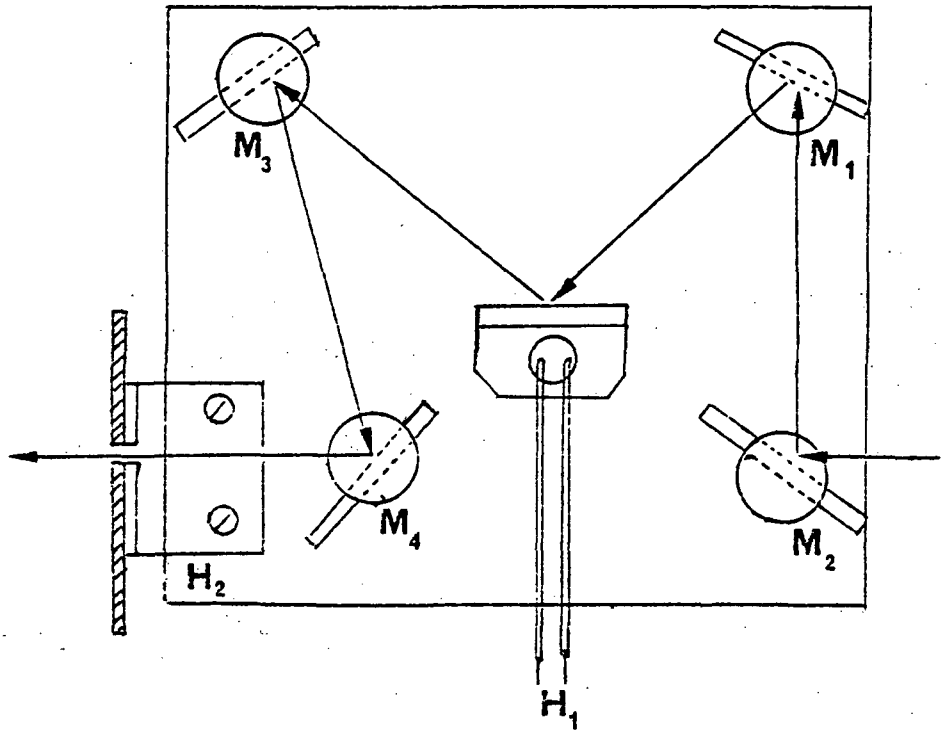

Where

M_1, M_2, M_3, and M_4 are reflectant mirror.

H_1 : heater

H_2 : holder

by heating at 200°C for various times.

A-5. Product Analysis

The products collected from the above preparations were identified by C-13 FT-NMR and FT-IR spectroscopy (Figs. 8-9, and Table 2). $CDCl_3$ (Aldrich; 99.8 atom %D, GOLD LABEL) was employed as solvent. The infrared spectra were obtained by KBr pellet. The endothermic/exothermic peak (under nitrogen atmosphere with a flow rate of 0.2 liter/min and a heating rate of 10°C/min) and char yield (under nitrogen atmosphere with a flow rate of 0.3 liter/min and a heating rate of 20°C/min) of each component were studied using DuPont 910 Differential Scanning Calorimeter and 951 Thermogravimetric Analyzer with 1090 Thermal Analyzer Record. Oxygen Indices were taken by using a General Electric CR 280FM 11B Oxygen Index Flammability Gauge. The epoxy resin was made into a pellet using a KBr die, and then placed in a sample cup mounted on the cup holder in the flame chamber. The mixture of oxygen and nitrogen was passed upward through the chimney at a flow rate of 3 to 5 cm/sec. The test followed the manual procedures[78]. The oxygen index was obtained from the equation as follows:

$$OI = \frac{[O_2]}{[O_2] + [N_2]}$$

where O_2 and N_2 are expressed in volume units.

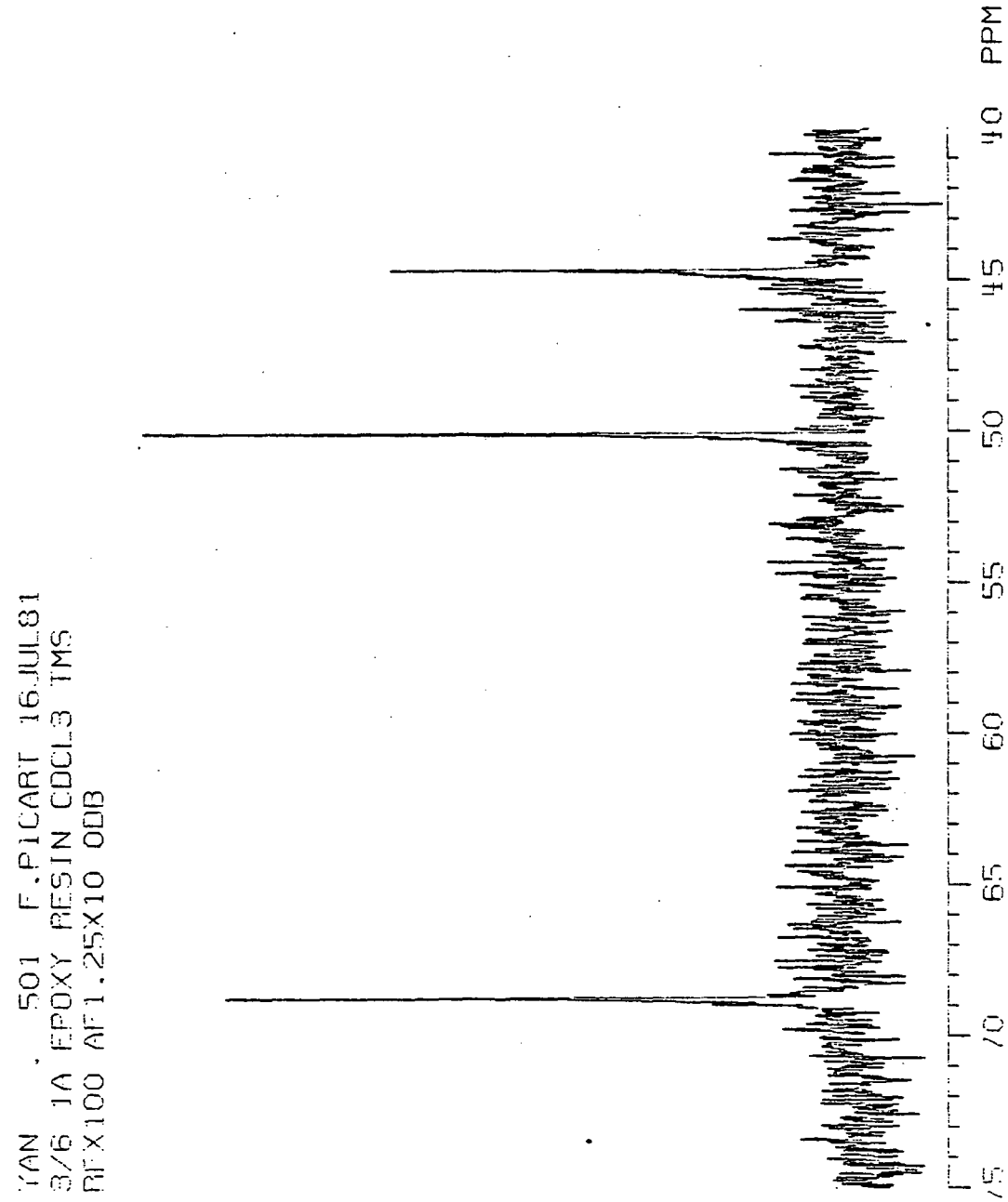

Figure 8. C-13 NMR spectrum of 2,6-DGESP in d-chloroform.

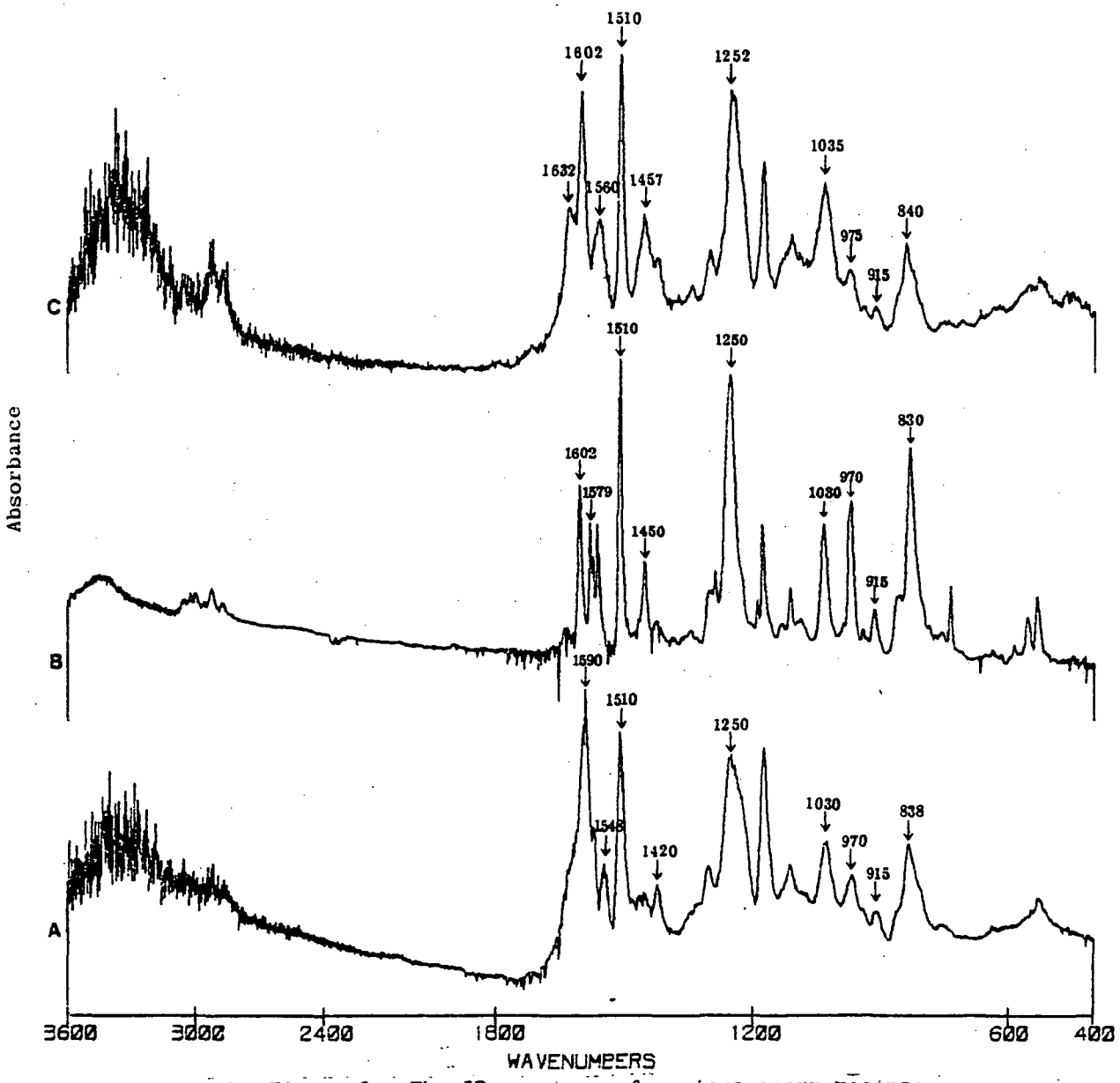

Figure 9. The IR spectrum of various epoxy resins: (A) 2,4-DGESP, (B) 2,6-DGESP, and (C) 2,4,6-TGESP (KBr pellet).

Table 2. The assignments of the IR spectra for 2,4-DGESP, 2,6-DGESP and 2,4,6-TGESP

vibration mode	Wavelength (cm^{-1})		
	2,4-DGESP	2,6-DGESP	2,4,6-TGESP
C=C stretching vibration with the benzene	1590 1450	1602 1450	1602 1632
C=C stretching vibration with the pyridine	1510 1548	1510 1579	1457 1510 1560
phenoxide	1250	1250	1252
C-H in-plane bending vibration of H-atom remains on a benzene	1030	1030	1030
C-H out-of-plane bending vibration of a H-atom remains on an ethylene (trans)	970	970	975
 epoxy ring	915	915	915
C-H out-of-plane bending vibration of 1,4-di-substituted benzene	838	830	840

B. Preparation of Polyarylates and Model Components

B-1. Preparation of Polyester from Hydroxy-Terminated Styrylpyridine with Terephthaloyl Chloride (TPC) and Isophthaloyl Chloride (IPC)

B-1-a. Model Components

(I) p-(β-2-vinylpyridyl)phenyl benzoate (p-VPPB)

(II) p,p'-Bis(β-2-vinylpyridyl)diphenyl isophthalate (p,p'-BVPDPI)

(III) p,p'-Bis(β-2-vinylpyridyl)diphenyl terephthalate-(p,p'-BVPDPT)

(IV) p,p'-2,6-(β-2-vinylpyridyl)diphenyl dibenzoate-(p,p'-2,6-VPDPDB)

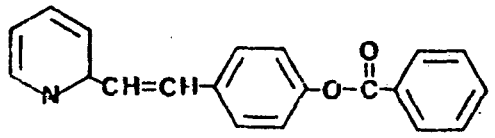

(I)

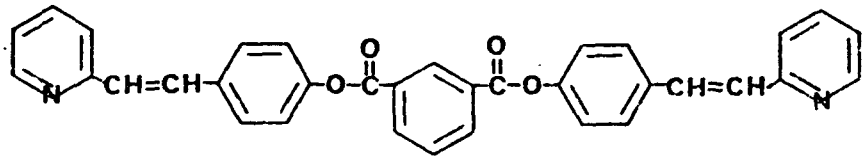

(II)

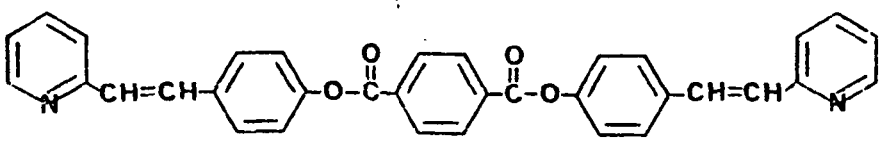

(III)

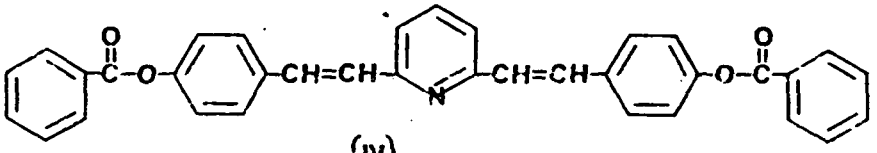

(IV)

The preparation of hydroxy-terminated styrylpyridine has been described on page 6 . The model esters were prepared by an interfacial reaction. The scheme for the reaction is as follows[79]:

INTERFACIAL REACTION

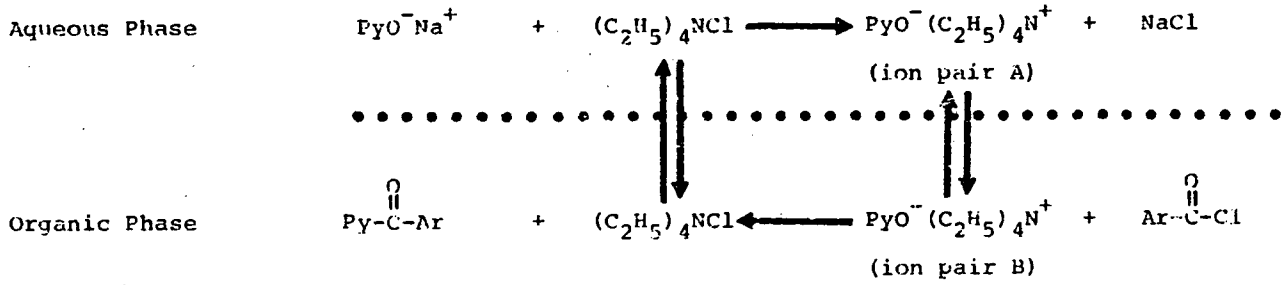

where: PyO^-Na: (p-hydroxystyryl)pyridine salt.

$Ar\text{-}\overset{O}{\overset{\|}{C}}\text{-}Cl$: Acyl chloride (benzoyl chloride, terephthaloyl chloride).

Solvent: organic phase (1,2 dichloroethane).

ion pair: depend on the partition coefficent of aqueous and organic solvent

$(C_2H_5)_4N^+Cl^-$: Phase-transfer agent.

In the above reaction, the water soluble nucleophile was dissolved in an aqueous NaOH solution, the phase-transfer catalyst, $(C_2H_5)_4N^+Cl^-$, allows for the transfer of the nucleophile as an ion-pair ($PyO^-(C_2H_5)_4N^+$) into the organic phase where later reaction with the organic reagent, $Ar\text{-}\overset{O}{\overset{\|}{C}}\text{-}Cl$ occurred. Migration of the cationic catalyst back to the aqueous phase completes the cycle, which continues until equilibrium has been established or until the nucleophile, PyO^-, or the organic compound,

$Ar-\overset{O}{\overset{\|}{C}}-Cl$, have been completely consumed.

A 500ml resin kettle was fitted with stirrer, dropping funnels, and a condenser connected with a drying tube. All the equipment was dried and flushed with nitrogen for 10 minutes. Monohydroxy-terminated styrylpyridine (0.02 mole), NaOH (0.05 mole) and 200ml of distilled water were placed in the resin kettle and cooled with stirring to $0^{o}C$ in an ice-water bath. A solution of mono or diacid chloride (0.01 to 0.02 mole) in 150ml of 1,2 dichloroethane was placed in a dropping funnel. The $(C_2H_5)_4NCl \cdot H_2O$ (10 gram), a phase transfer agent, was dissolved in 50ml of 1,2 dichloroethane and poured into the resin kettle. The rate of addition of diacid chloride was controlled; the complete addition required 3 hours. After completion of the reaction, stirring was continued for one more hour until the reaction kettle reached room temperature. The solids were filtered, washed twice with 20% NaOH (300 ml) subsequently rinsed with water. Recrystallization was done from 1,2 dichloroethane/ethanol (in a 4:1 volume ratio) and dried in vacuum oven at $80^{o}C$ for 2 days. The products were characterized by various methods (Tables 3,4; and Fig.10 with Table 5). In the case of p,p'-2,6-VPDPDB, the acid chloride and dihydroxy-terminated styrylpyridine were mixed by dropping dihydroxy-terminated styrylpyridine into the acid chloride.

Table 3.The chemical and physical constant for p-VPPB, p,p'-BVPDPI, p,p'-BVPDPT, p,p'-2,6VPDPDB, and p,p'-BVPDPC.

compound	melting point (^{0}C) (observed)	λ_{max}(nm)	log ε	H/C*	H/C**
p-VPPB	159.5-161.5	318	4.52	4.98/79.73	4.87/79.48
p,p'BVPDPI	213.2-214.5	319	4.85	4.58/77.86	4.61/77.62
p,p-BVPDPT	260.5-263.0	319	4.79	4.58/77.86	4.30/77.23
p,p'2,6VPDPDB	188.1-189.7	345	4.67	4.78/80.31	4.56/80.23
p,p'-BVPDPC	210.0-214.0	319	4.85	4.76/77.14	4.87/77.10

* : theoretical ratio of hydrogen/carbon

**: found ratio of hydrogen/carbon

Table 4. The oxygen index and char yield (TGA residue, 800 °C, under nitrogen) for model components and polymers.

component	(I)	(II)	(III)	(IV)	(V)	(VI)	(VII)	(VIII)	(IX)	(X)	(XI)
char yield	1.0	34.8	35.5	54.5	53.5	31.0	54.5	51.2	18.0	53.8	54.3
oxygen index	21.5	28.0	27.5	33.2	34.6	24.7	33.0	33.9	23.2	33.9	34.9

I. : p-(β-2-vinylpyridyl)phenyl benzoate (p-VPPB).
II. : p,p'-Bis(β-2-vinylpyridyl)diphenyl isophthalate (p,p'-BVPDPI).
III. : p,p'-Bis(β-2-vinylpyridyl)diphenyl terephthalate} (p,p'-BVPDPT).
IV. : poly-{2,4(β-vinylpyridyl)diphenyl isophthalate} poly(2,4VPDPI).
V. : poly-{2,4(β-vinylpyridyl)diphenyl terephthalate poly(2,4VPDPT).
VI. : p,p'-2,6(β-2-vinylpyridyl)diphenyl dibenzoate (p,p'-2,6VPDPDB).
VII. : poly-{2,6(β-vinylpyridyl)diphenyl isophthalate} poly(2,6VPDPI).
VIII. : poly-{2,6(β-vinylpyridyl)diphenyl terephthalate} poly(2,6VPDPT).
IX. : p,p'-Bis(β-2-vinylpyridyl)diphenyl carbonate (p,p'-BVPDPC).
X. : poly-{2.4(β-vinylpyridyl)diphenyl carbonate} poly(2,4VPDPC).
XI. : poly-{2,6(β-vinylpyridyl)diphenyl carbonate} poly(2,6VPDPC).

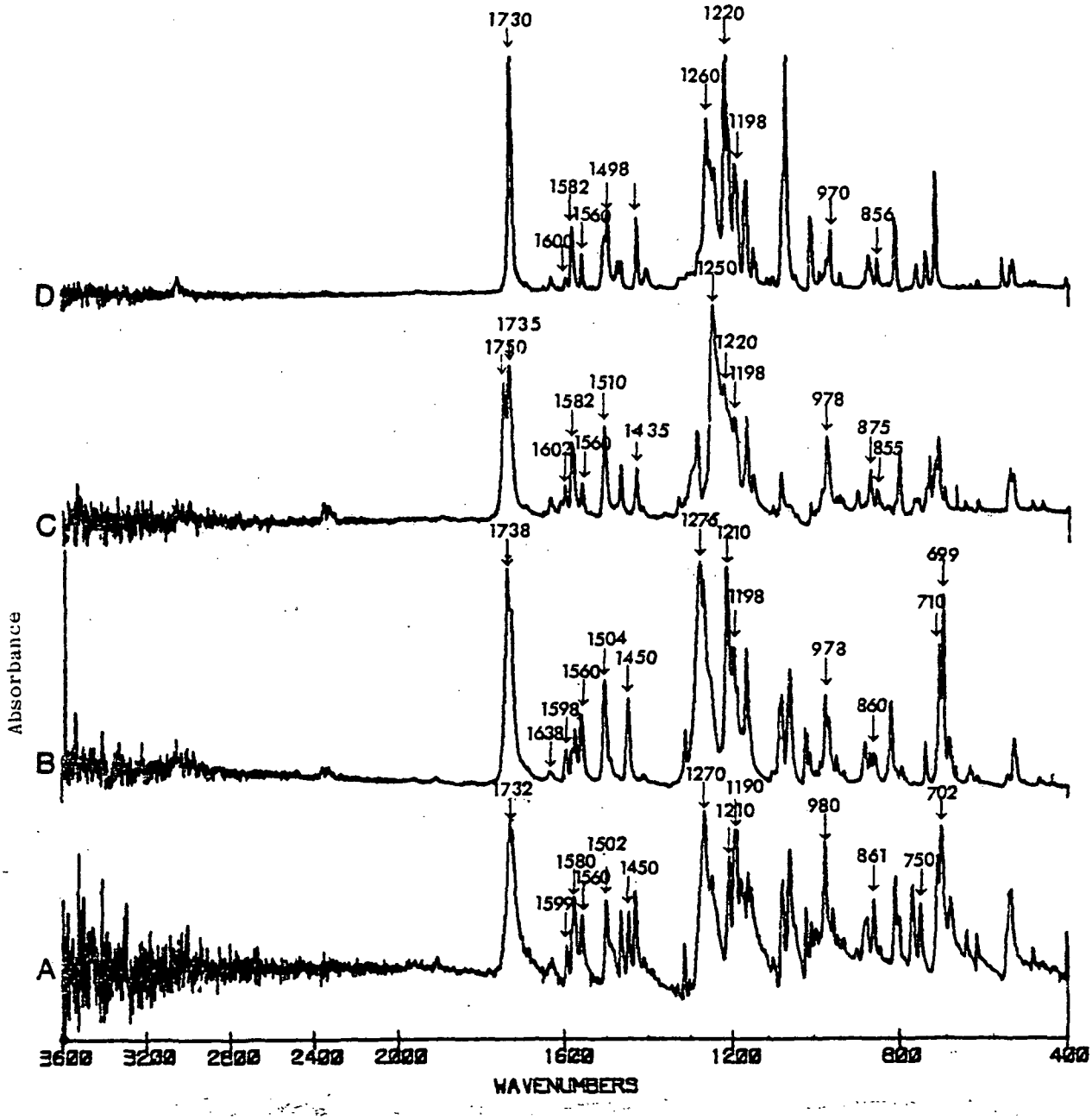

Figure 10. The IR spectrum of various components: (A) p-VPPB, (B) p,p'-2,6-VPDPDB, (C) p,p'-BVPDPI, and (D) p,p'-BVPDPT (KBr pellet).

Table 5. The assignments of the IR spectrum for p-VPPB, p,p'-2,6VPDPB, p,p'-BVPDPI, and p,p'-BVPDPT.

vibration mode	wavelength(cm^{-1})			
	p-VPPB	p,p'-2,6VPDPB	p,p-BVPDPI	p,p'-BVPDPT
C=O stretching vibration	1732	1739	1750	1730
C=C stretching vibration with the benzene ring	1509, 1580 1502, 1450	1638, 1598 1504, 1450	1602, 1582 1510, 1435	1600, 1582 1498, 1430
C=C stretching vibration with the pyridine ring	1560	1560	1560	1560
Ph-O C-O stretching vibration	1270	1250	1260	1276
O ‖ -C-O C-O stretching vibration	1210, 1190	1210, 1198	1220, 1198	1220, 1198
C-H out-of plane bending vibration of a H-atom remains on an ethylene (trans)	980	978	978	970
C-H bending vibration aromatic, one adjacent H atom			875	
C-H bending vibration aromatic, two adjacents H atom	861	860	855	856
C-H bending vibration aromatic, five adjacents H atoms	750, 702	710, 699		

B-1-b. Polyester Synthesis[75a]

(V) poly 2,4(β-vinylpyridyl)diphenyl isophthalate
poly(2,4-VPDPI)

(VI) poly 2,4(β-vinylpyridyl)diphenyl terephthalate
poly(2,4-VPDPT)

(VII) poly 2,6(β-vinylpyridyl)diphenyl isophthalate
poly(2,6-VPDPI)

(VIII) poly 2,6(β-vinylpyridyl)diphenyl terephthalate
poly(2,6-VPDPT)

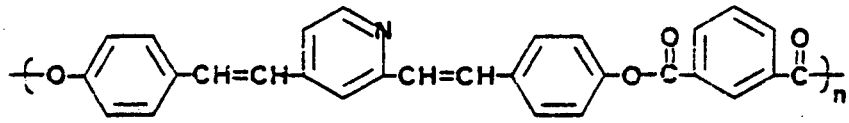

(V)

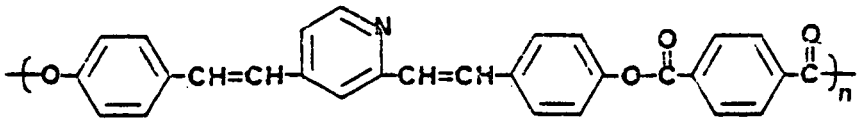

(VI)

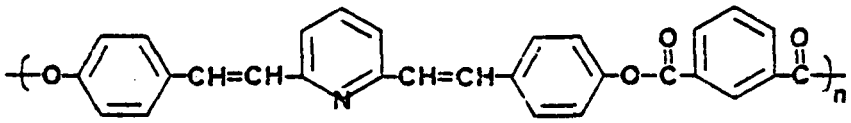

(VII)

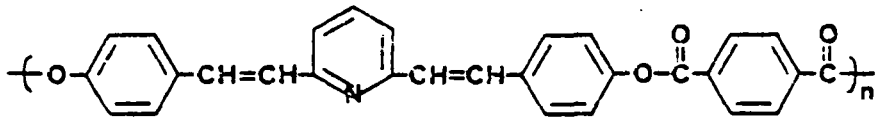

(VIII)

0.01 mole of di(p-hydroxystyryl)pyridine, 0.8 gram of NaOH, and 1.5 gram of tetraethylammonium chloride monohydrate were dispersed in 200 ml of water using a high-speed blender. To this mixture, 0.01 mole of diacid chloride in 50 ml dichloroethane was added quickly and the resulting mixture was stirred vigorously for five minutes. The polymer was rapidly precipitated on the wall of the blender. After five minutes, 250 ml of n-hexane was added and stirring was continued. The polymer was collected, washed twice with 100 ml portion of 20% NaOH; the product was then washed with water and subsequently with ethanol and then dried in vacuum oven at 80°C fot 2 days. The characterization data were shown in Table 4 , Fig.11, and Table 6 for assignment of FT-IR.

B-2. Preparation of Polycarbonates from hydroxy-terminated Styrylpyridine with Phosgene[75,80]

B-2-a. Model Component

(IX) p,p-Bis(β-2-vinylpyridyl)diphenyl carbonate (p,p'-BVPDPC)

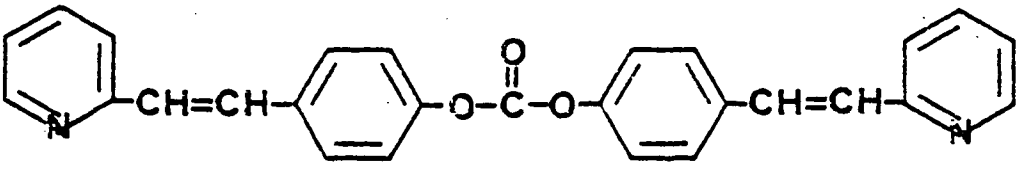

A 500 ml round-bottom flask was fitted with a stirrer, a condenser with a drying tube, and a gas inlet adapter tube which reached the bottom of the flask. All the equipment

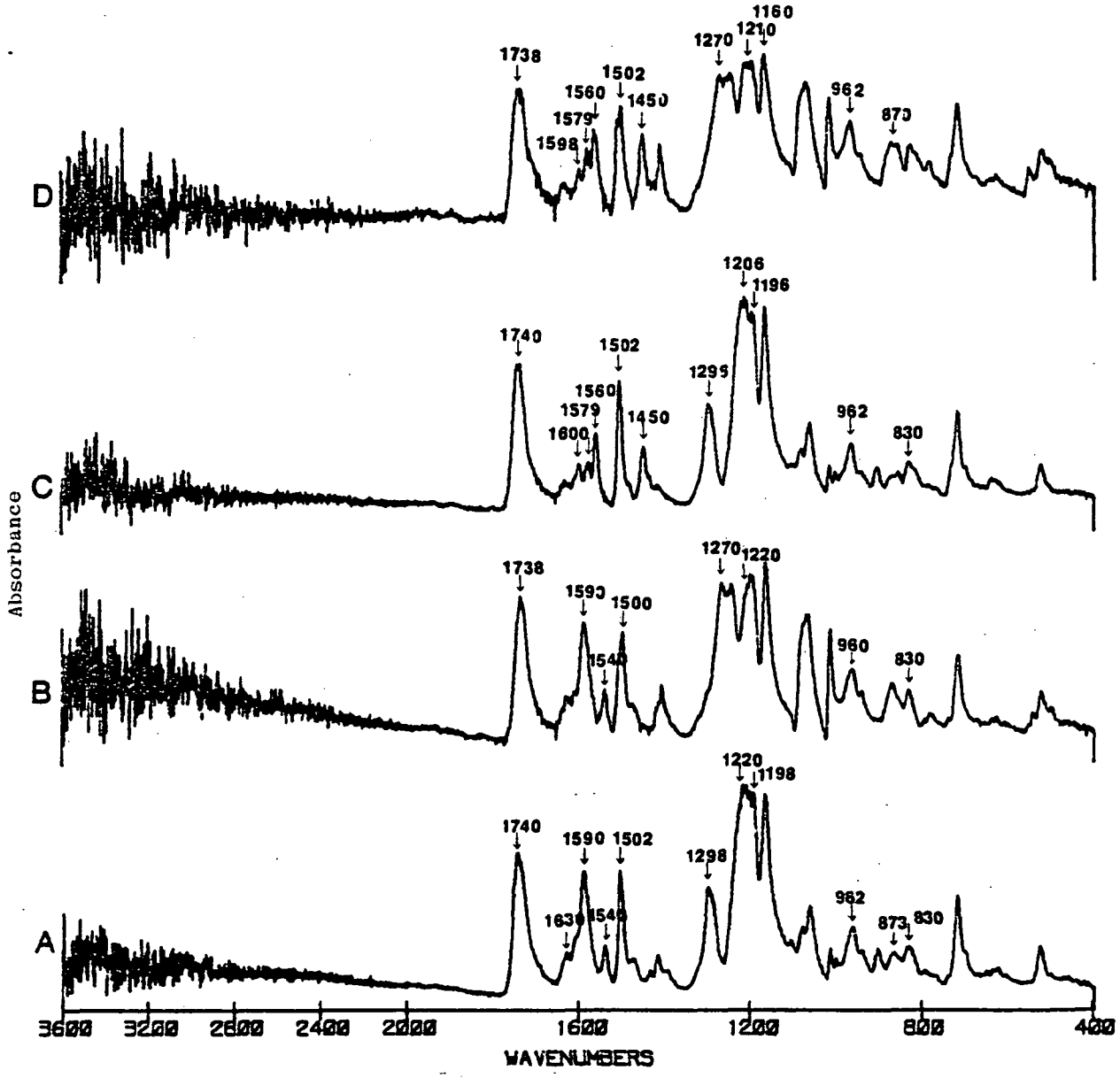

Figure 11. The IR spectrum of various components: (A) poly(2,4-VPDDPI), (B) poly(2,4-VPDPT), poly(2,6-VPDPI), and (D) poly(2,6-VPDPT) (KBr pellet).

Table 6. The assignments of the IR spectrum for poly(2,4VPDPI), poly(2,4VPDPT), poly(2,6VPDPI), and poly(2,6VPDPT).

vibration mode	wavelength (cm^{-1})			
	poly(2,4VPDPI)	poly(2,4VPDPT)	poly(2,6VPDPI)	poly(2,6VPDPT)
C=O stretching vibration	1740	1738	1740	1738
C=C stretching vibration with the benzene	1630, 1590 1502	1590, 1500	1600, 1579 1502, 1450	1598, 1579 1502, 1450
C=C stretching vibration with the pyridine	1540	1540	1560	1560
Ph-O C-O stretching vibration	1298	1270	1296	1270
O ‖ -C-O C-O stretching vibration	1220, 1198	1220	1206, 1196	1210, 1160
C-H out-of plane bending vibration of a H-atom remains on an ethylene (trans)	962	960	962	962
C-H bending vibration aromatic, one adjacent H atom	873			870
C-H bending vibration aromatic, two adjacent H atom	830	830	830	

was dried and flushed with nitrogen for 10 minutes. Monohydroxy-terminated styrylpyridine (0.01 mole), 0.015 mole of NaOH and 200 ml of distilled water were placed in the flask. The mixture was stirred vigorously and kept in an ice-water bath. The $(C_2H_5)_4NCl \cdot H_2O$ (0.08 mole), a phase transfer agent, was dissolved in 50 ml of 1,2-dichloroethane and poured into the flask. Phosgene gas was then bubbled into the solution at a controlled rate of 1 ml/min. After 2 minutes, the solution was observed to become cloudy and the pH of the solution decreased as a result of the addition of phosgene, a small amount of product was obtained, and in order to increase the yield, 10 ml of 20% NaOH was added and phosgene was again bubbled through the solution for 30 minutes. The product was pale yellow in color. The product was then washed twice with 50 ml of 20% NaOH, the color of the material became white. Subsequently, the product was washed generously with water and recrystallized from ethanol. The characterization data is shown in Tables 3,4, Fig. 12 and Table 7 for FT-IR assignments.

B-2-b Polycarbonates Synthesis

(X) poly 2,4(β-vinylpyridyl)diphenyl carbonate

poly(2,4-VPDPC)

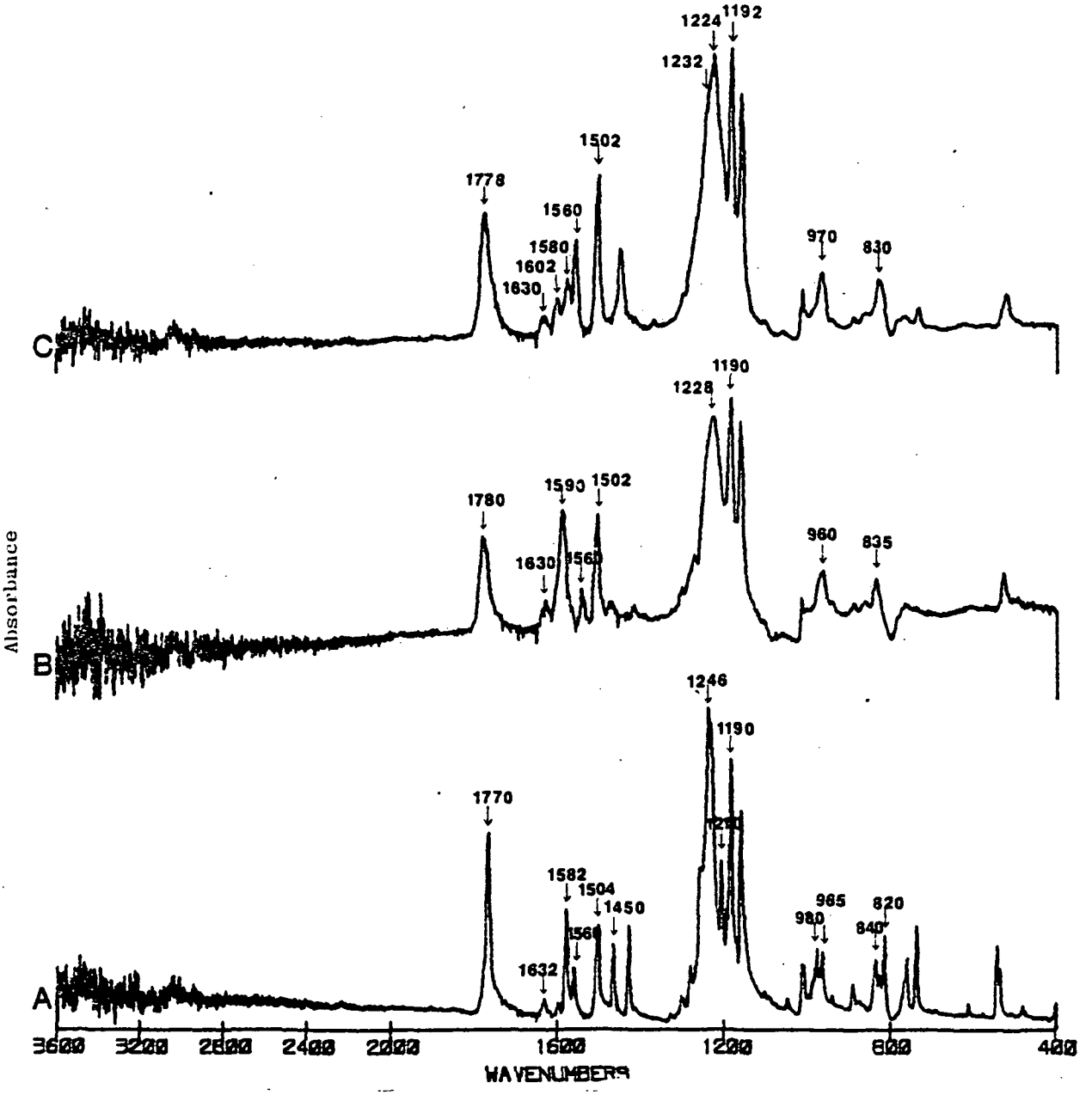

Figure 12. The IR spectrum of various components: (A) p,p'-BVPDPC, (B) poly(2,4-VPDPC), (C) poly(2,6-VPDPC)(KBr pellet).

Table 7. The assignments of the IR spectrum for p,p'-BVPDPC, poly(2,4VPDPC), and poly(2,6VPDPC).

vibration mode	wavelength (cm^{-1})		
	p,p'-BVPDPC	poly(2,4VPDPC)	poly(2,6VPDPC)
C=O stretching vibration	1770	1780	1778
C=C stretching vibration with the benzene	1632, 1582 1504, 1450	1630, 1590 1502	1630, 1602 1580, 1502
C=C stretching vibration with the pyridine	1560	1560	1560
Ph-O C-O stretching vibration	1246	1228	1232
O ‖ -C-O C-O stretching vibration	1210, 1190	1190	1224, 1192
C-H out-of plane bending vibration of a H-atom remains on an ethylene (trans)	980, 965	960	970
C-H bending vibration aromatic, two adjacents H-atom	840, 820	835	830

(XI) poly 2,6(β-vinylpyridyl)diphenyl carbonate

poly(2,6-VPDPC)

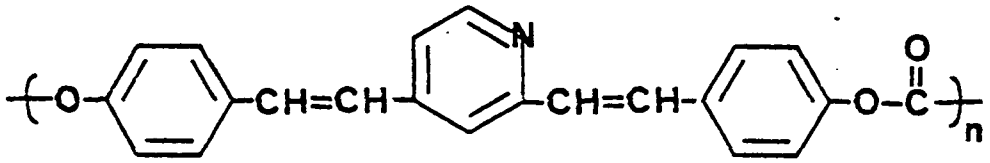

(X)

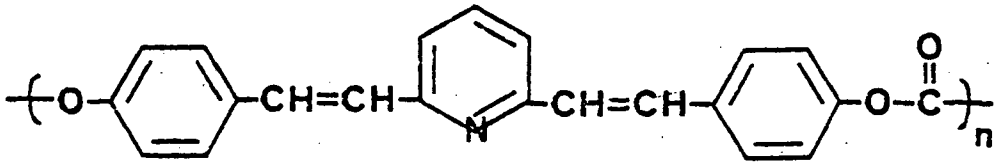

(XI)

The procedure used for the preparation of the above compounds was the same as the procedure mentioned in the proceding section. The only difference was that di-(p-hydroxystyrylpyridine was used instead of mono-(p-hydroxystyryl)pyridine.

C. Preparation of Styrylpyridine Based Polytriazines(PTP)

C-1. Synthesis of Cyanobenzaldehyde[81,82]

To a cooled mixture of 38 grams of para-tolunitrile, 450 ml acetic acid, and 450 ml acetic anhydride was added 67 ml of concentrated H_2SO_4. Stirring was vigorous so that the temperature did not exceed 25°C. The solution was then cooled to 5°C, and 72 grams of finely ground chromic acid were added at a very slow rate of one gram per minute. During the addition, the temperature was maintained between 5 to 8°C. Ninety minutes

after the chromic acid was added, the temperature began to rise slowly. When the temperature reached 10°C, the stirring was interrupted and the reaction mixture was left overnight. The contents of the reaction vessel were then poured over 2.5 Kg of ice and 2 Kg of water. The fine colorless precipitate was filtered, washed with water, resuspended in 400 ml of 2% Na_2CO_3, filtered, washed, dried and finally refluxed for thirty minutes with a mixture of 7 ml concentrated sulfuric acid, 75 ml ethyl alcohol, and 100 ml water. From the filtered solution, a mixture of p-cyano-benzaldehyde and oil separated upon standing. The mixture of cyanobenzaldehyde and oil was left overnight to allow the cyanobenzaldehyde to crystallize. The mixture was filtered and cyanobenzaldehyde was isolated. Then it was sublimated and subsequently recrystallized from ethanol.

The oil from which the cyanobenzaldehyde was separated, was diluted with an equal volume of water. Thereby the oil was induced to crystallize, yielding the para-carbamidobenzaldehyde. This sample was later refluxed with a mixture of acetic anhydride and one drop of sulfuric acid. The crystals which separated upon standing were recrystallized from dilute ethanol, producing a small amount of para-carbamidobenzaldiacetate, which was later used to produce more cyanobenzaldehyde. m.p. 76-77°C (lit. 75-76°C)[81].

A mixture of 6.4 grams of para-carbamidobenzaldiacetate and 12 ml of thionyl chloride was refluxed for two hours and the excess thionyl chloride was distilled off. Then the remaining red oil, 20 ml of alcohol, 20 ml of water, and 4 ml of 0.1 N sulfonic acid were added and the mixture was refluxed again for one hour. The filtered solution was diluted with an equal volume of water and cooled to 0°C, whereupon p-cyanobenzaldehyde crystallized, and was then recrystallized from ethanol.

C-2. Monomer Synthesis

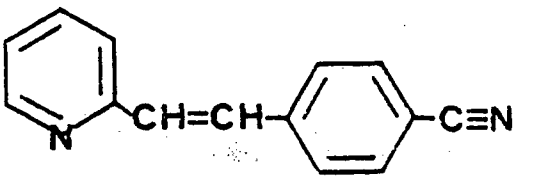

(2-(p-CN)SP)

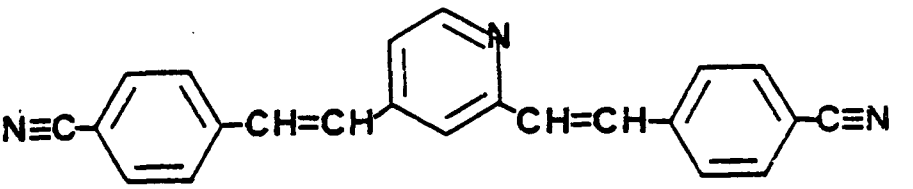

(2,4-D(p-CN)SP)

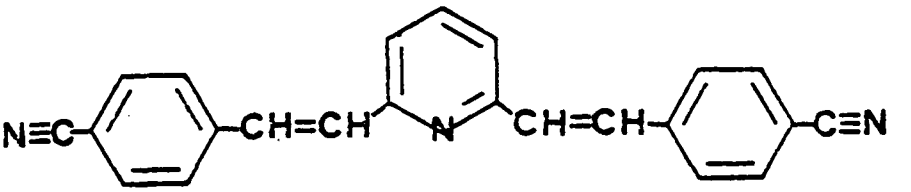

(2,6-D(p-CN)SP)

A mixture of 2-picoline (0.01 mole; lutidine 0.01 mole) p-cyanobenzaldehyde (0.012 mole; 0.023 mole of lutidine), and acetic anhydride (0.01 mole; 0.02 of lutidine) was refluxed under nitrogen for 10 hours using an oil bath at 160 170°C. After 10 hours, the solution was poured into 400 ml of ice-water and stirred for about 30 minutes to hydrolyze the excess acetic anhydride. The brown solid which remained was filtered, washed several times with water, and recrystallized repeatedly from 80% ethanol. Characterization results are shown in Table 8. IR spectra are shown in Fig. 13, and the assignments for each of the characteristic peaks in the IR spectra are listed in Table 9.

C-3. Polymer Synthesis[71,83]

Three portions of 0.01 mole of di-cyanostyrylpyridine were placed in three 100 ml three-necked round bottom flasks at 0°C under nitrogen. During a period of 30 minutes, 0.3 mole (20 ml) of chlorosulfonic acid was slowly added to the flasks with stirring. The mixture was allowed to stand at room temperature for varying time periods, then poured into ice-water, filtered and washed several times with water and ethanol. Dark-yellow polymers were obtained. The characterization data is shown in Table 10.

D Preparation of Styrylpyridine Prepolymers(PSP)[84]

To a 100 ml three-necked round bottom flask

Table 8. The characterization data for 2-(p-CN)SP, 2,4-D(p-CN)SP and 2,6-D(p-CN)SP

component	M.P. ^{o}C (reported)	M.P. ^{o}C (observed) onset	melted	LOI	$Y_{800^{o}C}$	H/C (1)	H/C (2)
2-(p-CN)SP		127.0	133.3	28.1	2.05	4.85/81.55	4.90/81.43
2,4-D(p-CN)SP		213.3	218.6	31.5	13.56	4.50/82.88	4.60/82.24
2,6-D(p-CN)SP	175-176*	171.5	176.1	32.0	19.97	4.50/82.88	4.45/82.26

* E. D. Bergmann and S. Pinchas, J. Org. Chem., 15, 1184 (1950).

$Y_{800^{o}C}$: char yield at 800^{o}C under nitrogen; measured by TGA

(1) : theoretical ratio of H/C

(2) : found ratio of H/C

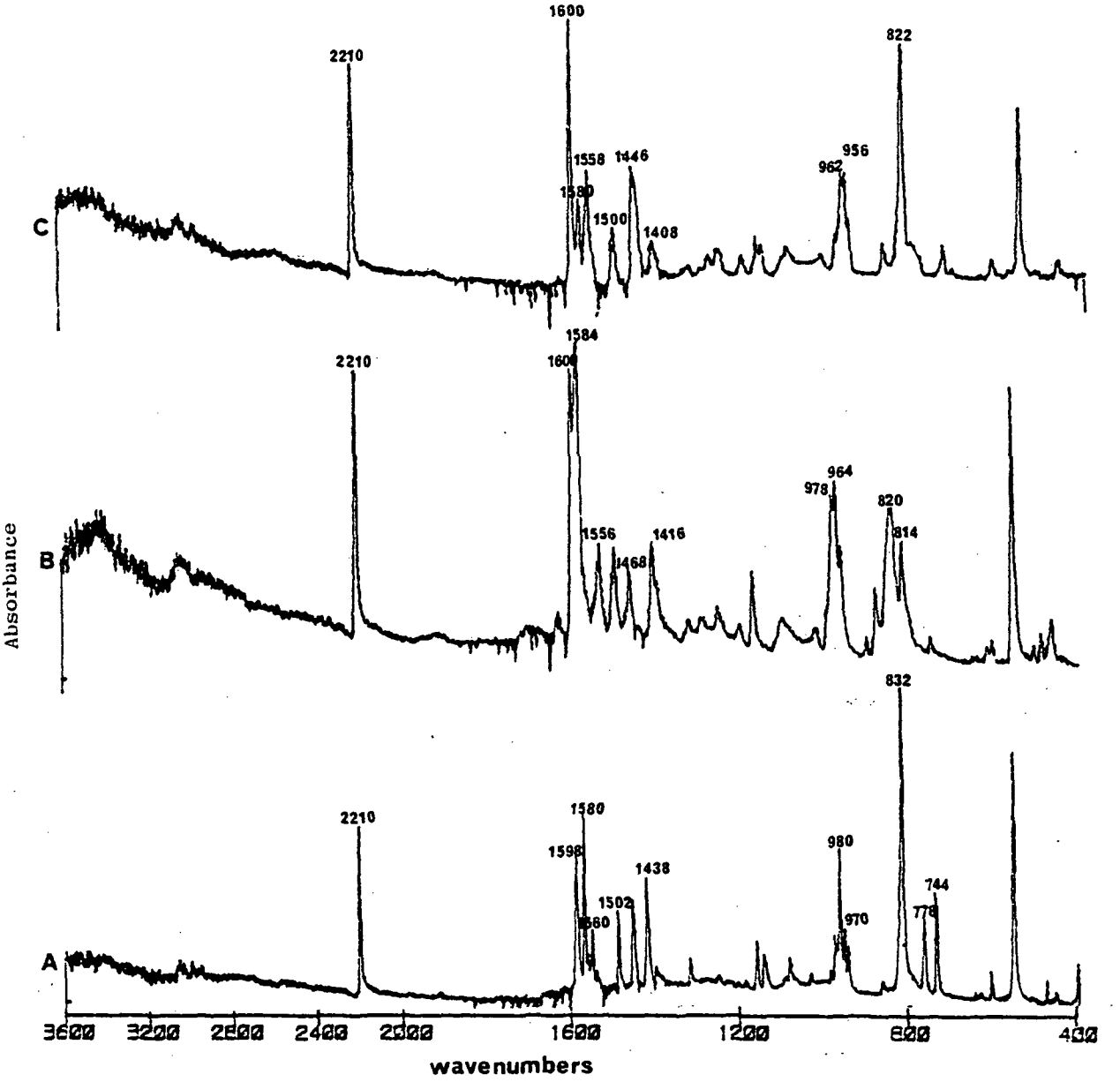

Figure 13. The IR spectrum of various components: (A) 2-(p-CN)SP, (B) 2,4-D(p-CN)SP, and (C) 2,6-D(p-CN)SP (KBr pellet).

Table 9. The assignment of the IR spectra for 2-(p-CN)SP, 2,4-D(p-CN)SP, and 2,6-D(p-CN)SP. KBr pellet.

vibration mode	wavelength (cm^{-1})		
	2-(p-CN)SP	2,4-D9p-CN)SP	2,6-D9p-CN)SP
C≡N stretching vibration	2210	2210	2210
C=C stretching vibration with the benzene	1598, 1580 1502, 1438	1600, 1584 1500	1600, 1580 1500, 1446
C=C stretching vibration with the pyridine	1560	1556	1558
C-H out-of-plane bending vibration of a H-atom remains on an ethylene(trans)	980, 970	978,964	962, 956
C-H bending vibration aromatic, two adjacents H-atom	832	820,814	822

Table 10. The characterization data for styrylpyridine triazine polymers (SPT)

polymer	trimerization time (hour)	softening point[a]	exotherm peak[a]	$Y^{b}_{800^{o}C}$	LOI[c]
2,4-SPT	48	235.2-264.2	321.6-338.1	50.37	33.9
2,6-SPT	24	225.9-239.1	320.6-345.0	42.36	29.5
2,6-SPT	48	218.4-238.1	320.0-350.0	43.52	36.0

a : measured by DSC, as a broad endotherm.

b : char yield at $800^{o}C$ under nitrogen; measured by TGA.

c : limiting oxygen index.

provided with stirrer, a thermometer and a reflux condenser, there was introduced 0.1 mole of terephthalic dialdehyde and 0.11 mole of the methyl derivatives of pyridine. After the reactants were dissolved at 60°C under a nitrogen stream, 0.003 mole of zinc chloride was added as a catalyst. The mixture was heated with refluxing for three hours. After three hours, the viscous solution was dissolved in acetone and then poured into ethyl ether with stirring. The prepolymer, PSP, precipitated and was washed several times with 0.01 N NaOH, water, and ethanol, then dried under vacuum at 60°C for 2 days. The characterization data is shown in Table 11.

Table 11. The characterization data for polystyrylpyridine (PSP)

polymer	Softening point[a] ^{o}C	exotherm peak[a] ^{o}C	$Y_{800^{o}C}$[b]	LOI[c]
2,4-PSP	164.0-223.4	397.2-446.0	73.28	32.5
2,6-PSP	177.6-207.1	337.8-379.8	67.79	33.2
2,4,6-PSP	195.0-219.2	393.2-441.6	72.37	33.9

a : measured by DSC, as a broad exotherm.

b : char yield at $800^{o}C$ under nitrogen; measured by TGA.

c : limiting oxygen index.

III. RESULTS AND DISCUSSION

A. Styrylpyridine Based Polymers : Epoxy Resins

A-1. Equivalent Weight Study on 2,6-Diglycidyl Ether of Styrylpyridine

Carbon -13 NMR has become an extremely valuable technique for analysis of organic polymers. This is due to the large C-13 chemical shift range and high sensitivity of the C-13 nucleus to chemical substituents effects. Modern Fourier Transfer NMR (FT-NMR) spectrometer systems have made the technique extremely efficient and easy to apply. In polymer chemistry, C-13 NMR has been used mostly for the analysis of thermoplastic polymers. W.B. Moniz [85] studied and characterized the cure of an epoxy resin system in a standard C-13 FT-NMR spectrometer. W.B. Moniz and C.F. Poranski [86a] have developed a method to determine the EEW of epoxy resins by C-13 NMR. In their paper, the three lines (Fig. 14) at 44, 50, and 70 ppm form the basis for the C-13 method of EEW determination. As n in the general oligomer structure increased, the number of bridging carbon increased, but the number of terminal epoxide group remained the same, at two per oligomer molecule. For the idealized n-oligomer, the ratio of terminal glycidyl ether carbons of types c, d, or e, to bridging carbons (type b) is 2/3n.

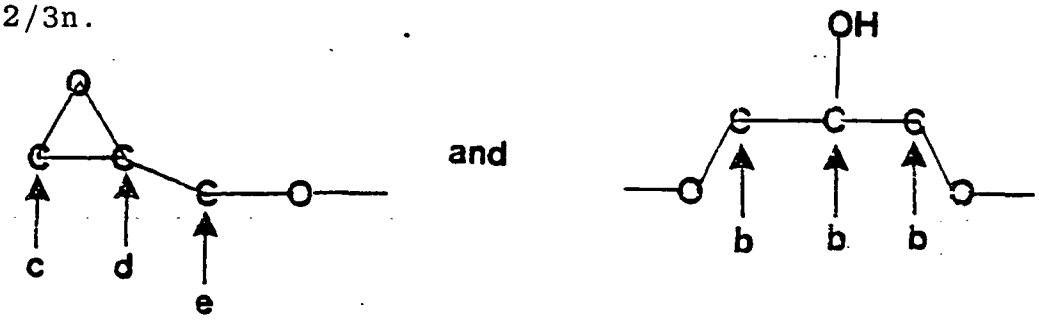

Figure 14. The 40-70 ppm region of the carbon 13 NMR spectra (15 MHz) of two epoxy resins.

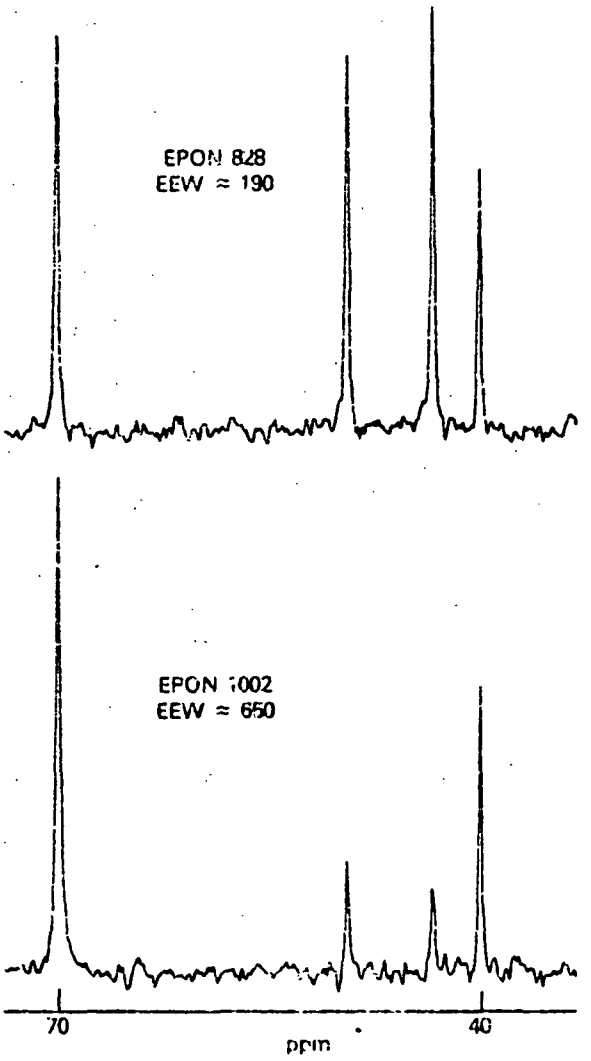

The 40–70 ppm region of the carbon-13 NMR spectra (15 MHz) of two epoxy resins

The intensity of the carbon 13 line at 70 ppm is the sum of the intensities of the line due to the terminal ether methylene carbon, I_e, and those due to the bridging carbons, I_b. Although I_e can not be measured directly, its value can be obtained by measuring either the line at 44 ppm (I_c) or the line at 50 ppm (I_d) or their average value, I'. Thus the ratio, 2/3n, can be expressed by I'/I_b-I' and

$$n = 2 (I_b-I')/ 3I'$$

The above equation is ambiguous [86b]. Subsequently, this equation was corrected to

$$I_e = I' = \frac{Ic + Id}{2} = \frac{I_{44} + I_{50}}{2}$$

$$I_{70} = I_b + I_e$$

$$I_b = I_{70} - I_e = I_{70} - I'$$

$$2/3n \cong \frac{\text{terminal glycidy ether carbon of types c,d, or e}}{\text{bridge carbon}}$$

$$2/3n = \frac{I'}{I_{70}-I'}$$

$$\therefore n = \frac{2(I_{70} - I')}{3I'}$$

Page Intentionally Left Blank

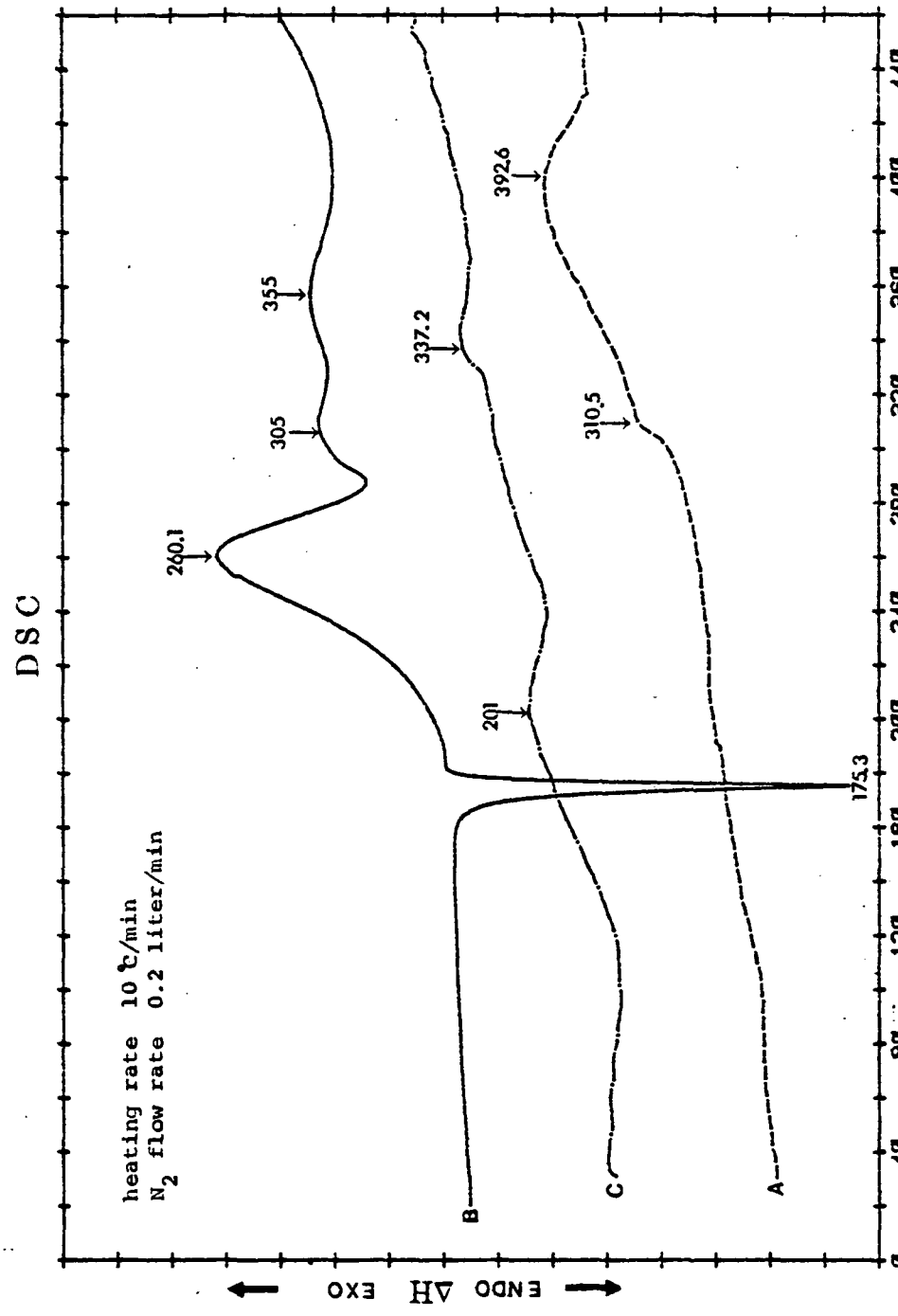

Figure 15. The DSC thermogram of various epoxy resins: (A) 2,4-DGESP, (B) 2,6-DGESP, and (C) 2,4,6-TGESP.

resin. Lopata [30] showed that the process seemed likely for unreacted epoxide groups by comparing the cured and uncured epoxy resin using infrared spectroscopy. The exothermic peaks in Fig. 13 are not only due to the epoxy group, but also to (i) thermal reaction (Diels-Alder reaction), (ii) isomerization of the unreacted epoxide group resin to the carbonyl group, and (iii) the thermal decomposition of the epoxy resin. The first two processes are known to be highly exothermic, and thus they could contribute to the observed exothermic behavior. That the unreacted epoxide groups and Diels-Alder reaction contributed to the exotherms at 310° and 390°C in the thermally cured epoxy resin was also shown by studying the polymerization reaction via infrared spectroscopy and DSC. Early in the thermal cure cycle, many of the epoxide rings and double bonds are unreacted, as shown by strong absorptions at 915 cm^{-1} and 970 cm^{-1} in the IR spectrum and also a large exotherm (390°C) in the DSC thermogram. As the cure proceeded, the epoxide ring was opened to give an ether linkage, and the absorption bands, at 1250, and 915 cm^{-1} decreased in intensity (see Figs. 16, 17; and Table 12). Meanwhile, the Diels-Alder reaction was occuring to form a ring, and the absorption band at 970 cm^{-1} decreased in intensity (Figs. 16, 17). Simultaneously, diminished exotherm peak at 390°C were

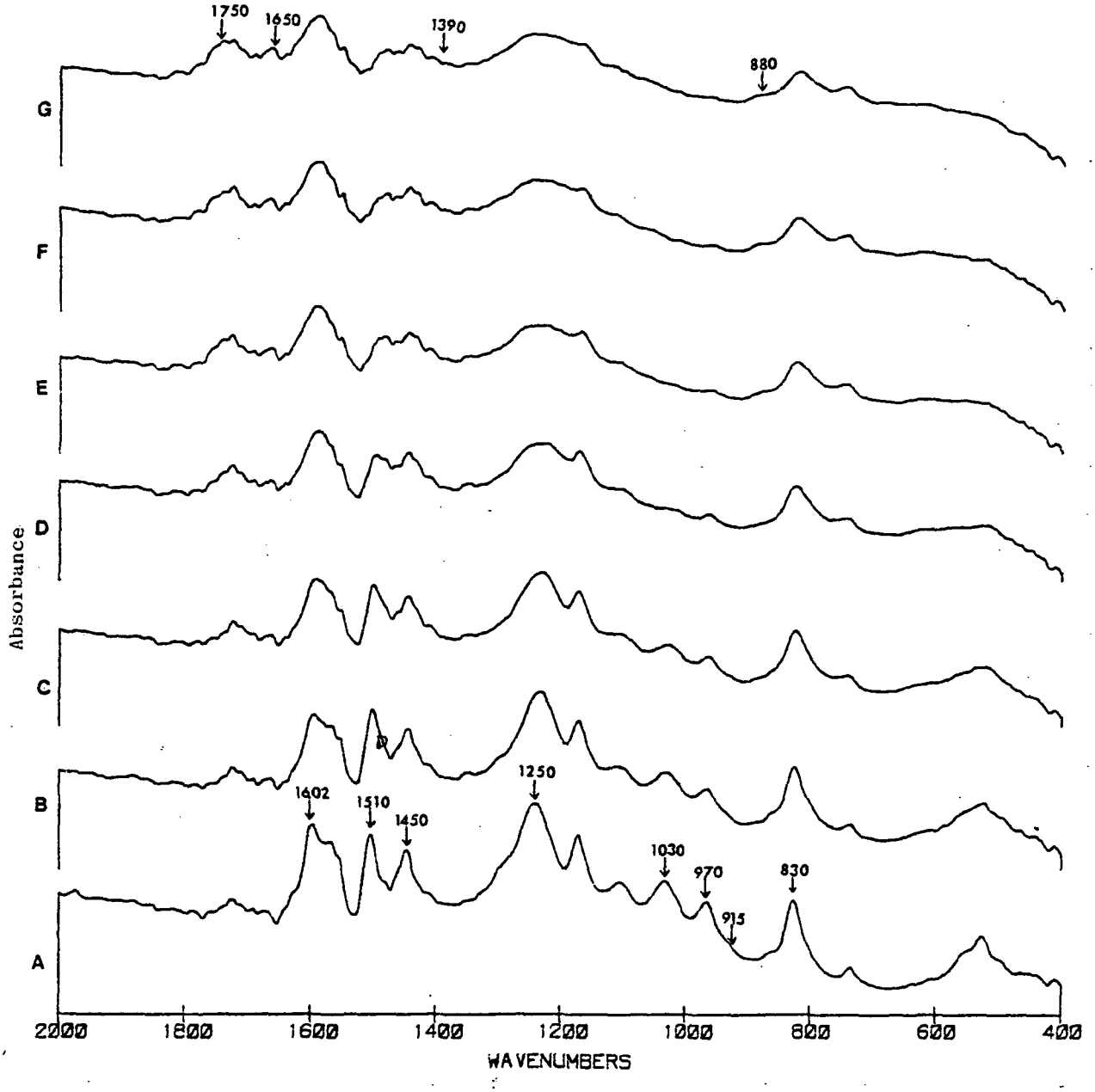

Figure 16. The IR spectrum of 2,6-DGESP cast on Al surface under nitrogen and after heating at 250°C and various times. (A) 0 hr , (B) 0.5 hr, (C) 1 hr, (D) 2 hr, (E) 3 hr, (F) 4 hr, and (G) 5 hr.

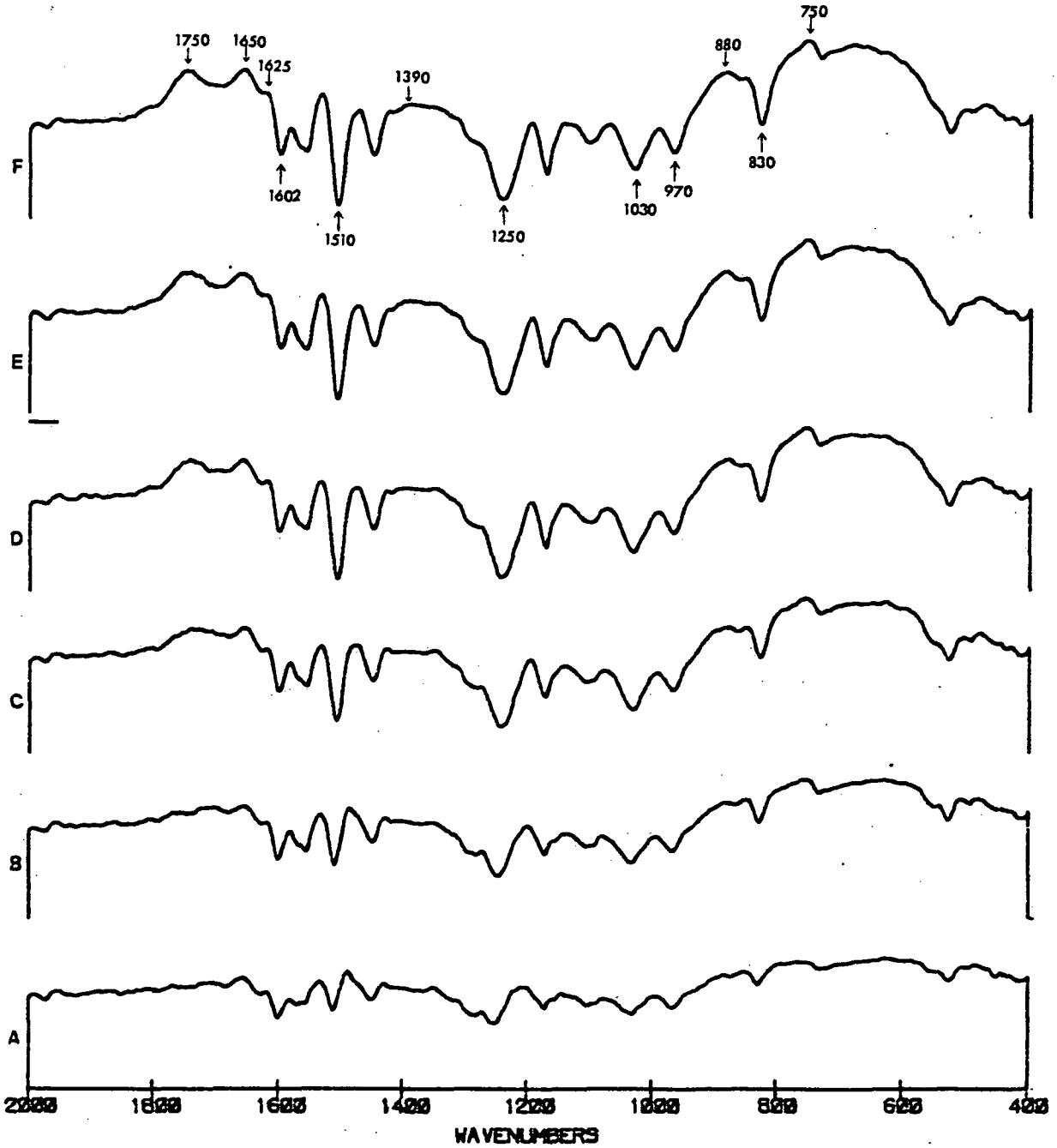

Figure 17. Difference infrared spectrum of 2,6-DGESP cast on Al surface under nitrogen before and after heating at 250°C and various times. (A) 0.5 hr, (B) 1 hr, (C) 2 hr, (D) 3 hr, (E) 4 hr, and (F) 5 hr.

Table 12. The assignment of the IR spectrum for each characteristic peak change during the thermal degradation for 2,6-DGESP.

vibration mode	wavelength (cm^{-1})		
	increase	decrease	formation
C=O	1750		carbonyl
C=C	1650,1625		naphthalene
C-H	1390		aldehyde
C-H out-of-plane bending vibration	880,750		aromatic ring
C=C aromatic ring		1600,1504	Diels-Alder reaction and ring formation
C-H out-of-plane bending vibration		970	
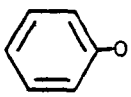		1250	hydroxy group
		915	epoxy ring

obtained (Fig. 15). Both of these findings were consistent with the hypothesis that unreacted epoxide groups and double bonds do in fact contribute to the exotherm at 390°C in the thermally cured resin.

A-3 Structure Study on The Thermal Cured Glycidyl Ethers of Styrylpyridine

Owing to the data storage capability of the FT-IR system, difference spectroscopy can be used as a sensitive method for detecting the small peak change in a sample during its thermal cure. The common features in the spectra are cancelled and only the change is recorded. Koenig[40] originally applied this technique for the oxidation of polybutadiene and used the elimination of the interfering absorbance process to isolate the particular absorbance due to a certain component. Similar approaches were subsequently used on epoxy resin systems.

Thermally cured epoxy resins were investigated under various thermal degradation conditions by Fourier Transform Infrared (FT-IR) spectroscopy. The epoxy resins were the 2,4-diglycidyl ether of styrylpyridine (2,4-DGESP), 2,6-diglycidyl ether of styrylpyridine (2,6-DGESP), and 2,4,6-triglycidyl ether of styrylpyridine (2,4,6-TGESP) respectively. Park and Blount[90] first studied the difference spectrum in epoxy resin thermal oxidative degradation studies. They found a decrease in the -OH absorption and an increase in the C=O absorption, but they could not

obtain detailed information on the degradation reactions. Fig. 9 showed the FT-IR spectra of 2,4 -DGESP, 2,6-DGESP, and 2,4,6-TGESP, and assignments for each peak are listed in Table 2. The different temperature of IR spectra and difference spectra of thermal cured 2,4-DGESP and 2,6-DGESP are shown in Fig. 18 to Fig. 23, respectively. The increase in intensity of the band near 1750 cm^{-1} resulted from the formation of a carbonyl group which may be due to isomerization of the epoxy group during the high temperature thermal curing process. The bands near 1650 cm^{-1} and 1625 cm^{-1} which increased in intensity were probably related to the structure of naphthalene or formation of a double bond of an unsymmetrical conjugated diene. The band at 1390 cm^{-1} which increased in intensity is typically characteristic for aldehyde formation which strongly supported M.B. Neiman [91] and H.C. Anderson[92] hypotheses (see equation 1). The increased intensity of the bands near 880 cm^{-1} and 750 cm^{-1} resulted from the formation of double bonds and rings for C-H out-of-plane bending vibrations. The noticeable decreases in the 1600 cm^{-1}, 1504 cm^{-1} and 965 cm^{-1} were due to the formation of the proposed Diels-Alder product. The significant decrease at 1250 cm^{-1} was probably due to bond scission of the phenoxide of 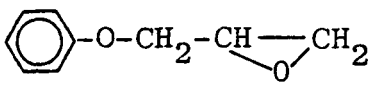 forming an aldehyde and hydroxy containing products. The major thermal curing reaction appeared to be equations 1 and 2.

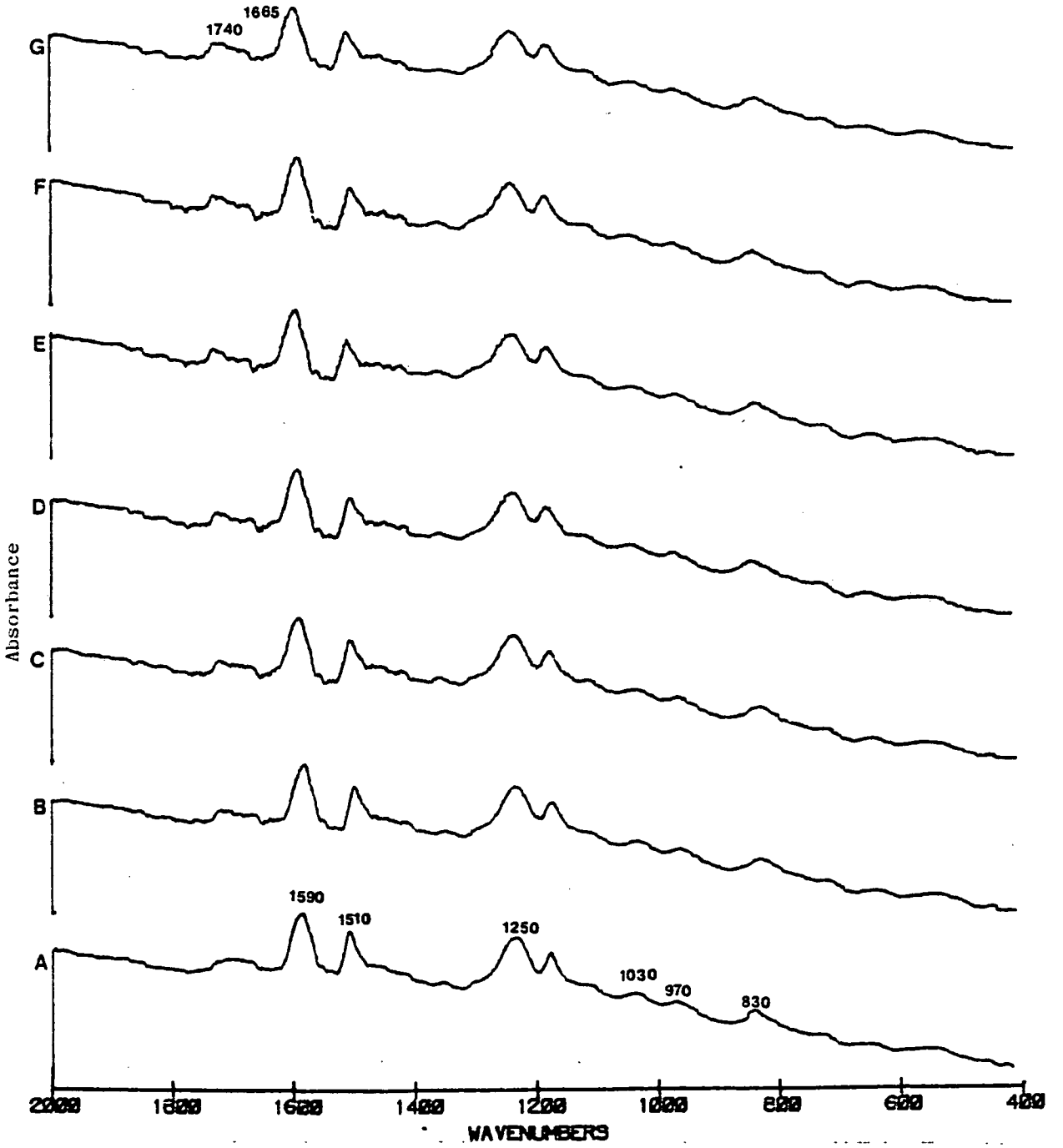

Figure 18. The IR spectrum of 2,4-DGESP cast on Al surface under nitrogen and after heating at 200‡C and various times. (A) 0 hr, (B) 0.5 hr, (C) 1 hr, (D) 2 hr, (E) 3 hr, (F) 4 hr, (G) 5 hr.

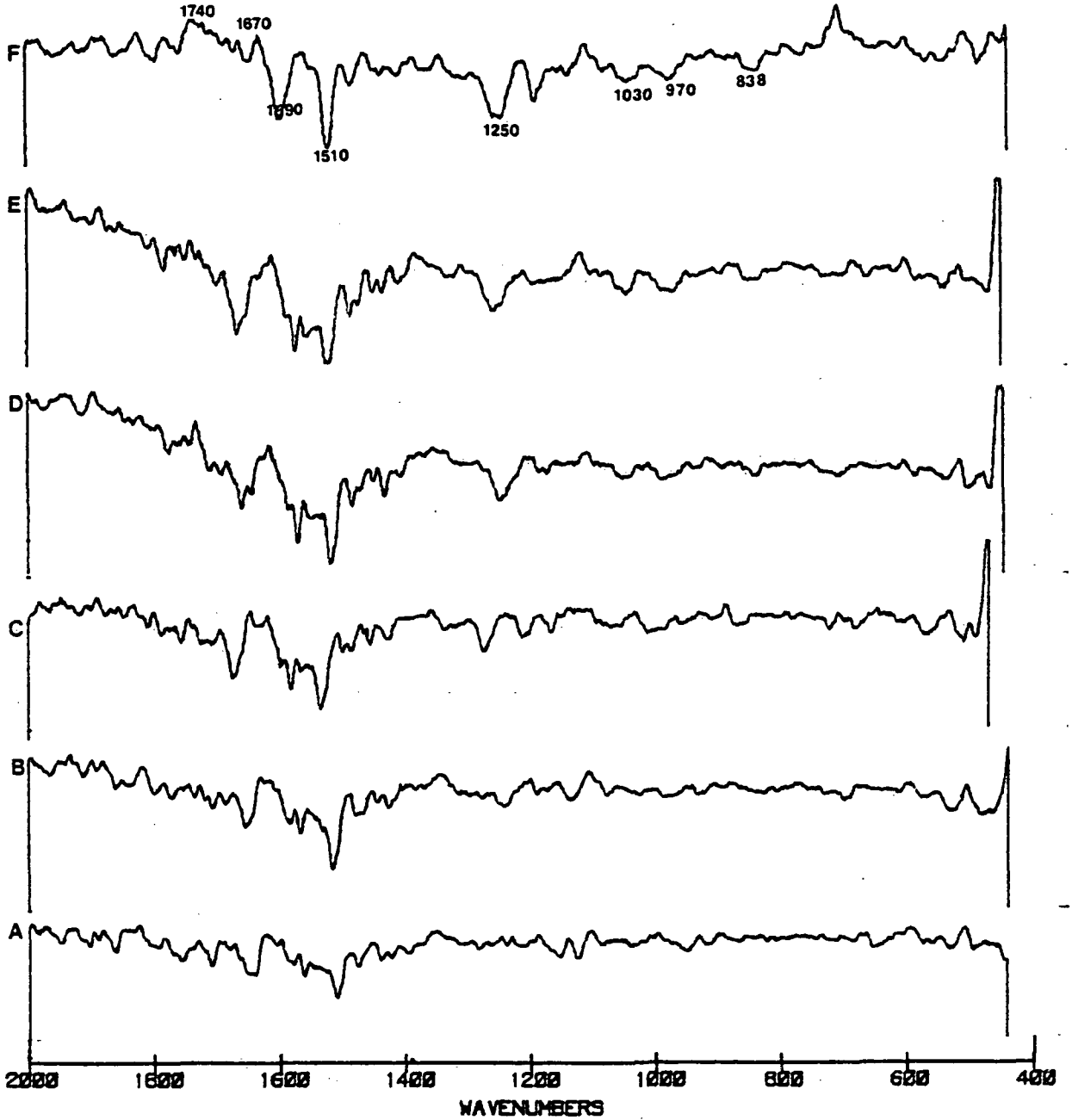

Figure 19. Difference infrared spectrum of 2,4-DGESP cast on Al surface under nitrogen before and after heating at 200°C and various times. (A) 0.5 hr, (B) 1 hr, (C) 2 hr, (D) 3 hr, (E) 4 hr, (F) 5 hr.

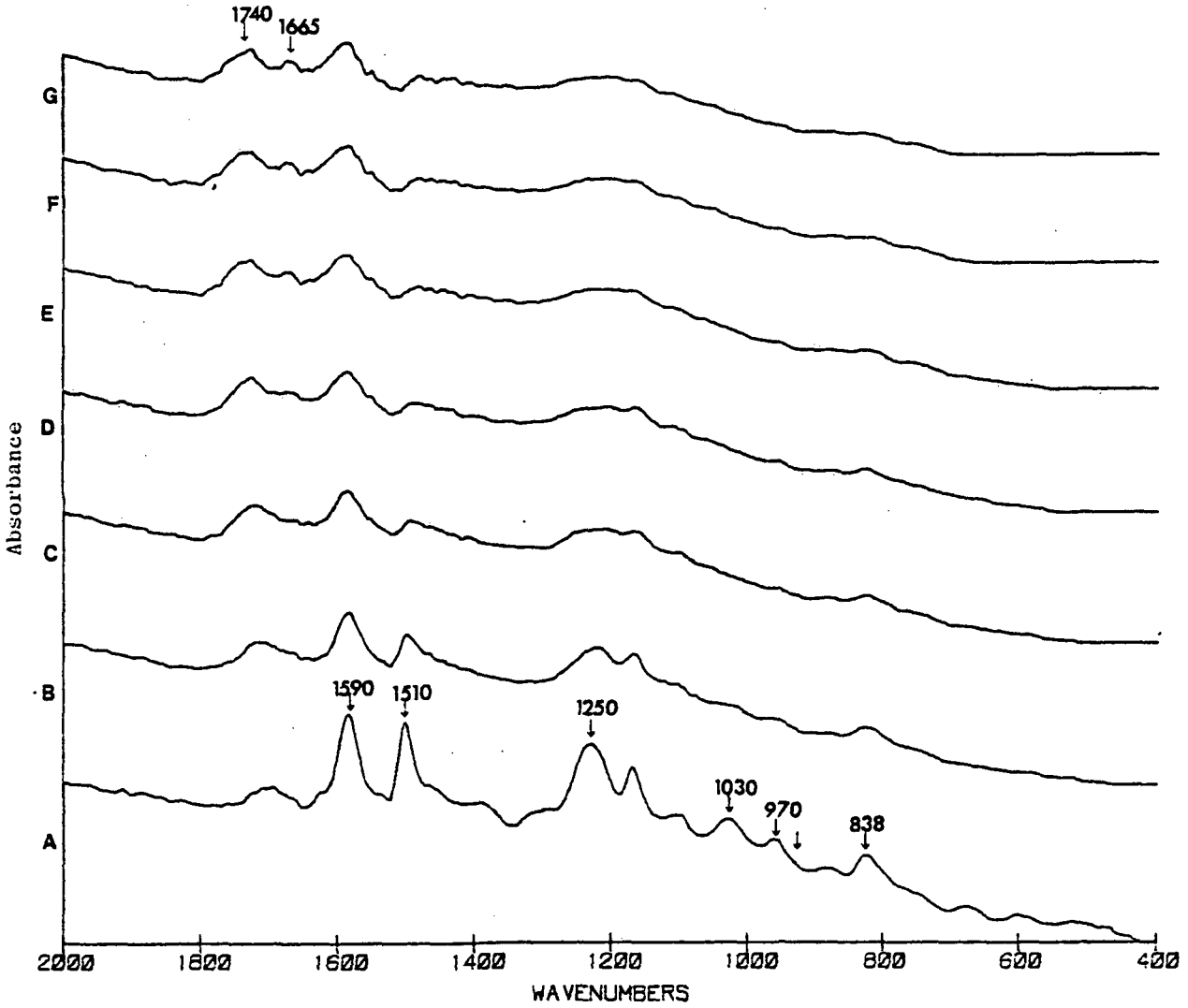

Figure 20. The IR spectrum of 2,4-DGESP cast on Al surface under nitrogen and after heating at 250°C and various times. (A) 0 hr, (B) 0.5 hr, (C) 1 hr, (D) 2 hr, (E) 3 hr, (F) 4 hr, and (G) 5 hr.

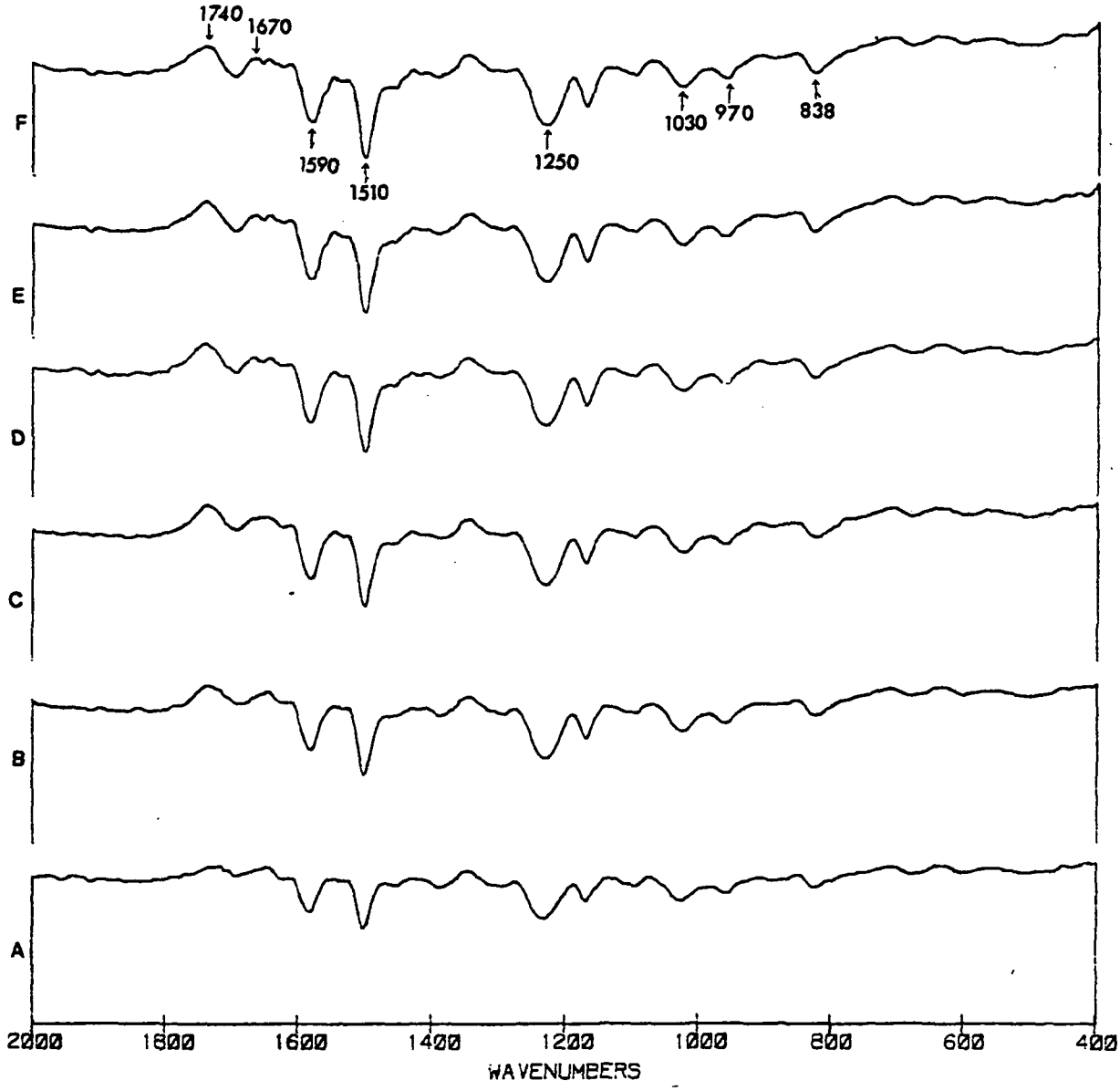

Figure 21. Difference infrared spectrum of 2,4-DGESP cast on Al surface under nitrogen before and after heating at 250°C and various times. (A) 0.5 hr, (B) 1 hr, (C) 2 hr, (D) 3 hr, (E) 4 hr, and (F) 5 hr.

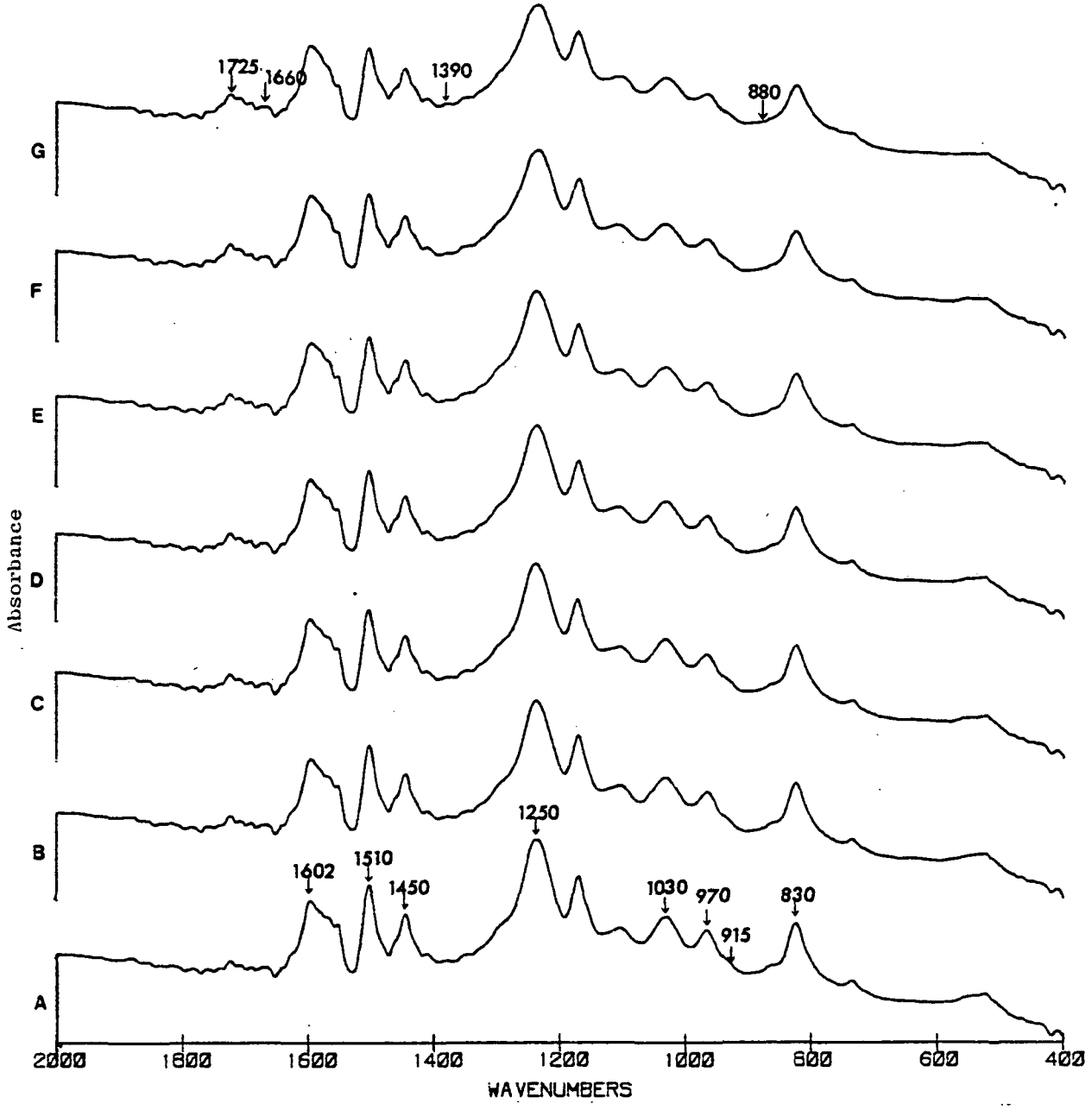

Figure 22. The IR spectrum of 2,6-DGESP cast on Al surface under nitrogen and after heating at 200°C and various times. (A) 0 hr, (B) 0.5 hr, (C) 1 hr, (D) 2 hr, (E) 3 hr, (F) 4 hr, and (G) 5 hr.

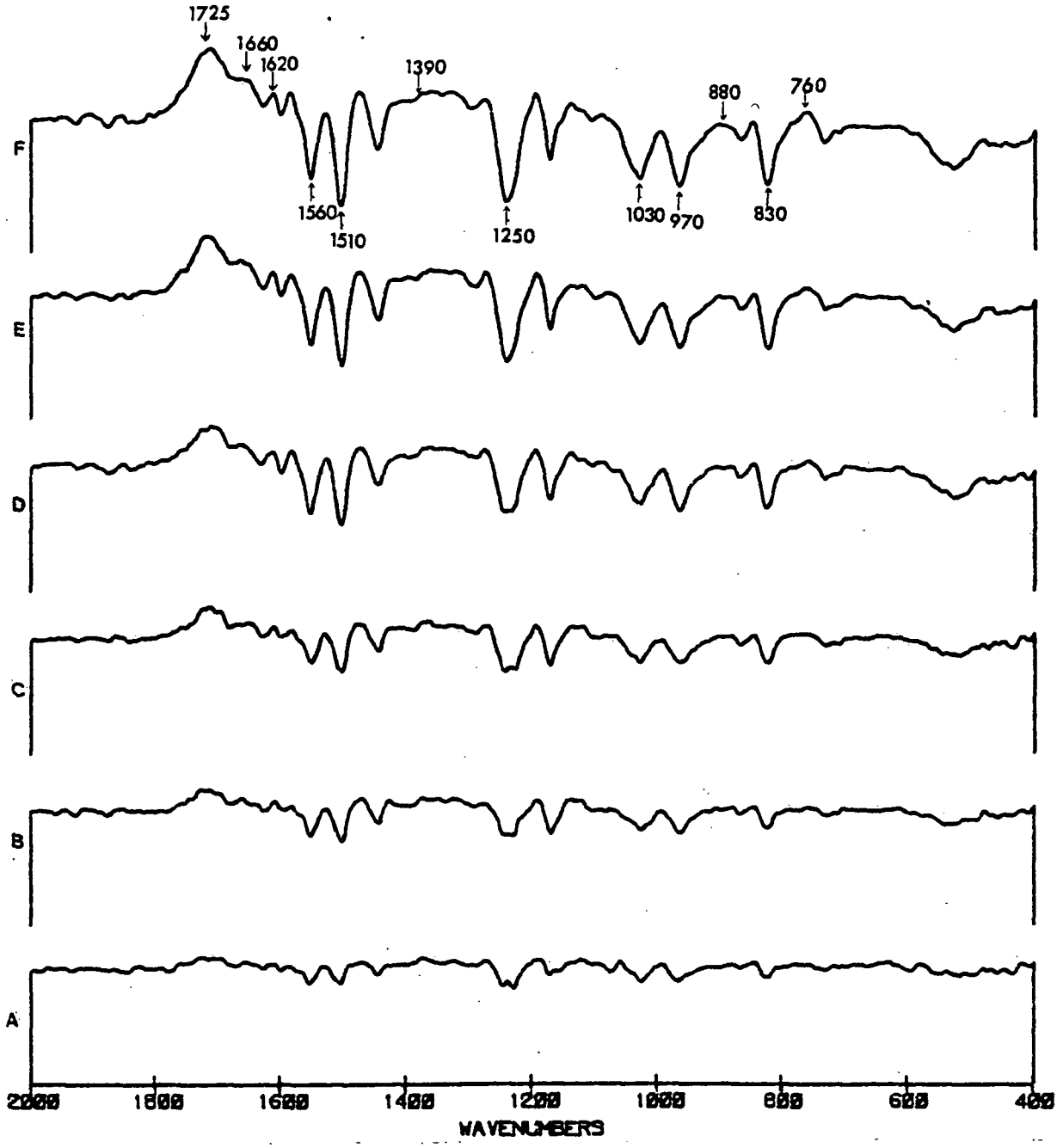

Figure 23. Difference infrared spectrum of 2,6-DGESP cast on Al surface under nitrogen before and after heating at 200°C and various times. (A) 0.5 hr, (B) 1 hr, (C) 2 hr, (D) 3 hr, (E) 4 hr, and (F) 5 hr.

Equation 1.[89]

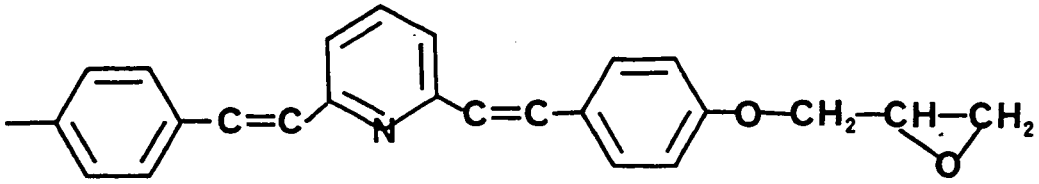

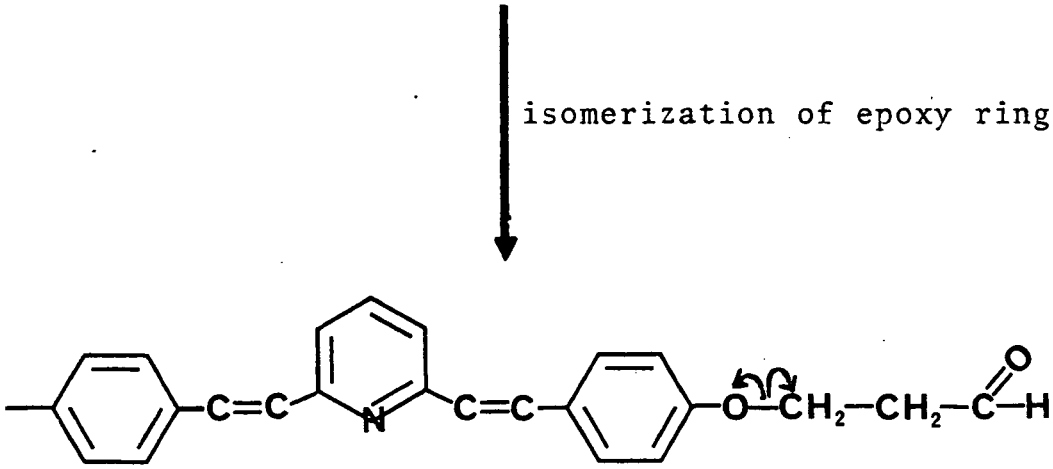

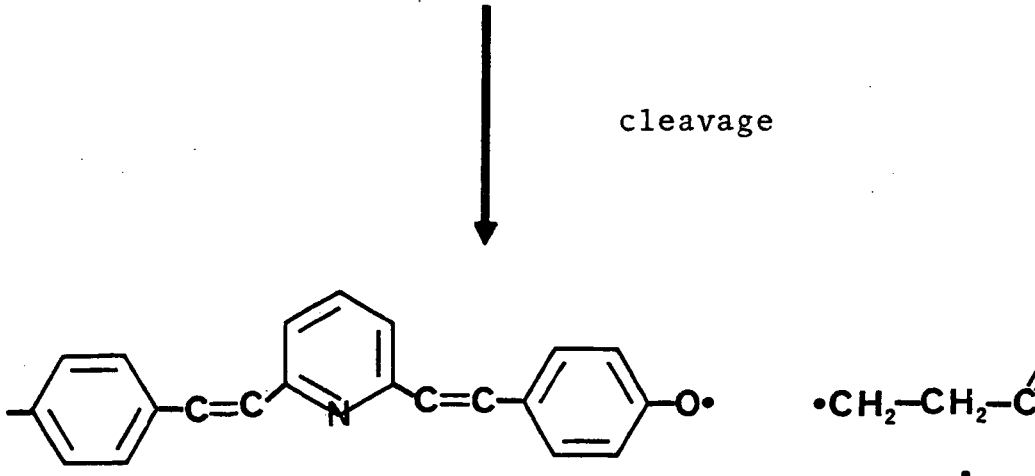

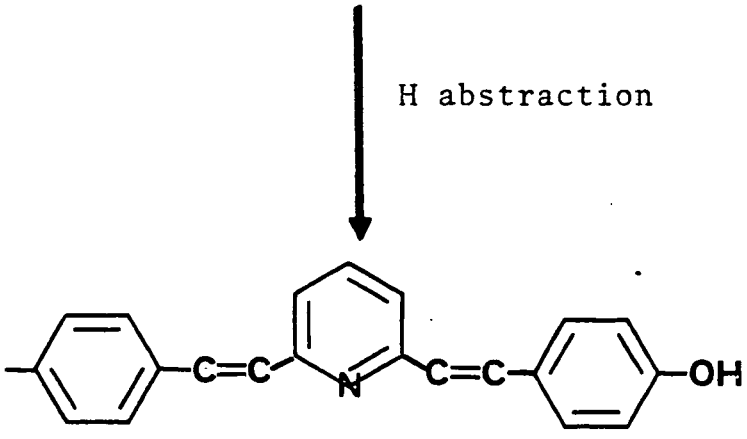

increasing the OH band

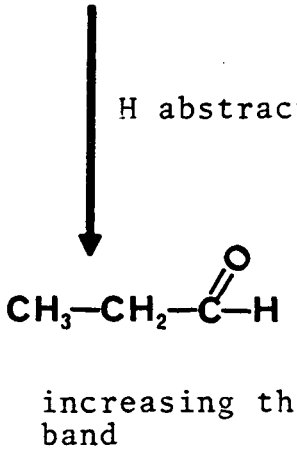

increasing the carbonyl band

Equation 2.[93] Intermolecular Diels-Alder reaction

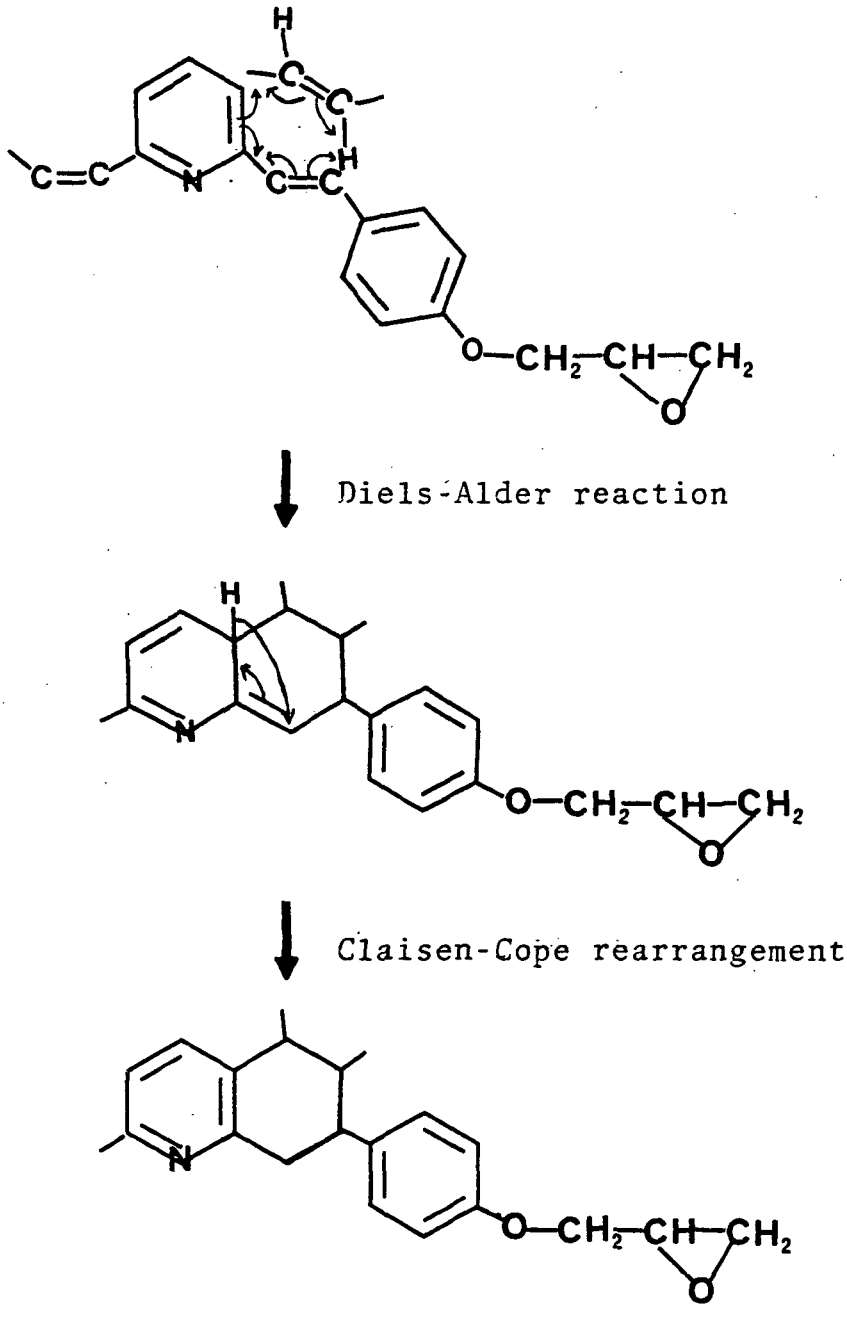

From the FT-IR difference spectra, (Fig. 17 and 23), one can expect that the high temperature thermal curing process favored the Diels-Alder reaction, because the typical bands for formation Diels-Alder product are increased as those for reactants decreased.

A-4 Curing Reaction Studies

The TGA thermograms of 2,6-DGESP with different amounts of TMB were run (Fig. 24). It was expected that the cured 2,6-DGESP with TMB would have a higher char yield than without TMB due to epoxy crosslinking. The IR spectrum of 2,6-DGESP with different amounts of TMB were run (Fig. 25) and the assignments for each peak are listed (Table 13). The oxygen indices and char yields, for 2,6-DGESP with different amounts of TMB were determined (Table 14). The cured TMB epoxy resins gave higher char yields than the thermally cured (no TMB curing agent) epoxy resin. However, they gave lower oxygen indices in a similar comparison. Perhaps unreacted TMB contributes to this anomaly (TMB,b.p. 130^{o}C) or was complexed and relatively unavailable and hence uncombined during the cure.

The char yields and oxygen indices of 200^{o}C thermally cured 2,6-DGESP at varying times was determined (Table 15). The oxygen index and char yield increased with increasing

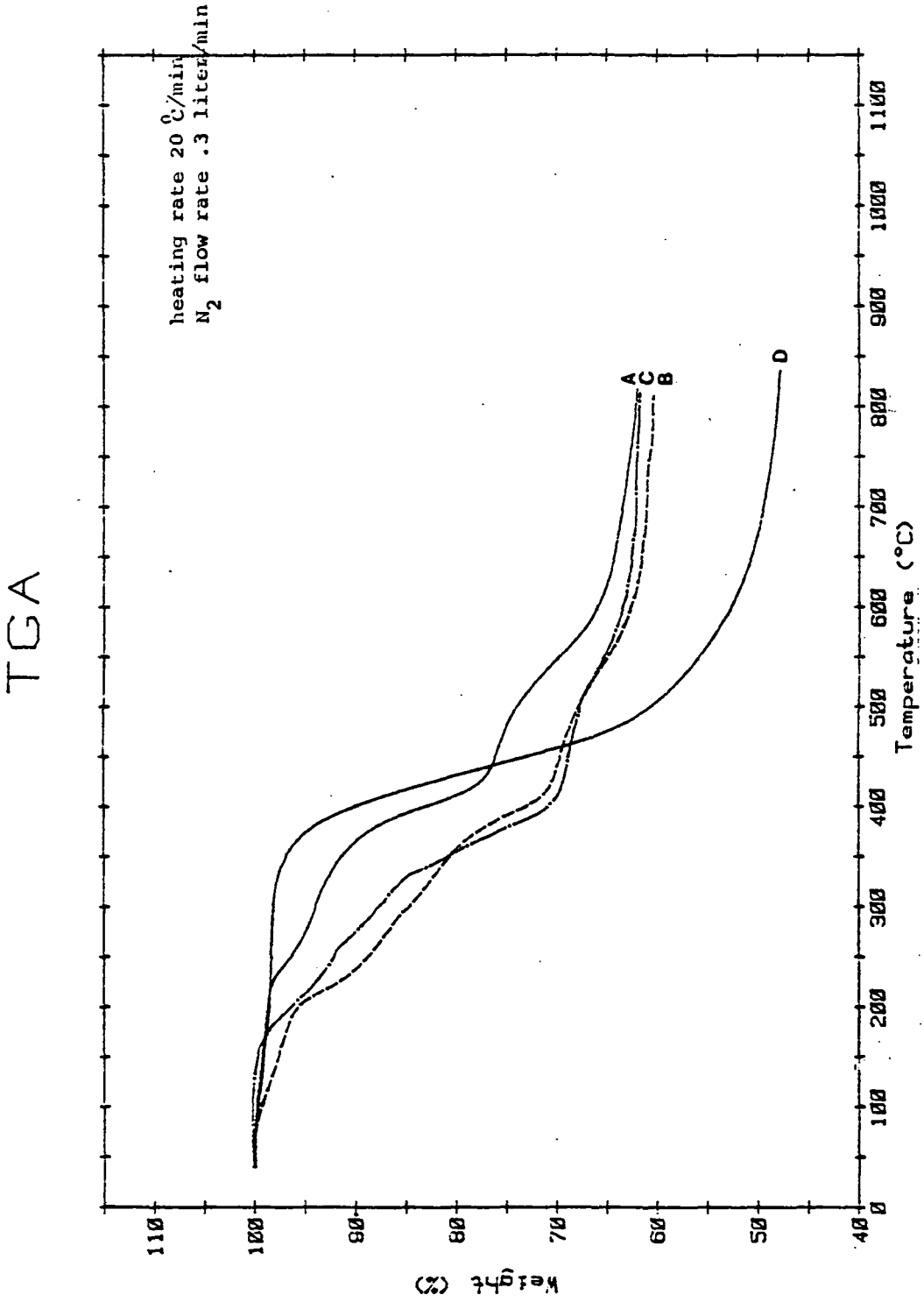

Figure 24. The TGA thermogram of 2,6-DGESP with different amounts of TMB. (A) 0.1624 eq. of TMB, (B) 0.3248 eq. of TMB, (C) 0.4872 eq. of TMB, and (D) without TMB.

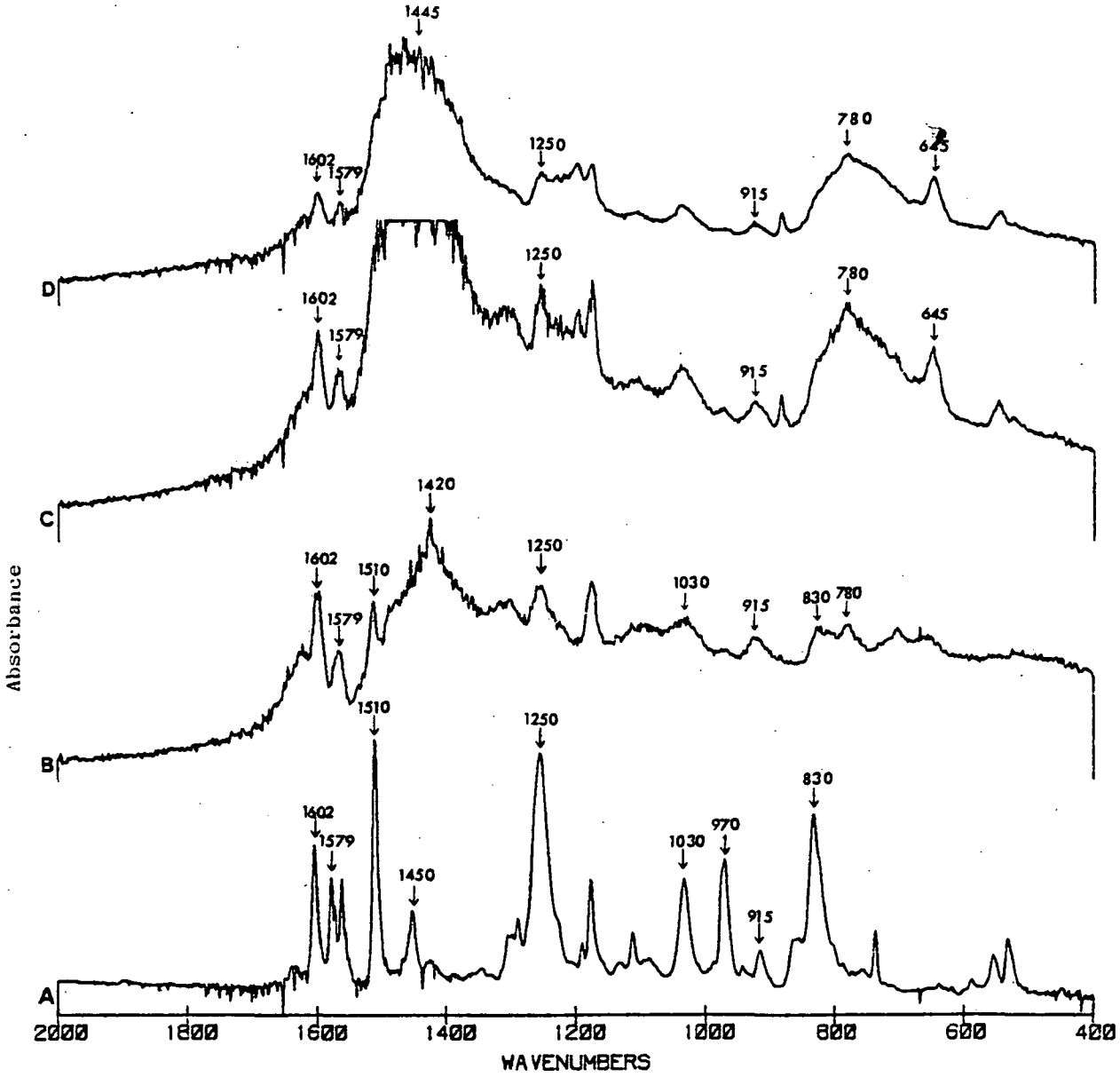

Figure 25. Infrared spectrum of 2,6-DGESP using KBr pellet under nitrogen before and after cure with different amounts of TMB. (A) no TMB present, (B) 0.1624 eq. of TMB, (C) 0.3248 eq. of TMB, and (D) 0.4872 eq. of TMB.

Table 13. The assignment of the IR spectrum for each characteristic peak change during the cured reaction for 2,6-DGESP with TMB.

vibration mode	wavelength (cm^{-1})	
	increase	decrease
$-CH_2-$	1420	
C-O-C	1030	
		915

Table 14. The oxygen index and char yield of 2,6-DGESP with different amounts of TMB.

TMB eq. wt.	without TMB	0.1624 eq.	0.3248 eq.	0.4872 eq
char yield	48.0%	62.3%	60.5%	61.5%
oxygen index	24.8%	25.8%	26.2%	27.0%

Table 15. The oxygen index and char yield of thermal cured 2,6-DGESP at 200°C with different times.

time	0 hr	1 hr	2 hr	3 hr	5 hr	6 hr	7 hr	10 hr
char yield	47.5%	47.7%	47.2%	50.0%	53.0%	59.5%	55.2%	62.3%
oxygen index	26.0%	28.2%	28.9%	29.8%	30.5%	33.0%	35.0%	36.0%

time and was probably related to increased crosslinking of the epoxy resin.

A-5 Conclusions

The reactions during the thermal curing of 2,6-DGESP can be followed by FT-IR. An intermolecular Diels-Alder reaction was proposed as the primary reaction during the thermal cure. Cured 2,6-DGESP with TMB gave a higher char yield than without TMB. Both char yield and oxygen index increased with increasing time for the thermally cured 2,6-DGESP. The Diels-Alder reaction was favored by high temperature.

B. Styrylpyridine Based Polymers: Polyarylates

B-1 Flammability Characterization of Styrylpyridine Polyesters and Polycarbonates and Their Related Model Compounds

Thermal characterization data (char yields) and oxygen indices for styrylpyridine based polyesters and their model compounds are shown in Fig. 26 and Table 4. An increase of char yield is generally reflected as an improved oxygen index. p,p'-BVPDPI, p,p'-BVPDPT and p,p'-2,6-VPDPDB have higher char yields and oxygen indices than p-VPPB. This was probably due to increased double bonds, pyridine, and phenyl rings in the backbone chain and/or occurrence of the Diels-Alder reaction with the C=C double bond in the backbone chain forming highly cross-

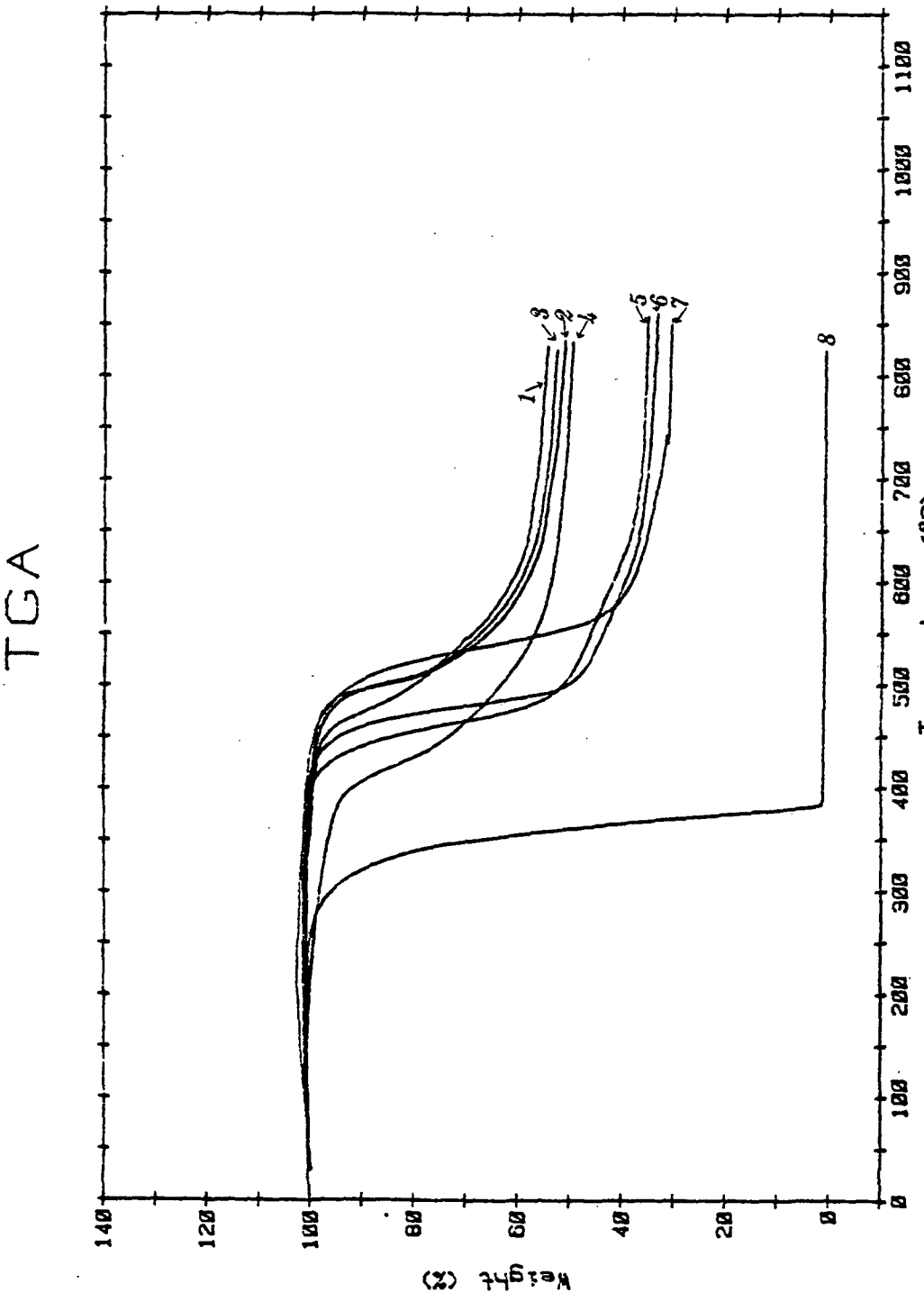

Figure 26. The TGA thermogram of various components: (1) poly(2,6-VPDPI), (2) poly(2,6-VPDPT), (3) poly(2,4-VPDPT), (4) poly(2,4-VPDPI), (5) P,p'-BVPDPT, (6) p,p'-BVPDPI, (7) p,p'-2,6-VPDPDD, and (8) p-VPPB; ATM: N2 (flow rate 0.5 LPM) and heating rate: 20°C/min.

linked C-C bonds. These conclusions were similar to van Krevelen's suggestion that polymers containing high aromatic ring content and/or double bonds in the polymer backbone unit usually gave large amounts of char[94]. The styrylpyridine based polyesters have greater char yields and oxygen indices than the model components for similar reasons. There is not great difference in char yields and oxygen indices of the polyesters based on isophthaloyl chloride (IPC) or terephthaloyl chloride (TPC) because of their similarity in chemical composition and structure.

The styrylpyridine based polycarbonates showed similar char yield and oxygen indices (Fig. 27 and Table 4) to that of the polyesters.

B-2 Photo-Fries Rearrangement of Styrylpyridine Based Ester and Carbonate- UV Spectroscopic Studies

The Ultraviolet (UV) rearrangement reaction of polyarylesters and their related model compounds have been previously studied[95,96]. The chemical changes which occur during the UV irradiation of styrylpyridine based ester and carbonate were investigated. The UV spectra of the p-VPPB and p,p'-BVPDPC in 1,2-dichloroethane was monitored during the irradiation (Fig. 28 and 29). The maximum absorption for unirradiated p-VPPB was at 319 nm. After

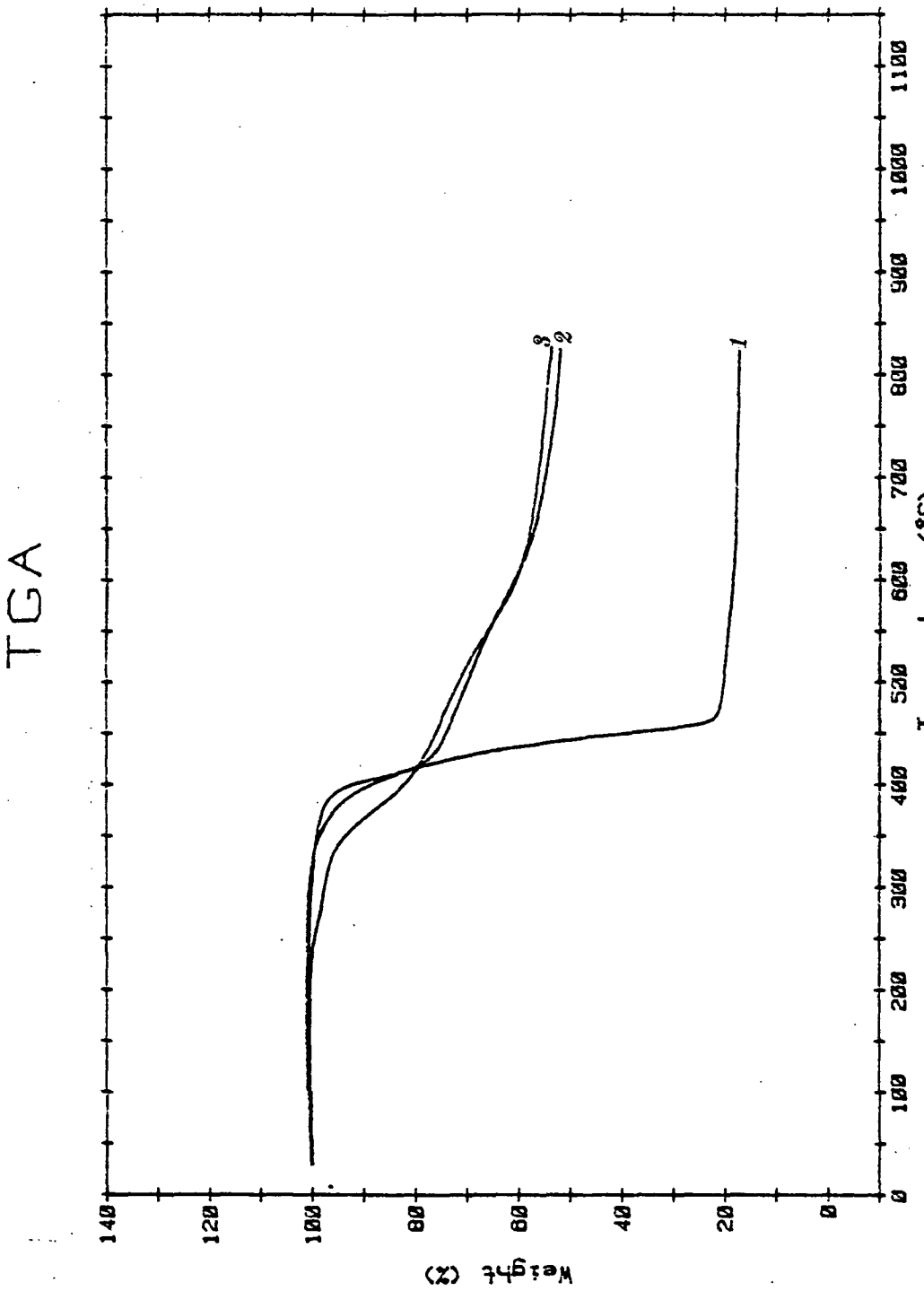

Figure 27. The TGA thermogram of various components: (1) p,p'-BVPDPC, (2) poly(2,4-VPDPC) and poly(2,6-VPDPC); ATM: N_2 (flow rate 0.5 LPM) and heating rate: 20°C/min.

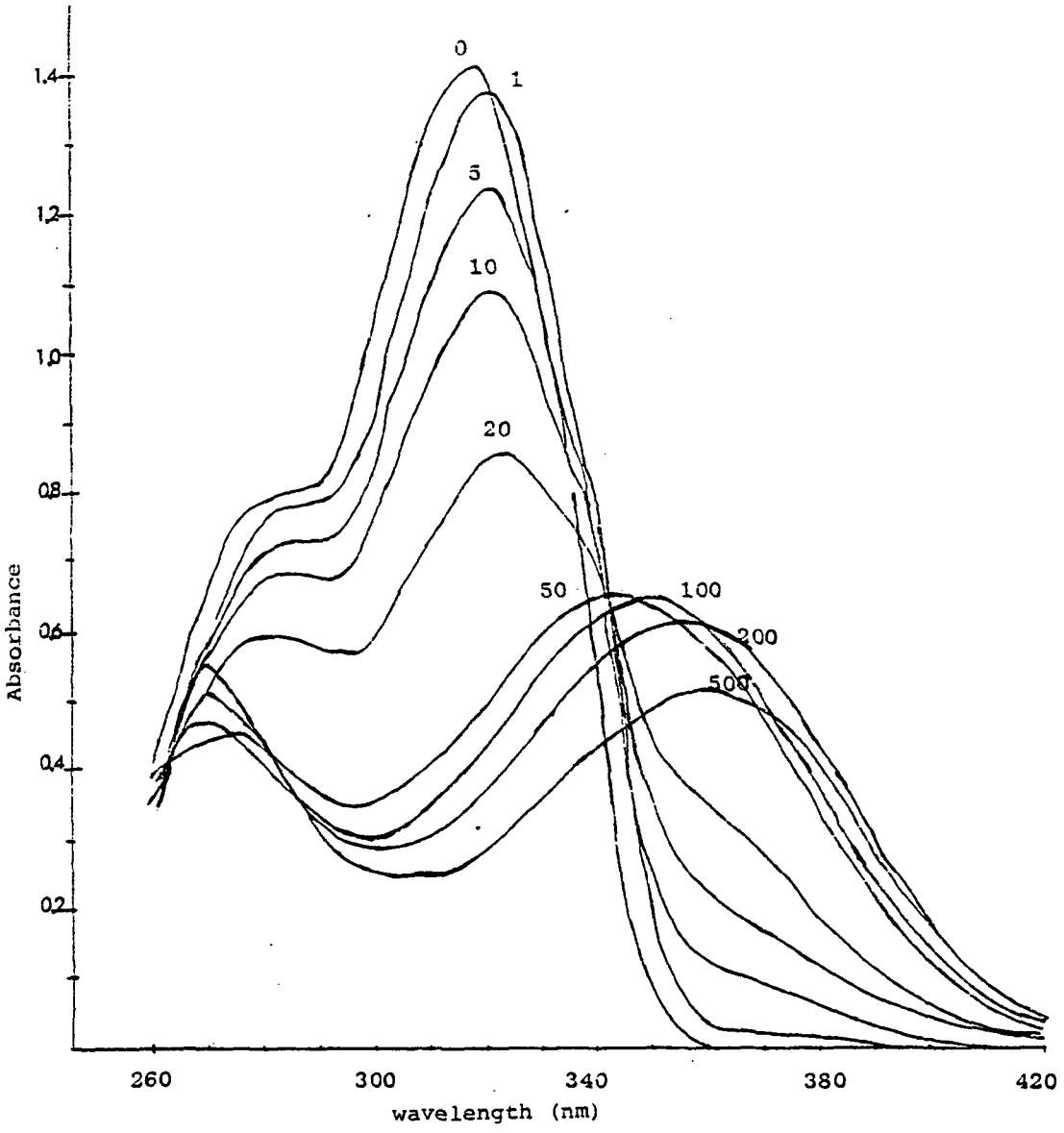

Figure 28. Change in UV spectra of p-VPPB in 1,2-dichloroethane solution before and after irradiation for different periods of time (seconds).

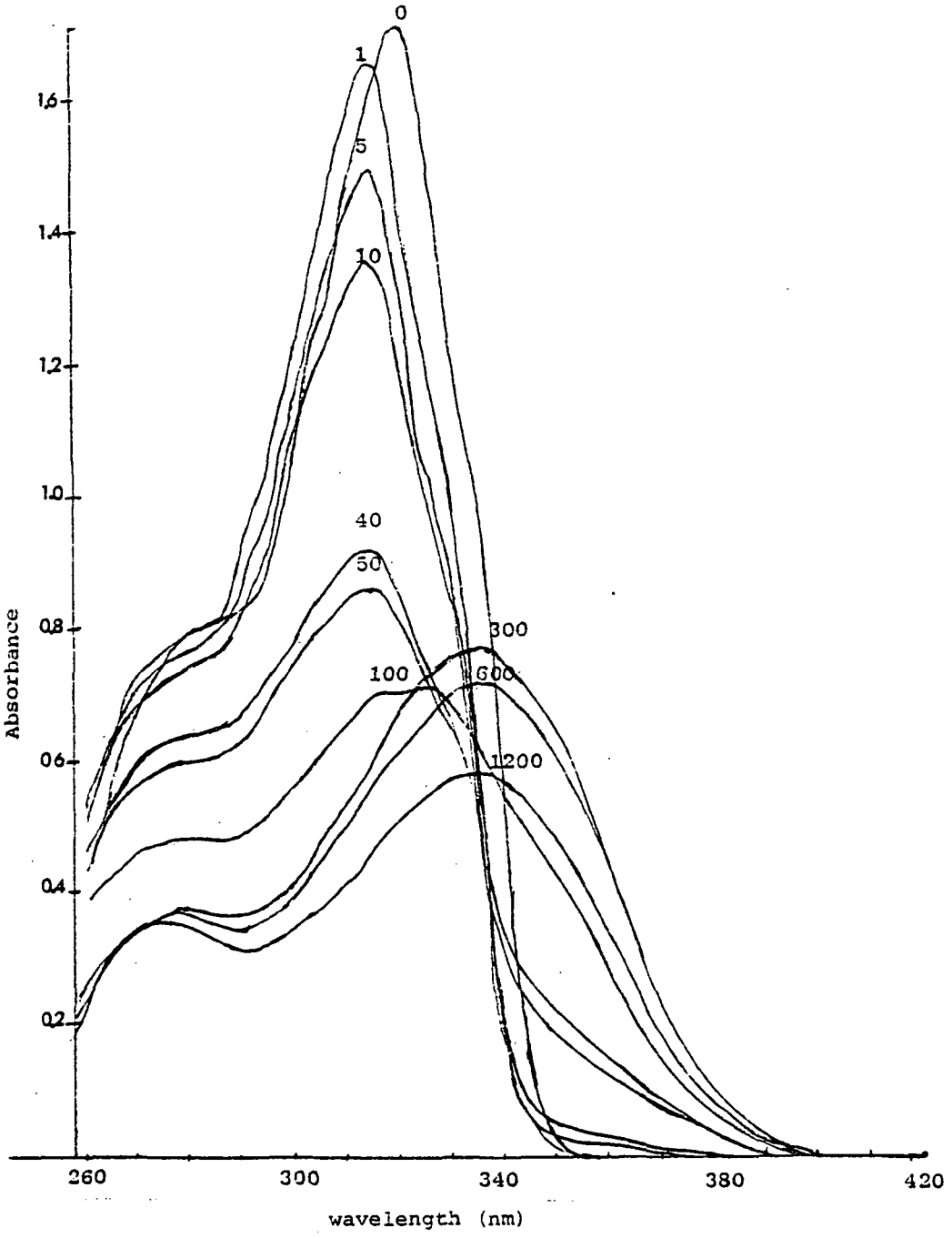

Figure 29. Change in UV spectra of p,p'-BVPDPC in 1,2-dichloroethane solution before and after irradiation for different periods of time (seconds).

UV irradiation, the maximum peak shifted from 319 nm to 350 nm and the observed increased absorption in the 340 nm range with a maximum at 350 nm was due to formation of the hydroxybenzophenone structure during the Fries rearrangement[95,97] (see eq. 3) primary absorption maximum (max= 319 nm) rapidly diminished in intensity, and a new absorption peak appeared on irradiation at 270 nm. This could probably be related to either the dimerization or to isomerization of the C=C between the phenyl and pyridine groups[98,99,100] (eq. 4). In the case of p,p'-BVPDPC, there was no increased absorption at 270 nm probably due to steric effects associated with a large molecule (ponderal effect) and to increased aplanarity of the styrylpyridine ring to suppress the dimerization and isomerication of the double bond preventing cis-isomer formation.

B-3 Conclusions

An increase of char yield is generally reflected as an improvement in oxygen index. In the styrylpyridine based polyesters and polycarbonates, an intermolecular thermally induced Diels-Alder reaction has occurred through the double bond increasing the char yield and decreasing the flammability. The Fries rearrangement, as well as dimerization and isomerication, occurred simul-

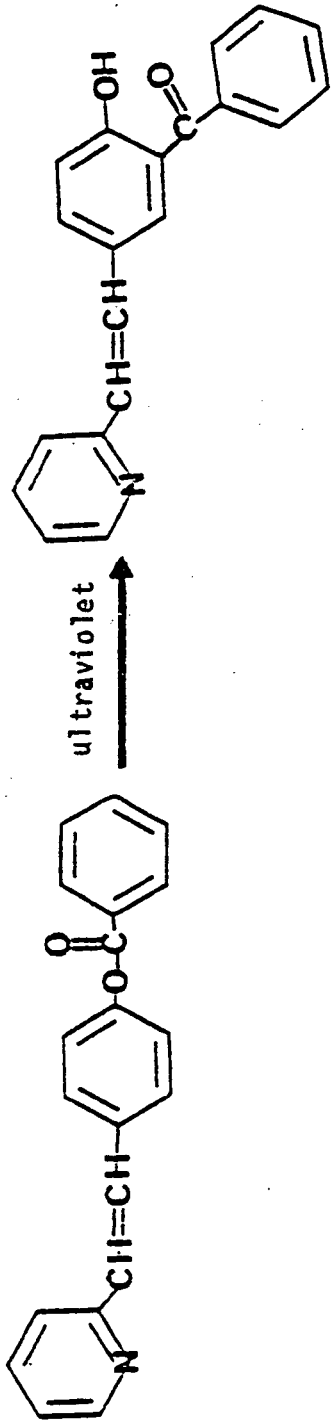

Equation 3.

Equation 4.

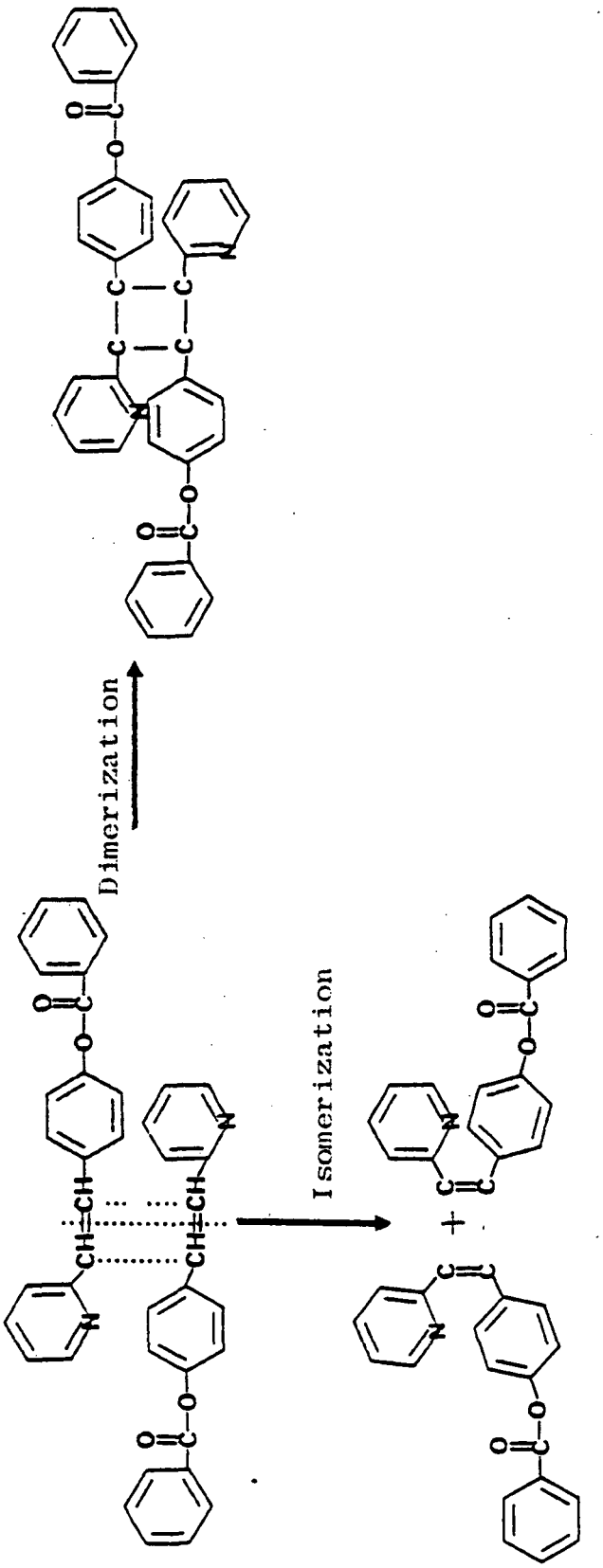

taneously during the UV irradiation of p-VPPB, but no dimerization or isomerization occurred for p,p-BVPDPC, probably due to steric effects.

C. Styrylpyridine Based polymers : Triazine and PSP

C-1 Aromatic s-Triazine Polymers-Structure and Thermostability Study

The aromatic s-triazines, 2,4-di-(p-cyanostyryl) pyridine (2,4-SPT), and 2,6-di(p-cyanostyryl)pyridine (2,6-SPT), were investigated by Fourier Transform Infrared (FT-IR) Spectroscopy after various reaction times. Several authors[70,71,73] have noted that triazine and aromatic structures fall in approximately the same infrared region. Because of the conventional IR could not give detailed information on the cyclotrimerization reaction. The FT-IR spectra and difference spectra of 2,6-SPT and 2,6-D(p-CN)SP are shown in Fig. 30 and 31, respectively. The decrease in intensity of the band near 2210 cm^{-1} is due to the disappearance of the C≡N group. The bands near 1720, 1660, 1620, 1240, 1180 cm^{-1} increased intensity of the C=N group in the s-triazine[101]. The increased intensity of the bands near 800 and 620 cm^{-1} resulted from the formation of an out of plane bending vibration of the C=N group[101]. Therefore, polymer 2,6-SPT structure gave the structure shown in Fig. 32.

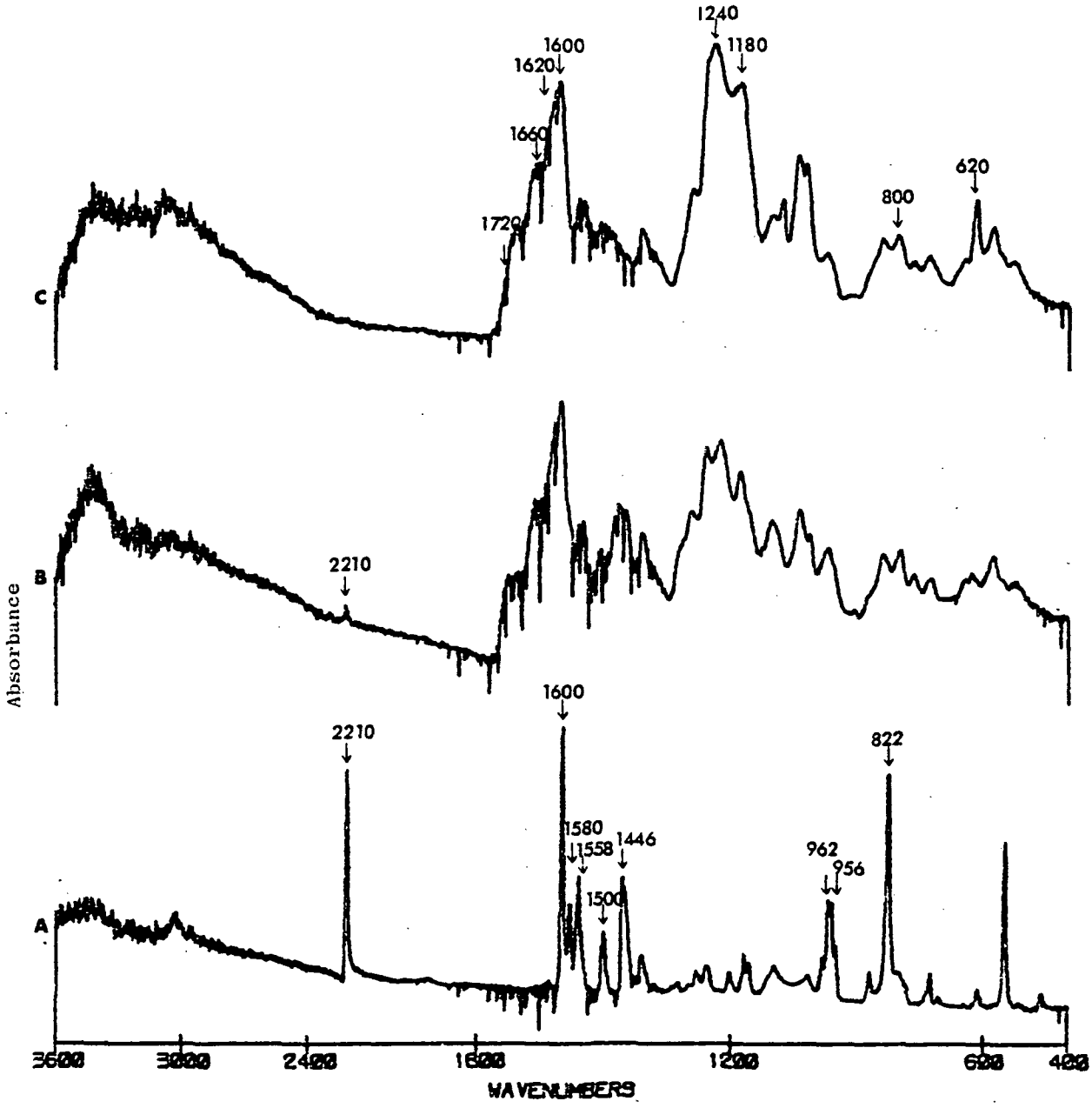

Figure 30. Infrared spectrum of monomer and polytriazine at various reaction times. (A) 2,6-D(p-CN)SP, (B) 2,6-SPT, 24 hr, (C) 2,6-SPT, 48 hr; (KBr pellet).

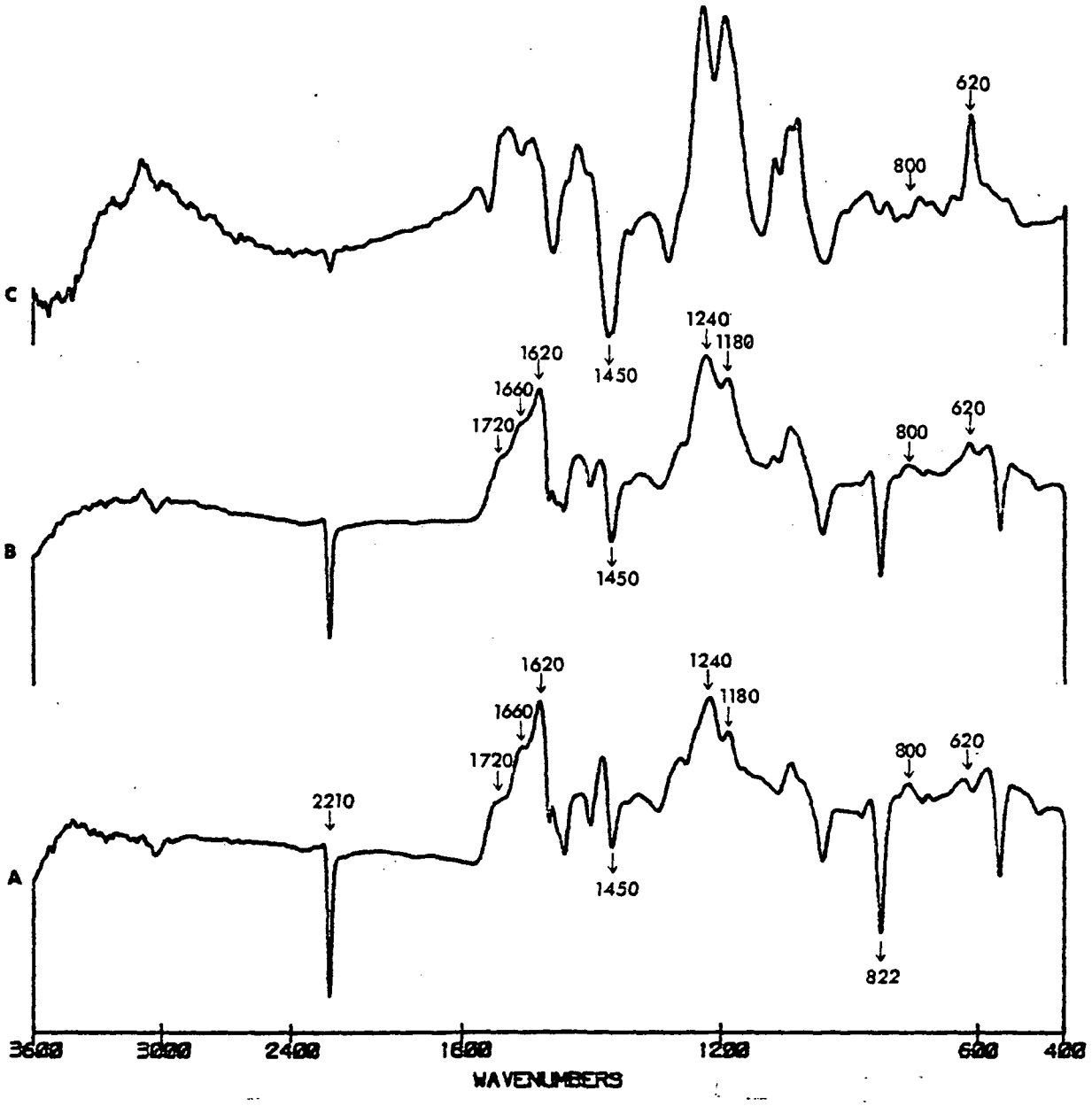

Figure 31. Difference spectra of (A) B-A, (B) C-A, and (C) C-B from Fig. 30.

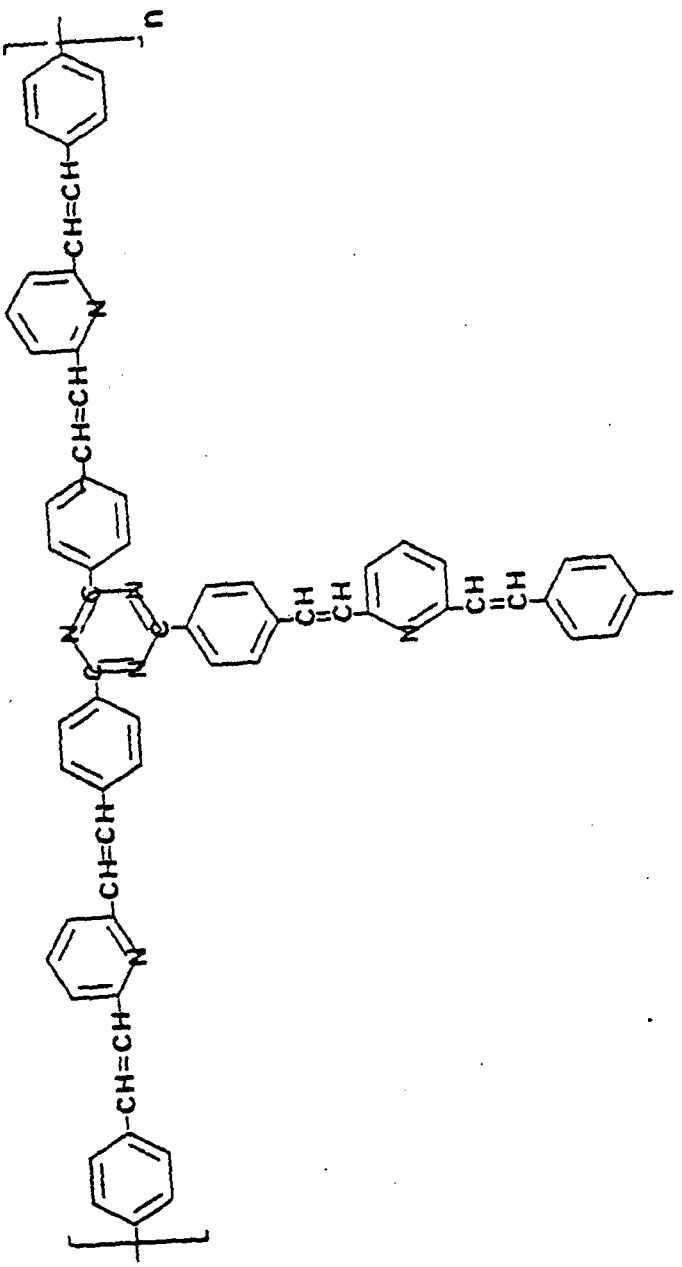

Figure 32. Polytriazine of 2,6-SPT structure.

Table 8 and 10 show the char yield and oxygen index of polytriazines and starting materials. It was expected that the corsslinked polytriazines would have a higher char yield than the starting materials. For the PSP structure unit increases in double bond, pyridine, and phenyl content, and crosslink formation usually gave higher char. An increase of char yield is generally reflected also in an improved oxygen index[5,45]. In the case of the polytriazine, the order of char formation is 2,6-SPT≈ 2,4-SPT >2,6-D(p-CN)Sp≈2,4-D(p-CN)SP >2-CNSP. A higher crosslink density related to the triazine ring formation appeared to account for this. These conclusions were similar to van Krevelen's suggestion that polymer containing highly aromatic content and/or double bonds in the polymer backbone unit usually gave large amounts of char yield[94].

C-2 Polystyrylpyridine (PSP)-structure and thermostability Study

Thermally cured polystyrylpyridine prepolymers, polymer 2-4-styrylpyridine (2,4-PSP), polymer 2,6-styrylpyridine (2,6-PSP) and polymer 2,4,6-styrylpyridine (2,4,6-PSP), were investigated under various thermal degradation conditions by FT-IR spectroscopy. The FT-IR and difference spectra of thermally cured 2,4-PSP, 2,6-PSP,

and 2,4,6-PSP are shown in Fig. 33 to 42, respectively. These studies were done at various curing temperatures. The increase in intensity of the band near 1620, 1600, 1500, and 1470 cm^{-1} were probably related to the ring stretching vibration of the C=C double bond structure of naphthalene[102]. The noticeable decrease in the 1670 and the 960 cm^{-1} were due to the formation of the proposed Diels-Alder products The significant increase at 1160 and 750 cm^{-1} (103,104) appeared to be related to the out of plane C-H deformation vibration of substituted naphthalene. The thermally cured 2,6-PSP structure would give such a structure (Fig. 43)

From the FT-IR different spectra results (see Fig. 38 and 40), the high temperature thermal curing appeared to favor the Diels-Alder reaction.

Various PSP's give high char yields and oxygen indices (Table 11) as a result of the Diels-Alder reaction during the thermal cure. There appeared to be no particular difference in char yield and oxygen index of 2,4-PSP, 2,6-PSP, and 2,4,6-PSP because of their similarity in chemical composition and structure.

C-3 Conclusions

FT-IR can be used to distinguish the structure

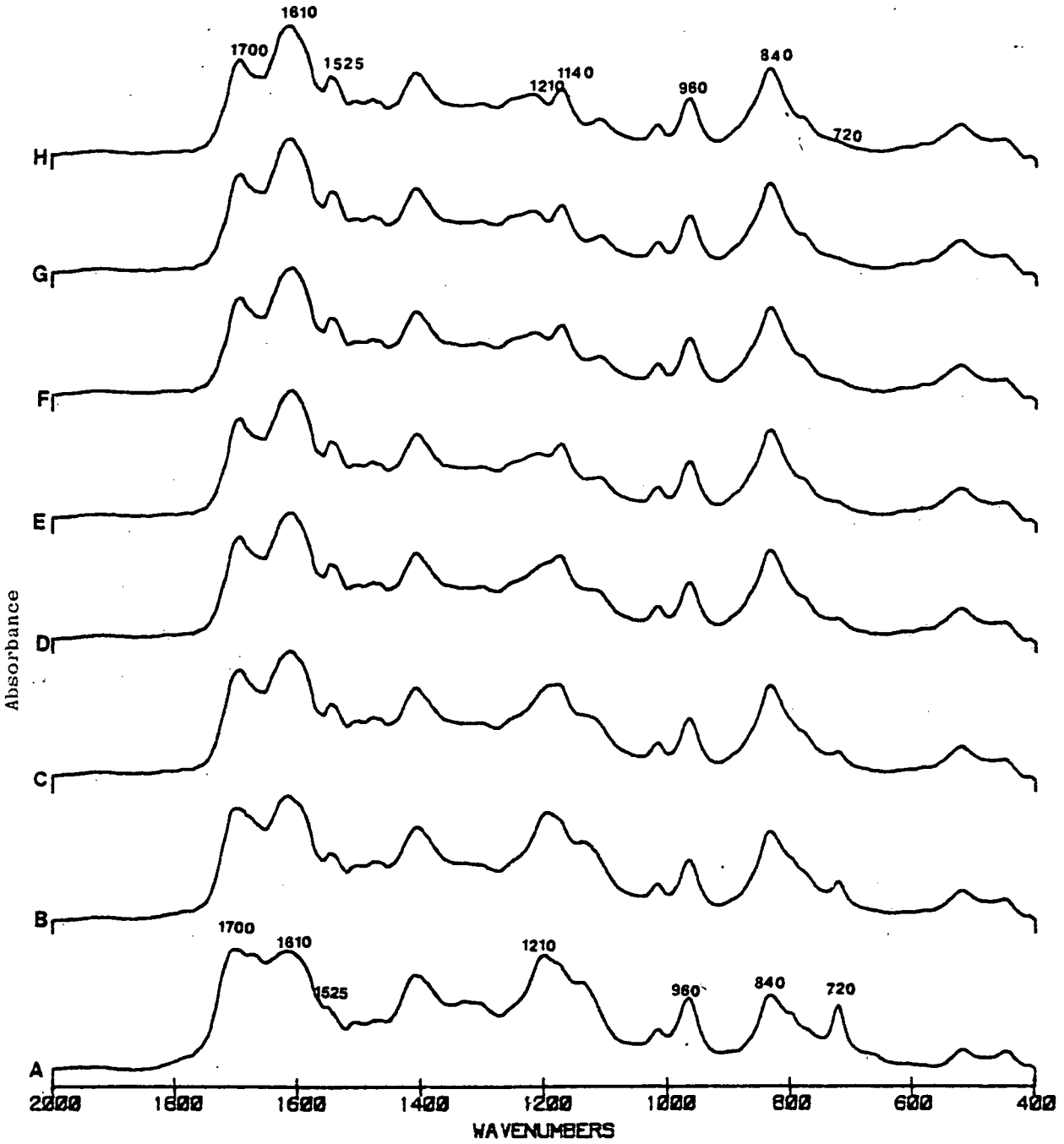

Figure 33. Infrared spectrum of 2,4-PSP cast on Al surface under nitrogen after heating at 180°C and various times. (A) 0 hr, (B) 0.5 hr, (C) 1 hr, (D) 1.5 hr, (E) 2 hr, (F) 3 hr, (G) 4 hr, and (H) 5 hr.

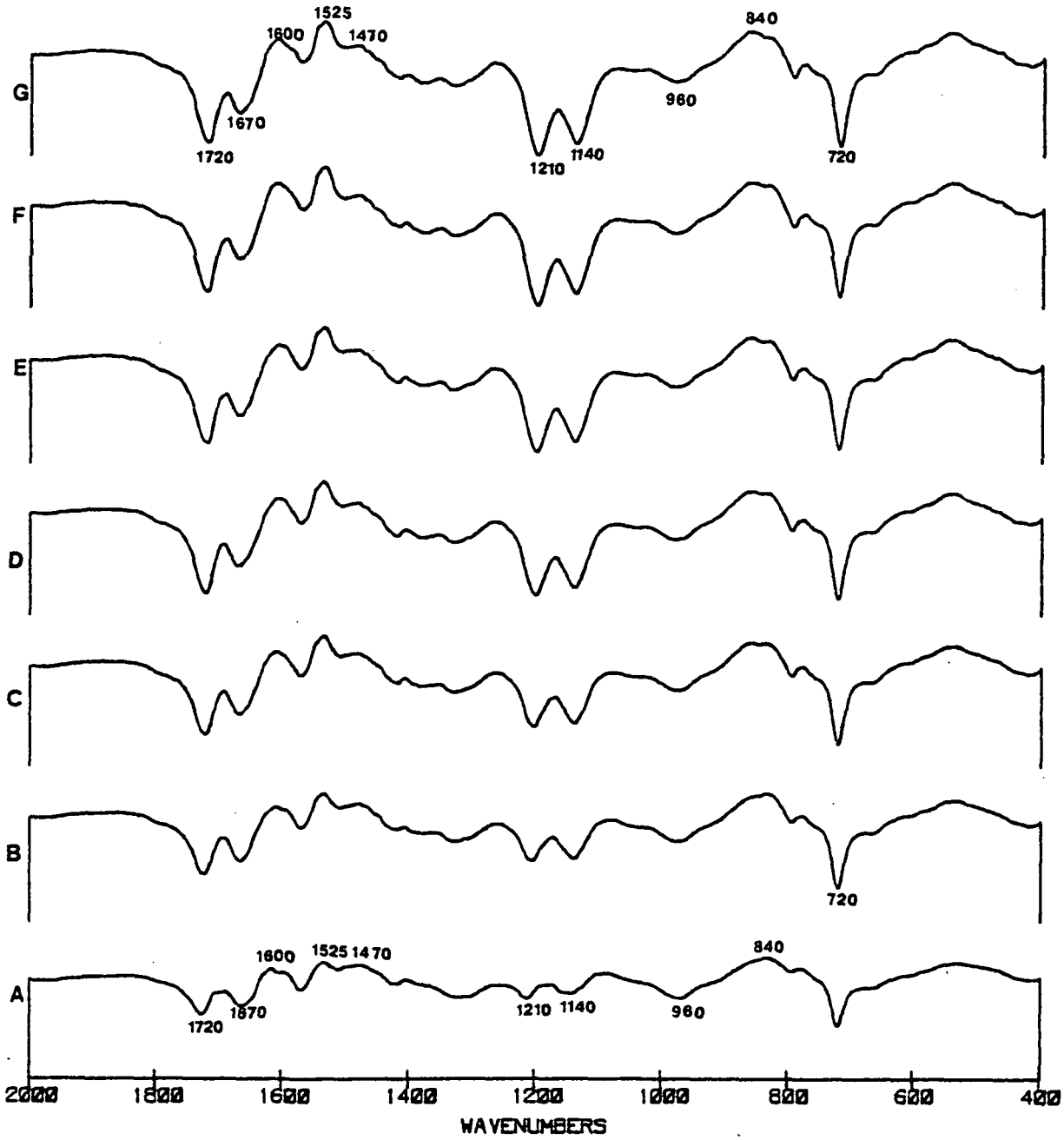

Figure 34. Difference infrared spectrum of 2,4-PSP cast on Al surface under nitrogen before and after heating at 180°C and various times. (A) 0.5 hr, (B) 1 hr, (C) 1.5 hr, (D) 2 hr, (E) 3 hr, (F) 4 hr, and (G) 5 hr.

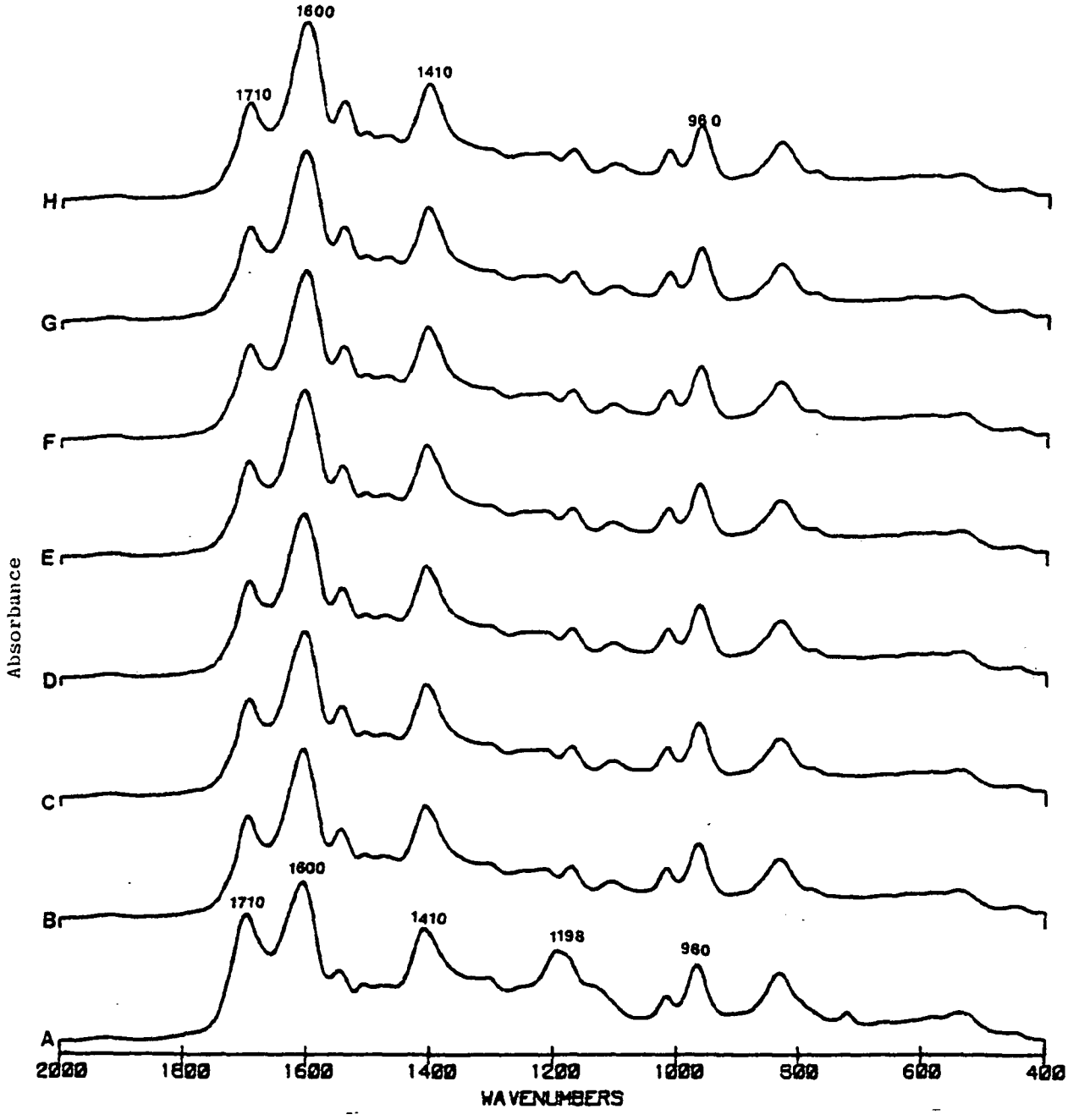

Figure 35. Infrared spectrum of 2,4-PSP cast on Al surface under nitrogen after heating at 200°C and various times. (A) 0 hr, (B) 0.5 hr, (C) 1 hr, (D) 1.5 hr, (E) 2 hr, (F) 3 hr, (G) 4 hr, and (H) 5 hr.

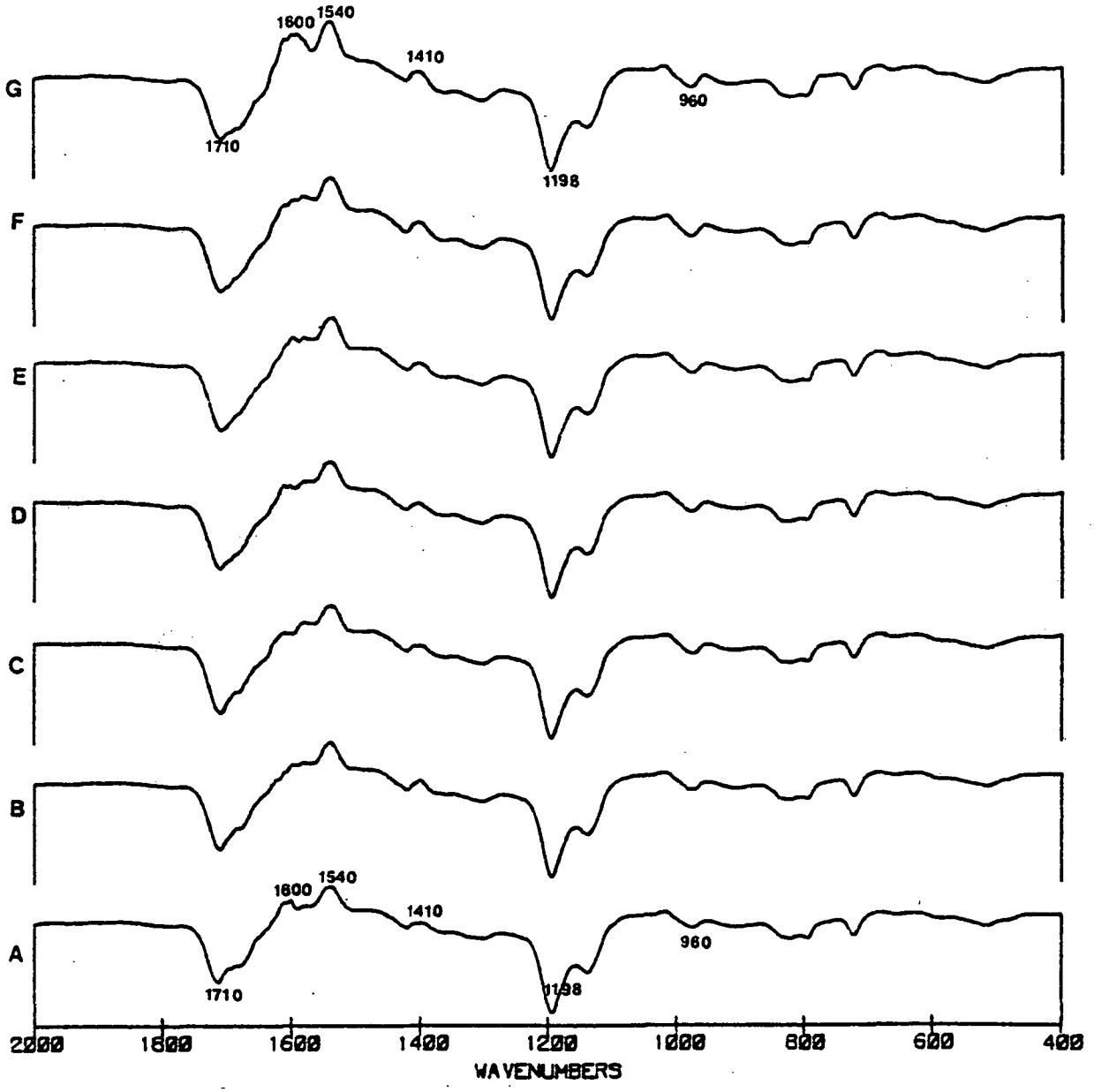

Figure 36. Difference infrared spectrum of 2,4-PSP cast on Al surface under nitrogen before and after heating at 200°C and various times. (A) 0.5 hr, (B) 1 hr, (C) 1.5 hr, (D), 2 hr, (E) 3 hr, (F) 4 hr, and (G) 5 hr.

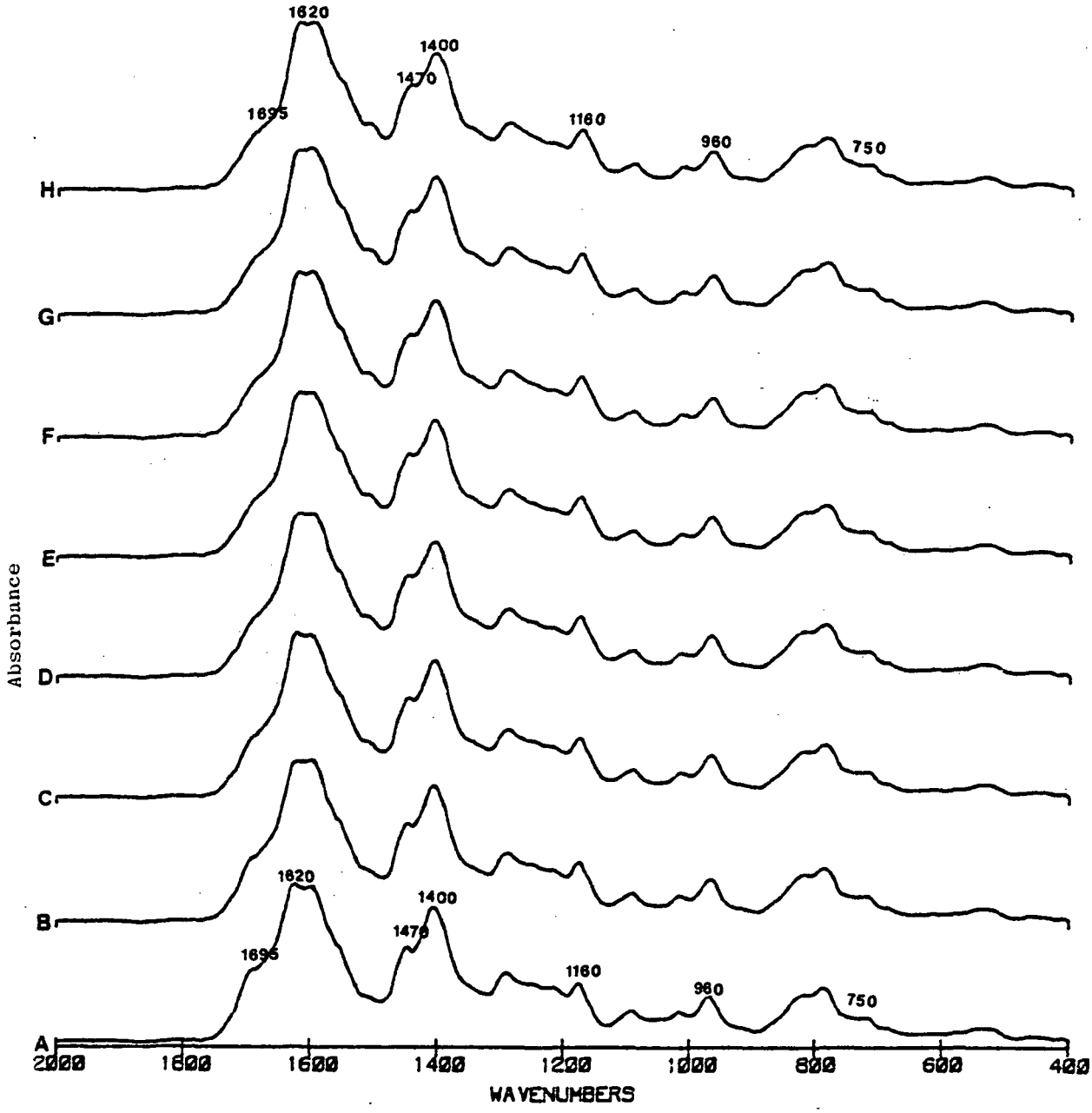

Figure 37. Infrared spectrum of 2,6-PVP cast on Al surface under nitrogen after heating at 180°C and various times. (A) 0 hr, (B) 0.5 hr, (C) 1 hr, (D) 1.5 hr, (E) 2 hr, (F) 3 hr, (G) 4 hr, and (H) 5 hr.

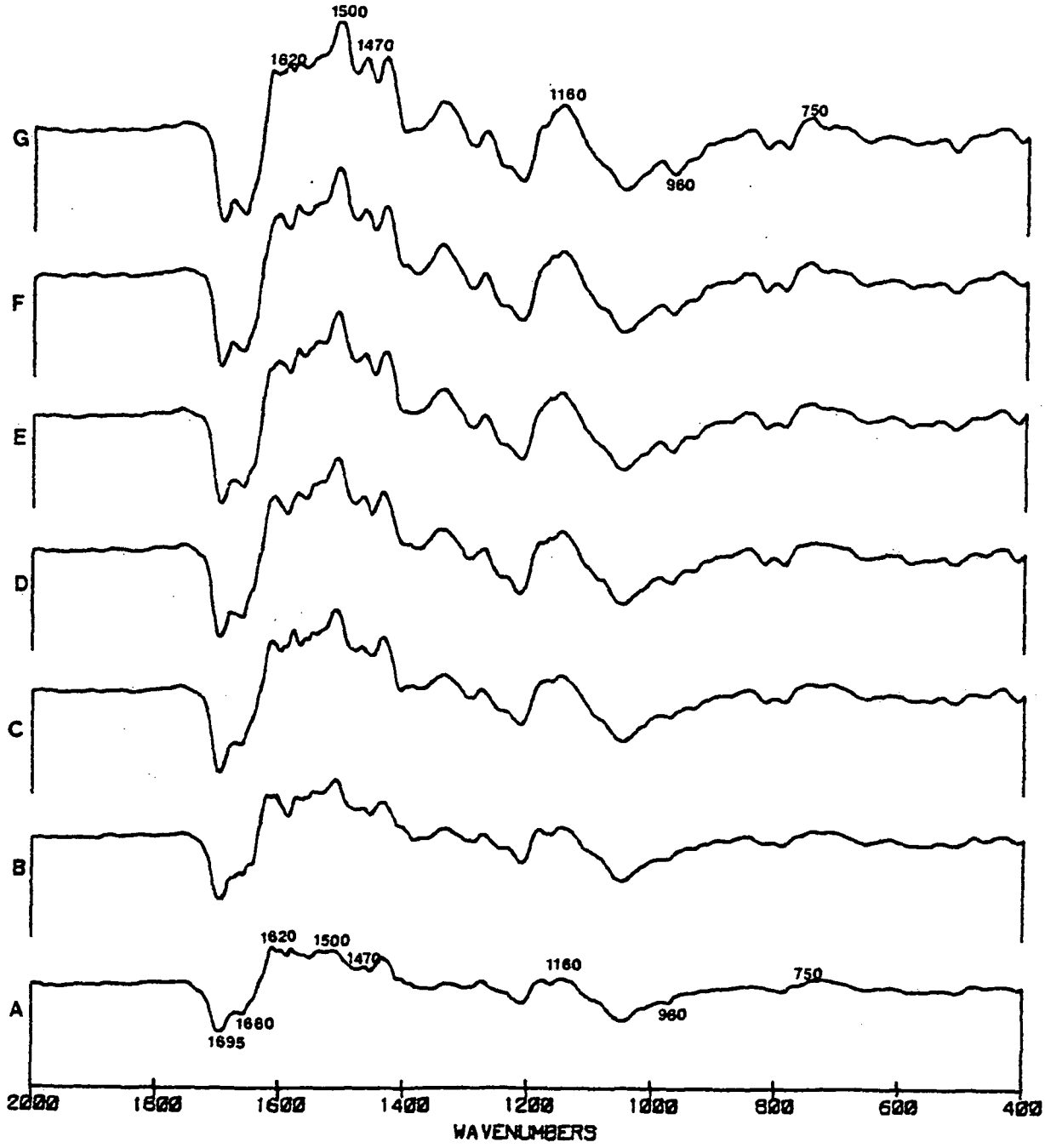

Figure 38. Difference infrared spectrum of 2,6-PSP cast on Al surface under nitrogen before and after heating at 180°C and various times. (A) 0.5 hr, (B) 1 hr (C) 1.5 hr, (D) 2 hr, (E) 3 hr), (F) 4 hr, and (G) 5 hr.

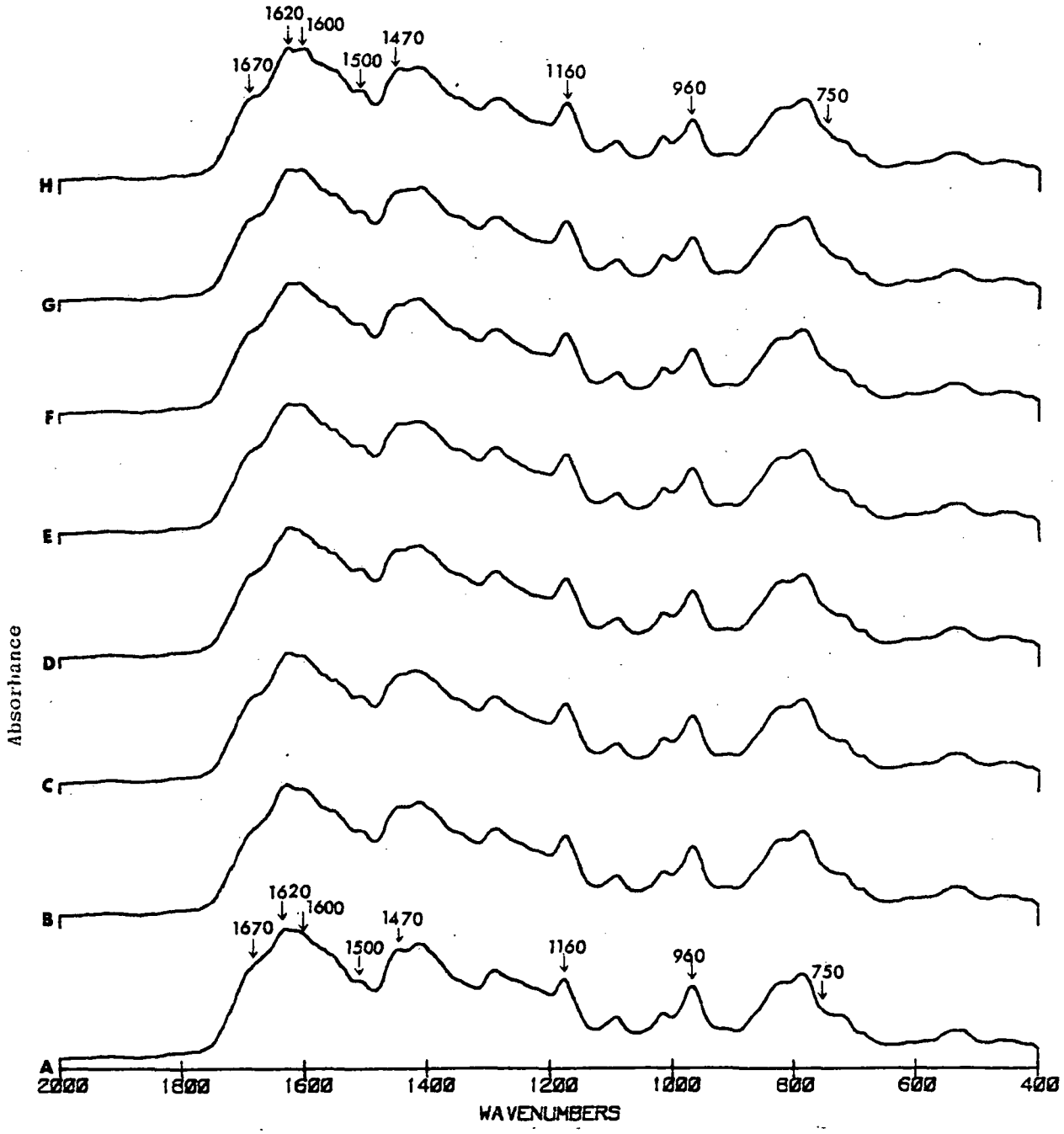

Figure 39. Infrared spectrum of 2,6-PSP cast on Al surface under nitrogen after heating at 200°C and various times. (A) 0 hr, (B) 0.5 hr, (C) 1 hr, (D) 1.5 hr, (E) 2 hr, (F) 3 hr, (G) 4 hr, and (H) 5 hr.

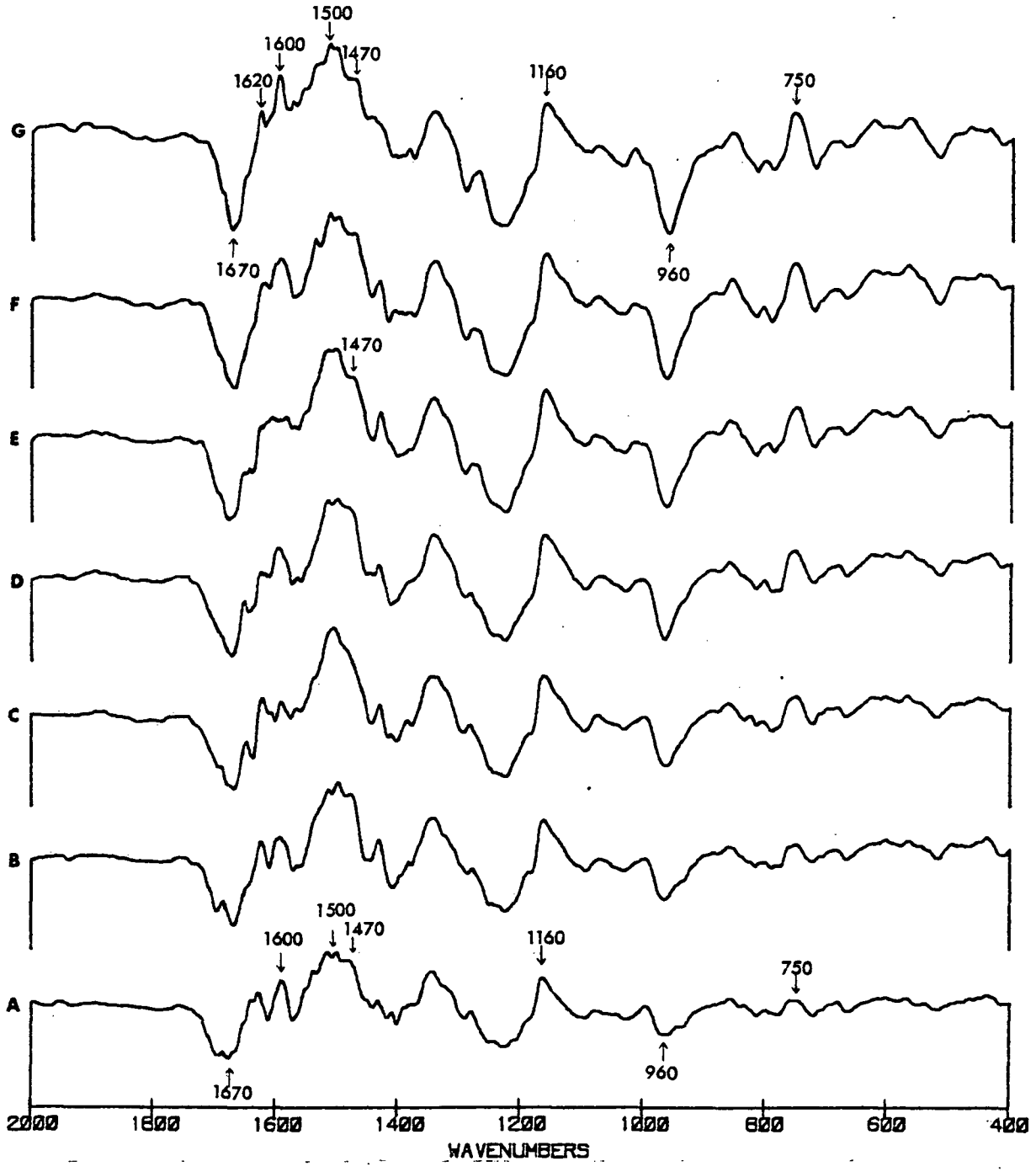

Figure 40. Difference infrared spectrum of 2,6-PSP cast on surface under nitrogen before and after heating at 200°C and various times. (A) 0.5 hr, (B) 1 hr, (C) 1.5 hr), (D) 2 hr, (E) 3 hr, (F) 4 hr and (G) 5 hr.

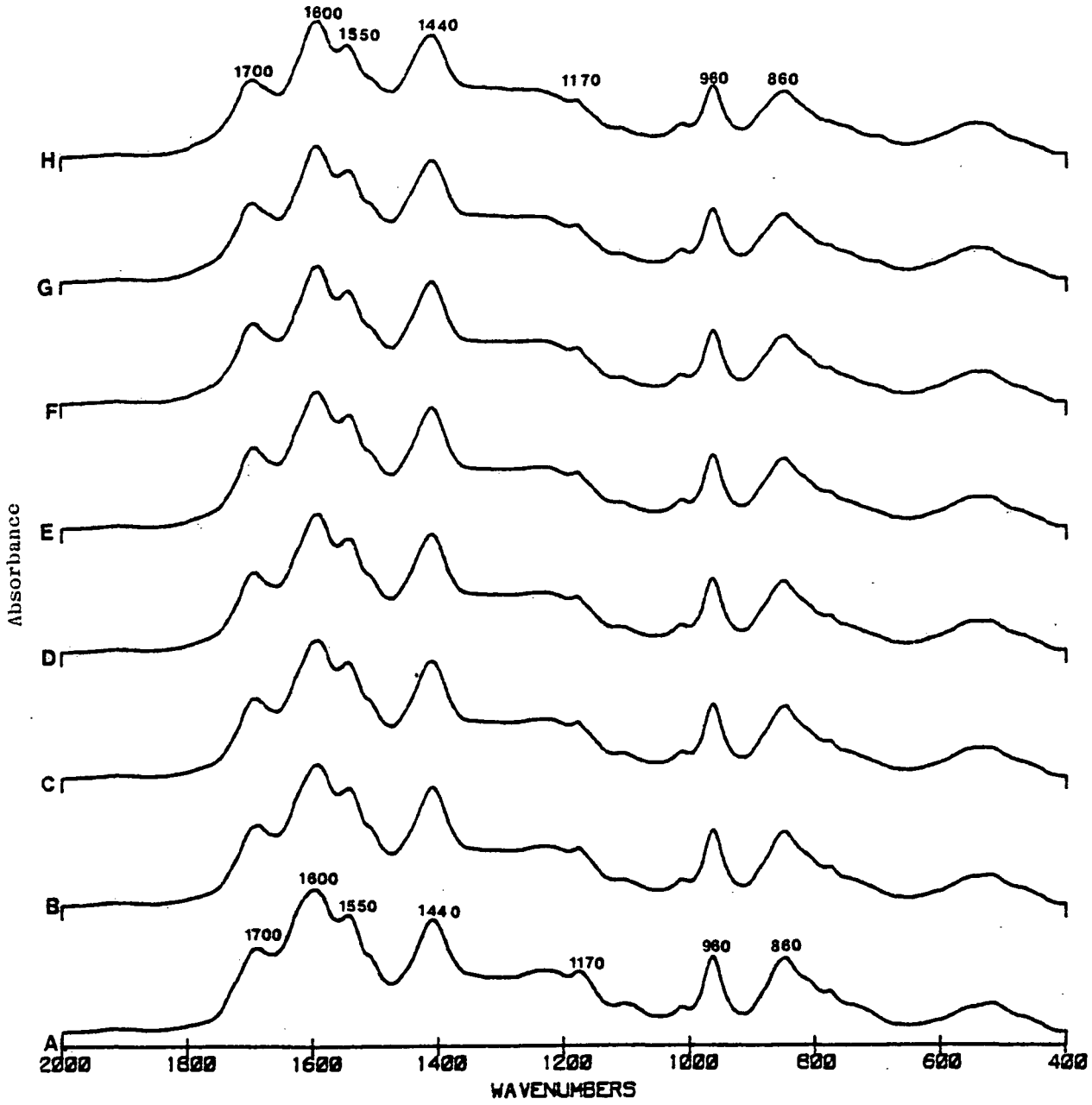

Figure 41. Infrared spectrum of 2,4,6-PSP cast on Al surface under nitrogen after heating at 250°C and various times. (A) 0 hr, (B) 0.5 hr, (C) 1 hr, (D) 1.5 hr, (E) 2 hr, (F) 3 hr, (G) 4 hr, and (H) 5 hr.

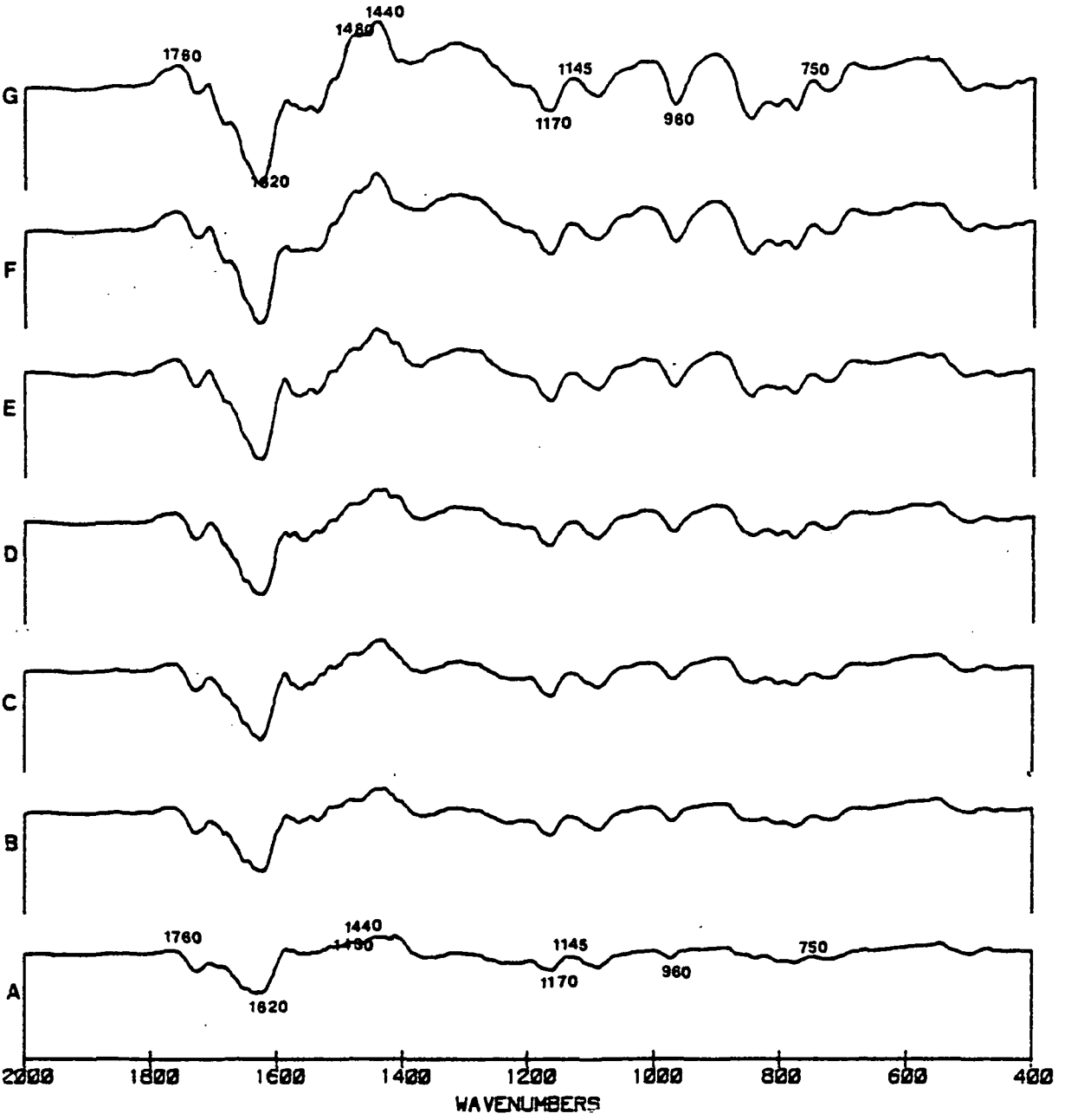

Figure 42. Difference infrared spectrum of 2,4,6-PSP cast on Al surface under nitrogen before and after heating at 250°C and various times. (A) 0.5 hr, (B) 1 hr, (C) 1.5 hr, (D) 2 hr, (E) 3 hr, (F) 4 hr, and (G) 5 hr.

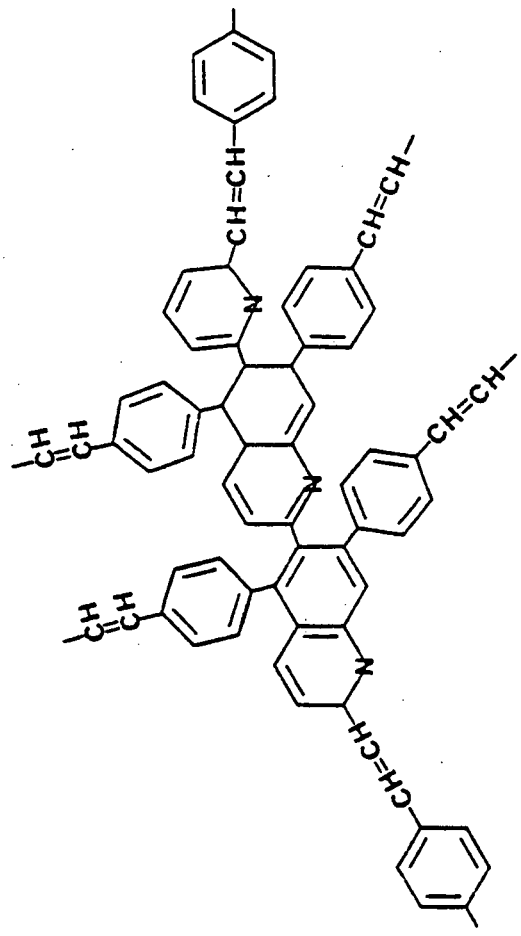

Figure 43. Thermally cured 2,6-PSP structure.

difference between the polymeric triazine and monomer and thus gave detailed information about the formation of the polymeric trazine structure. The char yield and oxygen index of polymeric triazine were increased as the cross-link density increased. The structure changes during thermal curing of 2,6-PSP can also be followed by FT-IR. An intermolecular Diels Alder reaction was proposed as the primary reaction during the thermal cure. In the case of those PSP polymers, there appeared to be no particular difference in char yield and oxygen index as a function of changes in structure.

Therefore, the equivalent weight can be expressed as follows:

$$EEW = \frac{\text{nx molecular weight of repeat unit + 2 x EEW of the resin when n=0}}{2}$$

The equivalent weight of 2,6-DGESP was calculated from Fig. 6 and listed in Table 1. The 2,4-DGESP and 2,4,6-TGESP had difficulty dissolving in the $CDCl_3$. In addition, the nitrogen atom on the pyridine can act as a catalyst to react with the epoxy ring [87]. Therefore, the content of epoxy resin may be diminished. The reaction between the epoxy ring and pyridine is as follows:

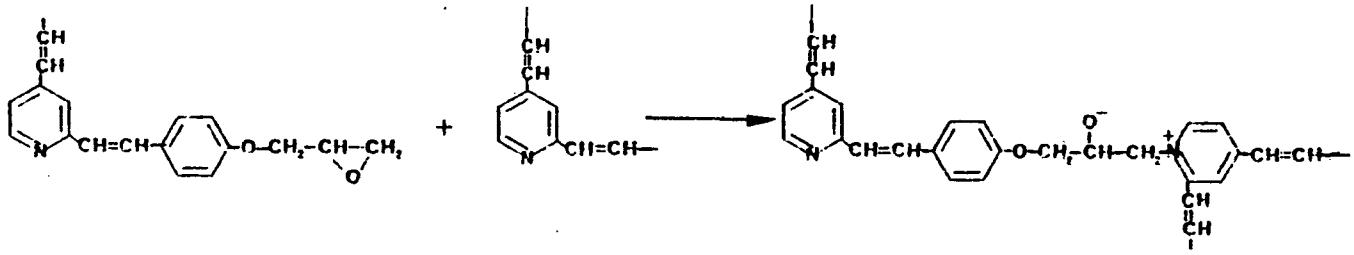

Hence, the EEW of 2,4,-DGESP and 2,4,6-TGESP were not obtained.

A-2 DSC Studies on the Glycidyl Ether of Styrylpyridine

The DSC thermogram of the epoxy-based aromatic polyether resin (Fig. 15) showed exothermic peaks (maximum) at 310.5° and 392.6° for 2,4-DGESP, at 260°, 305.4°, and 355° for 2,6-DGESP and at 210.0°, 337.2°C for 2,4,6-TGESP . Lee and Anderson [88,89] hypothesized that the exothermic peak at around 400°C could be attributed to reactions of the unreacted epoxide rings in the cured

IV. BIBLIOGRAPHY

1. W.W. Wright in "Degradation and Stabilization of Polymers", ed. by G. Geuskens, J. Wiley & Sons, N.Y., 1975, Chapter 3, pp. 43-75.

2. Lecture given by Prof. Eli M. Pearce, "Thermal Methods of Characterization", May 24, 1976, Annual Conference, Polytechnic Institute of New York.

3. H. F. Mark, S. M. Atlas, S. W. Shalaby, and E. M. Pearce, in "Flame-Retardant Polymeric Materials", ed. by M. Lewin, S. M. Atlas and E. M. Pearce, Plenum Press, N.Y., 1975, pp. 15.

4. C. P. Fennimore and F. J. Martin, Modern Plastics, 44, 141 (1966).

5. D. W. van Kevelen, Polymer, 16, 615 (1975).

6. E. M. Pearce and R. Liepins, Environ. Health Perspectives, 11, 69 (1975).

7. G. I. Nelson and J. L. Webb, J. Fire Flammability, 4, 325 (1973).

8. H. Lee and K. Neville, "Handbook of Epoxy Resins", McGraw-Hill, N.Y., 1967, Chapters 2 and 3.

9. N. Hata and J. Kumenotani, J. Appl. Polym. Sci., 17, 3545 (1975).

10. S. Y. Lee, S. Corbina and S. C. Chiang, Macromolecules, 12, 182 (1979).

11. G. J. Fleming, J. Appl. Polym. Sci., 13, 2579 (1969).

12. G. J. Fleming, J. Macromol. Sci., 3, 531 (1969).

13. J. W. Cooper, "Spectroscopic Techniques for Organic Chemists", John Wiley & Sons, N.Y., 1980, Chapter 2,pp. 25.

14. H. Lee and K. Neville, "Handbook of Epoxy Resins", McGraw-Hill, N.Y., 1967, Chapter 4.

15. ASTM D-1652-73, Standard Method of Test for Epoxy Content of Epoxy Resins, ASTM, 28, 341 (1975).

16. A. Durbetaki, Anal. Chem., 28, 2000 (1956).

17. D. W. Knoll, D. H. Nelson, and P. W. Keheres, 134th Am. Chem. Soc., Meet., Chicago, 1958, Division of Paint, Plastics, and Printing Ink Chemistry, Paper No. 5, 20 (1958).

18. B. Dobinson, W. Hoffmann, and B. P. Stark, "The Determination of Epoxide Groups", Pergamon, Oxford, 1969, Chapters 2 and 3.

19. J. G. Dorsey, G. F. Dorsey, A. C. Rutenberg, and L. A. Green, Anal. Chem., 49 (8), 1144 (1977).

20. W. B. Moniz and C. F. Poranski, "Epoxide Equivalent Weight Determination by Carbon-13 Nuclear Magnetic Resonance" in "Epoxy Resin Chemistry", edited by R. S. Bauer, ACS Symposium Series 114, ACS, Washington, D.C., 1979, Chapter 7.

21. H. D. Mak and M. G. Rogers, Anal. Chem., 44, (4), 837 (1972).

22. I. H. Tipton and M. J. Cook, Health Phys., 9, 103 (1963).

23. J. W. Shepherd, U.S. Patent 3,259,591 (1966); Chem. Abs., 65, 9131d (1966).

24. H. Brunner and M. J. Waghorn, Brit. Patent 910,899 (1962); Chem. Abs., 58,3564g (1963).

25. J. A. Parker, G. M. Fohlen, and P. M. Sawko, Development of Transparent Composites and Their Their Thermal Response, paper presented at Conference on Transparent Aircraft Enclosures, Las Vegas, Nevada, Feb. 5-8, 1973.

26. S. C. Lin, Ph.D. Thesis, Department of Chemistry, Polytechnic Institute of New York, 1978.

27. H. H. Chen and A. C. Nixon, Am. Chem. Soc., Div. Org. Coatings Plastic Chem., Preprints, 23 (1), 221 (1963).

28. L. E. Brown and J. D. Nutter, U.S. At. Energy Comm., Rept. No. MLM-1641 (1969).

29. H. Lee and K. Neville, Soc. of Plastics Eng. J., 16, 315 (1960).

30. E. S. Lopata and S. R. Riccitello, J. Appl. Polym. Sci., 19, 1127 (1975).

31. E. S. Lopata and E. R. Riccitello, J. Appl. Polym. Sci., 21, 91 (1977).

32. S. C. Lin and E. M. Pearce, J. Polym. Sci., Polym. Chem., 17, 3095 (1979).

33. S. C. Lin and E. M. Pearce, J. Polym. Sci., Polym. Chem., 17, 3121 (1979).

34. A. H. Frazer, "High Temperature Resistant Polymers", Interscience Publishers, N.Y., 1968, Chapter 1.

35. A. A. Askadskii and G. L. Slonimshii, Russian Chemical Reviews, 44 (9), 767 (1975).

36. R. H. Still, "The Use and Abuse of Thermal Methods of Stability Assessment", in "Developments in Polymer Degradation-1", ed. by N. Grassie, Applied Sciences Publishers, London, 1977, Chapter 1, pp 1-44.

37. S. V. Vinogradova and Ya. S. Vygodskii, Russian Chem. Rev., 42 (7), 551 (1973).

38. D. P. Bishop and D. A. Smith, Ind. Eng. Chem., 59 (8), 32 (1967).

39. R. T. Conley, "Thermosetting Resins" in "Thermal Stability of Polymers", ed. by R. T. Conley, Dekker, N.Y. 1970, Chapter 11, pp 507.

40. J. L. Koenig, Appl. Spectroscopy, 29, (4), 197, 293 (1975).

41. M. M. Coleman, Am. Chem. Soc., Polymer Preprints, 17 (2), 732 (1976).

42. R. D. Ritchie, Symposium on "High Temperature Resistance and Thermal Degradation of Polymers", London, September, 1960.

43. (a) Z. Jedlinski and A. Sek, Eur. Polym. J., 7,827(1971).
(b) Z. Jedlinski and D. Sek, J. Polym. Sci., Part A-1, 7, 2587 (1969).

44. D. W. van Krevelen, Chimia, 28, 504 (1974).

45. M. S. Lin and E. M. Pearce, J. Polym. Sci., Polym. Chem. Ed., 19, 2151, 2659 (1981).

46. A. M. Trozzolo, "Stabilization Against Oxidative Photodegradation", in Polymer Stabilization", ed. by W. L. Hawkins, Wiley Interscience, N.Y., 1972, pp 189.

47. R. A. Finnegan and J. J. Mattice, Tetrahedron, 21, 1015 (1965).

48. H. Kobsa, J. Org. Chem., 27, 2293 (1962).

49. G. C. Newland and J. W. Tanblyn, J. Appl. Polym. Sci., 8, 1946 (1964).

50. R. B. Fox, Pure Appl. Chem., 30, 87 (1972).

51. V. V. Korshak and S. V. Vinogradova, J. Polym. Sci., Part A-1, 7, 157 (1969).

52. D. Bellus, P. Slama and L. Durisinova, J. Polym. Sci., Part C, 22, 629 (1969).

53. L. Pauling, "Nature of the Chemical Bonds", 3rd ed., Cornell University Press, Ithaca, N.Y., 1960, Chapter 2, pp. 34-75.

54. J. G. Calvert and J. N. Pitts, "Photochemistry", J. Wiley & Sons, N.Y., 1966, Chapter 4, pp 240-365.

55. E. J. O'Connell, J. Am. Chem. Soc., 90, 6550 (1968).

56. A. Heller, Mol. Photochem., 1, 2571 (1969).

57. V. I. Stenberg, "Photo-Fries Reaction and Related Rearrangements" in "Organic Photochemistry", ed. by O. L. Chapman, Dekker, N.Y., 1967, Vol. 1, pp 127.

58. J. E. Guillet, Naturwissenschaften, 59, 503 (1972).

59. J. L. Lo. Ph.D. Thesis, Department of Chemistry, Polytechnic Institute of New York, 1981.

60. S. M. Cohen, R. H. Young, and A. H. Markhart, J. Polym. Sci., Part A-1, 9, 3263 (1971).

61. E. N. Zil'berman, Russ. Chem. Rev., 6, 331 (1960).

62. C. Grundamann, G. Weisse, and S. Seide, Annalen, 577, 77 (1952).

63. E. M. Smolin and L. Rappoport, "s-Triazines and Derivatives", Interscience, N.Y., pp 50, 149.

64. D. Martin, M. Bauer, and V. A. Pankratov, Russ. Chem. Rev., 47 (10), 975 (1978).

65. A. Damiani, E. Giglio, and A. Ripamont, Acta Cryst., 19, 161 (1965).

66. D. Belitskus and G. A. Jeffrey, Spectrochim. Acta, 21, 1563 (1965).

67. H. C. Brown, J. Polym. Sci., 44, 9 (1960).

68. H. Kon, Bull. Chem. Soc., Japan, 28, 275 (1955).

69. V. V. Korshak, T. M. Frunze, A. A. Izyneev, and V. G. Samsonova, Dokl.Akad.Nauk SSSR, 209, 862 (1973).

70. V. A. Kargin, V. A. Kabanov, and V. P. Zubov, Dokl. Akad. Nauk, SSSR, 139, 605 (1961).

71. D. R. Anderson and J. M. Holovka, J. Polym. Sci., Part A-1, 4, 1689 (1966).

72. H. P. Grinblat, I. V. Ikonitsku, et al., Polym. Sci., USSR, 21, 1434 (1979).

73. B. S. Wildi, U.S. Patent 3,284,418 (1966).

74. J. Verborgt and C. S. Marvel, J. Polym. Sci., Part A-1, 11, 261 (1973).

75. (a) P. W. Morgan, Macromolecules, 3, 536 (1972).
(b) S. R. Sandler and W. Karo, "Polymer Synthesis", Academic Press, N.Y., 1977, Vol. 2, Chapter 3, pp 74-113.

76. H. Lee and K. Neville, "Handbook of Epoxy Resins", McGraw-Hill, N.Y., 1966, Chapters 1 and 4.

77. J. W. Cooper, "Spectroscopic Techniques for Organic Chemists", Wiley-Interscience, N.Y., 1980, pp 166-169.

78. General Electric Model CR 280 KF 11A, Fluid Flammability Test Kit, Test Procedure Manual 4541K 25-001C.

79. R. A. Jones, Aldrichimica Acta, 9 (3),35 (1976).

80. S. R. Sandler and W. Karo, "Polymer Synthesis", Academic Press, N.Y., 1977, Vol. 1, Chapter 3, pp 73-86.

81. E. D. Bergmann and S. Pinchas, J. Org. Chem., 15, 1184 (1950).

82. Otto Schales and H. Graefe, J. Am. Chem. Soc., 74, 4486 (1952).

83. A. H. Cook and D. G. Jones, J. Chem. Soc., 278 (1941).

84. M. Ropers and B. Bloch, French Patent 2,261,296(1974); U.S. Patent 3,994,862 (1976).

85. C. A. Sojka and W. B. Moniz, J. Appl. Polym. Sci., 20, 1977 (1976).

86. (a) C. F. Poranski and W. B. Moniz, J. Coat. Tech., 49 (632), 57 (1977).
(b) C. F. Poranski, Private Communication.

87. W. Bradley, J. Forrest, and O. Stephenson, J. Chem. Soc., 1589 (1951).

88. L. H. Lee, J. Polym. Sci., A-3, 859 (1965).

89. H. C. Anderson, Anal. Chem., 32 (12), 1592 (1960).

90. W. R. R. Park and J. Blount, Ind. Eng. Chem., 49 (1), 1879 (1957).

91. M. B. Neiman and B. M. Kovarskaya, J. Polym. Sci., 56, 383 (1962).

92. H. C. Anderson, J. Appl. Polymer Sci., 6, 484 (1962).

93. Ming-Ta S. Hsu, M.L. Rosenberg, J. A. Parker, and A. H. Heimbuch, J. Appl. Polym.Sci., 26, 1976 (1981).

94. D. W. van Krevelen and P. J. Hoftyzer, "Properties of Polymers", Elsevier, N.Y., 1976, Chapter 21, pp. 459-465.

95. S. B. Maerov, J. Polym. Sci., Part A, 3, 487 (1965).

96. S. Bellus, P. Hrdlovic, et al., J. Polym. Sci., Part C, 16, 267 (1967); Part C, 22, 629 (1969); Part B,4, 1 (1966).

97. J. S. Humphrey,Jr. et al., Macromolecules, 6, 305 (1973).

98. N. R. Bertoniere, W. E. Franklin, et al., J. Appl. Polym. Sci., 15, 1743 (1971).

99. C. C. Unruh, J. Polym. Sci., 45, 325 (1960).

100. S. A. Zahir, J. Appl. Polym. Sci., 23, 1355 (1979).

101. L. J. Bellamy, "The Infrared Spectra of Complex Molecules", Chapman and Hall, Ltd., London, 1975, Chapter 16.

102. H. Luther, Z. Elektrochem., 59, 1008 (1955).

103. R. B. Barnes, R. C. Gore and V. Z. Williams, "Infrared Spectroscopy", Reinhold, N.Y., 1944, pp. 19-25.

104. R. L. Warner, W. Kennard, and D. Rayson, Austral. J. Chem., 8, 346 (1955).